A STUDY OF THE HYPERBOLIC HEAT CONDUCTION PROBLEM AND LAPLACE INVERSION USING GENERALIZED HAAR WAVELET OPERATIONAL MATRIX METHOD

SUAZLAN BIN MT AZNAM

FACULTY OF SCIENCE
UNIVERSITY OF MALAYA
KUALA LUMPUR

2012

A STUDY OF THE HYPERBOLIC HEAT CONDUCTION PROBLEM AND LAPLACE INVERSION USING GENERALIZED HAAR WAVELET OPERATIONAL MATRIX METHOD

SUAZLAN BIN MT AZNAM

DISSERTATION SUBMITTED IN FULFILLMENT OF THE REQUIREMENT FOR THE DEGREE MASTER OF SCIENCE

INSTITUTE OF MATHEMATICAL SCIENCES
FACULTY OF SCIENCE
UNIVERSITY OF MALAYA
KUALA LUMPUR

2012

UNIVERSITI MALAYA

ORIGINAL LITERARY WORK DECLARATION

Name : SUAZLAN BIN MT AZNAM   (I.C/Passport No: 820429-10-5459)

Registration/Matric No: SGP090001

Name of Degree: MASTER OF SCIENCE

Title of Project Paper/Research Report/Dissertation/Thesis ("this Work"):

A STUDY OF THE HYPERBOLIC HEAT CONDUCTION PROBLEM AND
LAPLACE INVERSION USING GENERALIZED HAAR WAVELET
OPERATIONAL MATRIX METHOD

Field of Study: PARTIAL DIFFERENTIAL EQUATIONS

  I do solemnly and sincerely declare that:

(1)   I am the sole author/writer of this Work;
(2)   This Work is original;
(3)   Any use of any work in which copyright exists was done by way of fair dealing and for permitted purposes and any excerpt or extract from, or reference to or reproduction of any copyright work has been disclosed expressly and sufficiently and the title of the Work and its authorship have been acknowledged in this Work;
(4)   I do not have any actual knowledge nor do I ought reasonably to know that the making of this work constitutes an infringement of any copyright work;
(5)   I hereby assign all and every rights in the copyright to this Work to the University of Malaya ("UM"), who henceforth shall be owner of the copyright in this Work and that any reproduction or use in any form or by any means whatsoever is prohibited without the written consent of UM having been first had and obtained;
(6)   I am fully aware that if in the course of making this Work I have infringed any copyright whether intentionally or otherwise, I may be subject to legal action or any other action as may be determined by UM.

Candidate's Signature   Date

Subscribed and solemnly declared before,

Witness's Signature   Date

Name:
Designation:

ABSTRACT

Wavelets have been applied successfully in image and signal processing. Many attempts have been made in mathematics to use wavelet function as numerical computational tool. In this study, an orthogonal wavelet function namely Haar wavelet function is considered. We used the operational matrix based on Haar basis to solve hyperbolic heat conduction equation problem and Laplace inversion.

It is remarkably known by many that one of the difficulties encountered in numerical method for non-Fourier heat conduction problem is the numerical oscillation within the vicinity of jump discontinuities at the wave front. We propose a new method of solving non-Fourier heat conduction equation problem which is also a hyperbolic partial differential equation. Our new method for solving partial differential equation of hyperbolic heat conduction equation is a hybrid of finite difference method and pseudo spectral method, where the former for time discretization and the latter for spatial discretization. The time discretization is performed prior to spatial discretization. In this sense, partial differential equation is reduced to ordinary differential equation and solved implicitly with Haar wavelet basis. For pseudo spectral method, Haar wavelet expansion has been used considering its advantage of the absence of the Gibbs phenomenon at the jump discontinuities. Furthermore, definition of Haar wavelet basis in this work allows a pleasant way in computing inverse of Haar wavelet matrix. We also derived generalized Haar wavelet operational matrix in the interval of $[0, X)$. The propose method have been applied into one physical problem namely, thin surface layers. It is found that the proposed numerical

results could suppress and eliminate the numerical oscillation in the jump vicinity at a certain value of discretization.

We also present a numerical method for inversion of Laplace transform using the method of Haar wavelet operational matrix. We prove the method for the case of the transfer function using the extension of Riemann-Liouville fractional integral. The proposed method extends the work of Wu et al. to cover the whole of time domain as we used the generalized Haar wavelet operational matrix. Moreover, this method gives an alternative numerical way to find the solution for inversion of Laplace transform in a simple way. The use of numerical generalized Haar operational matrix method is much simpler than the conventional contour integration method and it can be easily coded. Examples in finding Laplace inversion for rational, irrational and exponential transfer function are illustrated. Furthermore, examples on solving differential equation by Laplace transform method are also included.

Both of the proposed numerical methods are stable, convergent and easily coded. Numerical results also demonstrate good performance of the method in term of accuracy and competitiveness compared to other numerical methods. Additionally, few benefits come from its great features such as faster computation and attractiveness.

ABSTRAK

Penggunaan gelombang kecil telah berjaya diaplikasikan dalam bidang pemprosesan isyarat dan imej. Beberapa percubaan telah dilakukan untuk menjadikan fungsi gelombang kecil ortogon sebagai alat pengiraan berangka. Dalam kajian ini, fungsi gelombang kecil Haar yang juga merupakan fungsi gelombang kecil ortogon dipertimbangkan.

Diketahui umum bahawa ayunan berangka yang dikesan di sekitar ketakselanjaran lompatan di depan gelombang merupakan salah satu kesukaran yang dihadapi dalam kaedah berangka bagi masalah pengaliran haba bukan Fourier. Kami mencadangkan kaedah baharu bagi penyelesaian masalah persamaan pengaliran haba bukan Fourier yang juga merupakan persamaan pembezaan separa jenis hiperbolik. Kaedah baharu bagi penyelesaian persamaan pembezaan separa untuk persamaan pengaliran haba hiperbolik adalah gabungan kaedah perbezaan terhingga dan kaedah spektra pseudo. Antara kedua-dua kaedah ini, yang pertama digunakan untuk pendiskretan masa dan yang kedua digunakan untuk pendiskretan ruang. Pendiskretan masa dilakukan terlebih dahulu berbanding pendiskretan ruang. Menerusi pendekatan ini, persamaan pembezaan separa diturunkan kepada persamaan pembezaan biasa dan diselesaikan secara tersirat menggunakan fungsi asas gelombang kecil Haar. Bagi spektra pseudo, pengembangan fungsi gelombang kecil Haar digunakan setelah mempertimbangkan kelebihannya iaitu ketakhadiran fenomena Gibbs sekitar ketakselanjaran lompatan. Tambahan pula, takrifan fungsi asas gelombang kecil Haar dalam kajian ini menyenangkan pengiraan songsangan matriks gelombang

kecil Haar. Kami juga telah menerbitkan operasi matriks teritlak gelombang kecil Haar untuk selang masa [0,X). Kaedah berangka ini diaplikasi ke dalam suatu masalah fizikal iaitu lapisan permukaan nipis. Melalui keputusan kaedah berangka, kami berjaya mengekang atau melenyapkan ayunan berangka pada satu-satu nilai pendiskretan di sekitaran ketakselanjaran lompatan.

Kami juga menunjukkan kaedah berangka bagi mencari songsangan jelmaan Laplace menggunakan kaedah operasi matriks gelombang kecil Haar. Kami membuktikan kaedah ini dengan kes fungsi pindah tak nisbah menggunakan perluasan kamiran pecahan Riemann-Liouville. Kaedah berangka ini merupakan penerusan hasil kerja Wu dll bagi mencakupi keseluruhan domain masa dengan menggunakan operasi matriks teritlak gelombang kecil Haar yang telah diterbitkan. Tambahan lagi, kaedah berangka ini memberi pilihan mencari penyelesaian jelmaan Laplace songsang dengan cepat. Kaedah ini juga lebih mudah jika dibandingkan dengan kaedah kebiasaan pencarian songsangan jelmaan Laplace serta senang diaturcara. Contoh mencari songsangan jelmaan Laplace bagi fungsi pindah nisbah, tak nisbah dan eksponen ditunjukkan. Seterusnya, contoh bagi penyelesaian persamaan pembezaan menggunakan kaedah jelmaan Laplace juga disertakan. Kedua-dua kaedah berangka ini stabil, menumpu dan mudah diatur cara.

Dapatan kaedah berangka menunjukkan pencapaian yang baik dari segi kejituan dan setanding berbanding kaedah berangka yang lain. Di samping itu, kaedah berangka ini juga menarik dan cepat.

ACKNOWLEDGMENTS

PUBLICATIONS

1. Suazlan Mt Aznam and Amran Hussin (2012). Numerical Method for Inverse Laplace Transform with Haar Wavelet Operational Matrix. *Published in Malaysian Journal of Fundamental and Applied Sciences Vol.8 No.4 (2012).* UTM Malaysia.

2. Suazlan Mt Aznam and Amran Hussin (2012). Generalized Haar Wavelet Operational Matrix Method for Solving Hyperbolic Heat Conduction in Thin Surface Layers. *Under review for publication in Computers and Mathematics with Applications.*

PRESENTATIONS AND SEMINARS

1. One Day Seminar in Mathematics. (April 2010). Kuala Lumpur: Malaysia.

2. 6th International Education Symposium JUCTe (Japanese University Consortium for Transnational-Education). (November 2010). Kuala Lumpur: Malaysia.

3. Regional Annual Fundamental Science Symposium. (December 2011). Johor Bahru: Malaysia.

CONTENTS

LIST OF TABLES

LIST OF FIGURES

LIST OF NOTATIONS

η dimensionless length

$\mathbf{B}_m$ Block pulse matrix

$\mathbf{b}_m(x)$ block pulse function vector

$\mathbf{c}_m^t$ Haar series coefficient vector

$\mathbf{F}_m$ Generalized block pulse operational matrix

$\mathbf{H}_m$ Haar wavelet matrix

$\mathbf{h}_m(x)$ Haar function vector

$\mathbf{I}_m$ Identity matrix

$\mathbf{Q}_m$ Generalized Haar wavelet operational matrix

θ dimensionless temperature

ξ dimensionless time

$b_i(x)$ Block pulse function

C thermal wave propagation speed

c_i Haar series coefficient

$h_0(x)$ Haar wavelet scaling function

$h_1(x)$ Haar's mother wavelet function

m	Level of Haar wavelet
Q	dimensionless heat flux
q_r	reference heat flux
R	Average radius of curvature
T	temperature (^0C)
t	time (seconds)
x_j	collocation points

CHAPTER 1

INTRODUCTION

1.1 Overview of Thesis

The technology advancement that we are experiencing today would never had been at this level of achievement without continuous innovation efforts done by previous generations. Mathematicians had thoroughly studied mathematical equations as a tool for innovation in terms of computer aided programmes and softwares. These equations which are familiarly known as partial differential equations are becoming vital and play an important role in the field of science and engineering. It has been proven to be the best tools to describe naturally occurring physical phenomenon around us such as heat, sound, fluid flow, electrodynamics, electrostatics and elasticity. For example, we have better understanding on how heat propagates in a finite slab by computer simulation which is made possible by solving the partial differential equations. This understanding had helped IC chips designers in creating product prototype more efficiently by reducing the failure rate. Size of IC chips had decreased significantly in the last few decades, however the manufacturing process is facing new challenge in terms of failure due to overheating. In order to optimize the resources in designing the chip and to reduce failures due to overheating, designers are using computer simulation to find the optimal design. This is one of the many examples how computer simulation solving partial differential equation had contributed to the advancement of modern day technologies.

Partial differential equation is a differential equation with multiple variables that contains unknown multi variable functions and their partial derivatives. In the early history of solving partial differential equation, mathematicians were focusing on finding analytical solution. Among known analytical methods used to these days are separable variable method, integral transform method, method of characteristic and change of variables method. Most of these methods are limited to solve an ideal mathematical equation and if any attempts to solve a complex mathematical equation, for example nonlinear and non-homogeneous partial differential equations, very frequently will end up and involved with tedious calculation. Therefore, as computer technology became prominent in life today, numerical analysis of partial differential equation has received special attention by many scholars.

Numerical method based on wavelet is relatively a new mathematical tools for solving partial differential equations. Compared to other mathematical tools, wavelet analysis has captured mathematicians' attention due to its positive results in the field of signal and image processing. The most interesting features of wavelet is that their basis function localized in space or time came along with localization in frequency. The basis functions are usually orthogonal and compactly supported. These features resulting in sparse transformation in wavelet domain for non-stationary signals that contribute to fast algorithms. In numerical analysis these are some of a few desired properties of numerical analysis.

1.2 Scope of Research

The main focus on this work is to solve hyperbolic type partial differential equation numerically using generalized Haar wavelet operational matrix method. This partial differential equation comes from a non-Fourier heat conduction problem in thin surface layers. We derived generalized Haar wavelet operational matrix based on generalized block pulse function and Haar basis function. Generalized Haar wavelet operational matrix method is used for spatial discretization which is performed after reducing the partial differential equation into ordinary differential equation using finite difference method. Two sets of initial and boundary conditions are solved with this hybrid method.

We further our study utilizing our derivation of generalized Haar wavelet operational matrix in finding Laplace inversion numerically because Laplace transform method is usually opted for solvin partial differential equation. Finding Laplace inversion often faced difficulties as the inversion table of Laplace transform is limited and it involves Bromwich contour integral. We proved the method for the case of transfer function using the extension of Riemann-Liouville integral. A few examples of finding inversion of Laplace transform are illustrated, not only rational transfer function but also the irrational and exponential transfer function.

However, the numerical stability and error analysis of both propose numerical methods are not being mathematically proven. To justify the accuracy of these numerical results, a comparison with analytical solution given by others is being employed. The difference between the proposed numerical method and exact

solution is shown by absolute error.

1.3 Research Objectives

The objectives of this research are to :

1. establish generalized Haar wavelet operational matrix for integration.

2. establish numerical method of finite difference with generalized Haar operational matrix for solving partial differential equation of hyperbolic type with initial and boundary conditions.

3. solve non-Fourier heat conduction equation which is also a hyperbolic type partial differential equation in thin surface layers.

4. establish numerical method for Laplace inversion with generalized Haar wavelet operational matrix.

5. find Laplace inversion numerically for rational, irrational and exponential transfer functions using established Laplace inversion with generalized Haar wavelet operational matrix method.

1.4 Thesis Organization

This thesis consists of 6 chapters including this chapter and is organized as follows:

In Chapter 2, we present an overview of operational matrix in general. We list a few well known orthogonal function that has been used to derive operational matrix. Next, we narrow it down to a specific orthogonal function namely Haar basis function. The selection of this orthogonal function will be justified by

listing down a few of its advantageous compared to other orthogonal function. To justify why we choose Haar wavelet function, we list down a few advantages of this orthogonal function. We further review on our main problem of solving partial differential equation of non-Fourier heat conduction equation. At the end of this chapter, we look at numerical inversion of Laplace transform.

In Chapter 3, we show the basic mathematical background of Haar wavelet which are needed to understand the concept followed in this thesis. Most of literatures define Haar wavelet and its operational matrix within the interval $[0, 1)$. Therefore, we derive generalized Haar wavelet operational matrix which could cater the Haar series expansion domain greater than one.

In Chapter 4, we establish a new numerical method to solve non-Fourier heat conduction equation problem which is also a hyperbolic type partial differential equation. This numerical method is a combination of finite difference method and pseudo spectral method. The former is used for time discretization and the latter is used for spatial discretization. In spatial discretization, generalized Haar wavelet operational matrix is employed. Numerical solution for hyperbolic type equation often encounters difficulties eliminating numerical oscillation surrounding its jump discontinuities at wave front. It is found that from the numerical results, at a certain value of discretization, numerical oscillation can be suppressed or totally be eliminated.

In Chapter 5, we extend the work of Wu et al. (2001) in finding Laplace inversion from a transfer function. We prove the case of transfer function using the extension of Riemann-Liouville fractional integral. The usage of generalized Haar wavelet operational matrix enable us in finding the inversion of Laplace

transform that covers the whole time domain.

Finally, Chapter 6 summarizes the overall works and contributions of the study in numerical analysis of hyperbolic heat conduction equation in non-Fourier heat conduction problem and Laplace transform inversion. We also make some recommendation for future work.

CHAPTER 2

LITERATURE REVIEW

Operational matrix method have received considerable attention by many scholars in solving dynamical system analysis (Sinha and Butcher, 1997), system identification, optimal control systems (Mohan and Kar, 2005; Endow, 1989; Karimi, 2006) and numerical solution of integral and differential equations (Lepik, 2005; Kilicman and Zhour, 2007). Casting a differential or integral equation into a corresponding matrix system is the main characteristic of this operational matrix method. The approach is based on replacing the underlying differential equations into integral equations through integration operator and approximating the functions involved in the equation by truncated orthogonal series. An operation of integral operator is replaced by operational matrix.

To have a better view on operational matrix, let us consider the integral property of function vector, $\mathbf{\Phi}(x)$ in the following approximation:

$$\int_0^x \mathbf{\Phi}(\tau)d\tau = \mathbf{Q}\mathbf{\Phi}(x), \tag{2.1}$$

where

$$\mathbf{\Phi}(x) = \begin{bmatrix} \phi_0(x) & \phi_1(x) & \cdots & \phi_{m-1}(x) \end{bmatrix}^t \tag{2.2}$$

in which the elements $\phi_0(x), \phi_1(x), \ldots, \phi_{m-1}(x)$ are the orthogonal basis functions in the Hilbert space $L^2(R)$. The operational matrix, $\mathbf{Q}$ is an $m \times m$ constant matrix behaves as an integrator (Cheng and Tsay, 1977) and can be uniquely determined on the basis of the particular orthogonal functions, $\phi_i(x)$. From Eqn. (2.1), it can be observed that the problem of multiple integration is simplified by computing

7

the multiplication of matrices instead of performing the integration operations conventionally.

To date, there are hefty number of literatures deriving operational matrix from different orthogonal functions. Among orthogonal basis functions that have been given special attention are Walsh function (Chen and Hsiao, 1975), cosine-sine and exponential function (Paraskevopoulos, 1987), block pulse function (Chi-Hsu, 1983), normalized Bernstein polynomials (Singh et al., 2009), linear Legendre mother wavelets (Khellat and Yousefi, 2006), Chebyshev wavelet (Babolian and Fattahzadeh, 2007) and Haar wavelet (Gu and Jiang, 1996; Chen and Hsiao, 1997).

Chen and Hsiao (1975) derived Walsh operational matrix for performing integration and solving generalized state equations. Paraskevopoulos (1987) shows the operational matrix relationship between Fourier sine-cosine series and Fourier exponential series expansion. Babolian and Fattahzadeh (2007) have obtained Chebyshev operational matrix for integration in general and applied into solving continuous and discontinuous solution of Volterra type integral equations. All of these numerical computations share a number of advantageous in common. One of the advantage is the ability of finding the solution with only matrices manipulation rather than performing integration or differentiation in a conventional ways. Another advantage is that the ability of transforming the matrices into a sparse matrix and small number of significant coefficients (Hariharan and Kannan, 2011). This is the main factor that reduces computation time. The advantage remains even if big matrix is involved whereby big matrix usually requires large computer storage and a huge number of arithmetic

operations (Lepik and Tamme, 2004).

In this study we are going to work with Haar wavelet basis function and its operational matrix. Haar wavelet has a few numbers of advantages compared to other wavelet. Haar wavelet is the simplest wavelet function and it is one example of orthogonal function. Their bases are very compact support which means that the wavelet vanishes outside of a finite interval. Among admired properties of Haar wavelet orthogonal functions in numerical computation is that the sparse representation for piecewise constant function, fast transformation and the possibility of implementation of fast algorithm in matrix (Shahsavaran, 2011). Faster matrix transformation can be achieved with expansion of Haar series rather than expansion of Walsh series for the same amount of terms required for the computation, as the resolution order by Haar expansion is less than Walsh expansion (Khuri, 1993). Haar wavelet operational matrix for the integral of Haar wavelets is always positive definite, hence the existence of Haar wavelet operational matrix inverses and its square root are never unavailable. This factor nominates this method as computer oriented because no imaginary numbers are involved in the computation (Chen and Hsiao, 1997). Apart from that Haar wavelet is the only wavelet that does not exhibit Gibbs phenomenon (Kelly, 1996; Jerri, 1998; Raeen, 2008). This factor gives an extra advantage to proposed numerical method which will be covered in Chapter 4.

The first attempt that put Haar basis function into focus for solving differential equation was by Chen and Hsiao (1997), who first derived the Haar operational matrix for the integrals and brought the application of Haar analysis into the dynamic systems. They applied the proposed method to solve lumped

and distributed-parameter systems. It can be found that Lepik (2005, 2007a,b) has established Haar wavelet method to solve ordinary and partial differential equation and recently, solved PDE with two dimensional Haar wavelets (Lepik, 2011). Generalized Haar wavelet operational matrix is an extension work of Wu et al. (2001) that covers the whole domain for Haar series expansion intervals. We derived the Haar wavelet operational matrix based on Wu et al. (2001) works but extending it using generalized block pulse function operational matrix for integration done by Kilicman and Zhour (2007). It is expedient to do this way as it will fit the expansion of Haar series in the interval $0 \leq x < X$.

The main problem to be solved in this work is the partial differential equation problem of non-Fourier heat conduction in thin surface layers. Heat conduction problem often arises in a variety of problems in various branches of science and engineering. When the heat flux or the temperature involved in the heat transfer process is not very high, or the phenomena occurring at a time scale smaller than the thermal relaxation time of the material are not of interest, these problems are best described and analyzed with the heat conduction equation based on Fourier's law. This equation implies a presumption of infinite thermal propagation speed. Therefore, its prediction may underestimate the peak temperature during a rapid transient heat process. When someone is interested in the transient problems in an extremely short period of time, in very high flux, or for very low temperature, the classical diffusion theories may break down (Liu and Chen, 2004). Under these conditions, the theory with the finite propagation velocity of thermal wave will become dominant. In this event, modification is necessary to deal with finite propagation velocity of thermal wave for more precise heat flux model.

The simplest approach to construct a non-Fourier heat equation is through modified equation by Vernotte (1958) and Catteneo (1958) to the classical heat diffusion equation, which includes a component recognising the finite speed of heat signals that behave as wave propagation. Earlier successful applications of hyperbolic heat equation were used to predict transient heat conduction process in chemical and process engineering (Chan et al., 1971), in the process of laser pulse heating (Hess et al., 1981), in IC chips (Guo and Xu, 1992) and in thin surface layers (Kao, 1977; Chen, 2007). Table (2.1) below summarizes the differences between Fourier hyperbolic heat conduction equation and non-Fourier heat conduction equation (HCE).

Table 2.1: Comparison between Fourier and Non-Fourier heat conduction equation (HCE).

Item	Fourier HCE	non-Fourier HCE
1) conservation energy	same	same
2) heat flux equation	$q = -k\nabla T$	$\tau\dfrac{\partial q}{\partial t} + q = -k\dfrac{\partial T}{\partial r}$
3) equation form	parabolic	hyperbolic
4) heat propagation	infinite	finite
5) temperature gradient	moderate	extreme

Over the last 20 years, wavelet transforms have been applied extensively for applications in various fields like pattern recognition (Beylkin, 1993), data compression and signal processing (Mallat, 2009). However application of wavelet

transform to the solution of hyperbolic partial differential equation has been limited (Holmström and Waldén, 1998). Wavelets with their highly localized functions in spatial dimension, which are of varying scales, have the potential to combine the advantages of both spectral and finite difference bases. Another good feature of using wavelets is that there is a class of fast algorithm based on the fast wavelet transform which may be used to speed up the numerical schemes (Bindal et al., 2003). Historically, the wavelet transform was developed as an extension of Fourier transform in order to decompose the frequency content of a function in both spatial and frequency domain.

Numerous literatures are available for solving hyperbolic heat conduction equation. The major difficulty encountered in the numerical solution of the hyperbolic conduction is numerical oscillations in the vicinity of sharp discontinuities. Tamma and Railkar (1989) had successfully overcome this problem by introducing specially tailored transfinite-element formulations for the hyperbolic heat conduction equation. Carey and Tsai (1982) applied the central and backward difference schemes to examine numerical oscillation errors at the reflected boundary. Chen and Lin (1993) employed a new powerful hybrid technique based on the Laplace transform and control volume methods to solve hyperbolic heat conduction equation and their numerical method provides excellent results. They applied various examples of physical problems to verify the accuracy of their method. Chen (2007) solved hyperbolic heat conduction equation in thin surface layer using hybrid method combining Laplace transform, weighing function scheme (Shong-Leih, 1989) and hyperbolic shape function. Shen et al. (2010) present anti-diffusive solutions to the hyperbolic heat transfer

equation using Bokanowski and Zidani's second-order method (Bokanowski and Zidani, 2007) and Xu and Shu's fifth-order method (Zhengfu and Chi-Wang, 2005) in one and two dimensional. Analytical solution of one dimensional hyperbolic heat conduction equation was given by Kao (1977), Baumeister and Hamill (1969), Ozisik and Vick (1984) and Taitel (1984).

Focus in this research is on the pseudo spectral method for spatial discretization, by using Haar wavelet expansion to implicitly solve hyperbolic heat conduction in thin surface layers. As mentioned before, Haar wavelet is the only orthogonal wavelet that does not exhibit numerical oscillation near the jump discontinuity at any points (Raeen, 2008; Kelly, 1996). This is the utmost concern when attempting to solve numerical hyperbolic type heat conduction equation as the numerical solution will encounter oscillation in the vicinity of jump discontinuity. It will be a great advantage for this method to suppress oscillation that might appear, since finite difference is being used to discretize time. To the best of our knowledge, the proposed method in this work is the first time attempt to solve hyperbolic heat conduction equation. Analytical solution for prescribed wall temperature conditions has been given by Kao (1977).

Apart from that we establish a method in finding inversion of Laplace transform using generalized Haar wavelet operational matrix. This method is an extension work of Wu et al. (2001) that covers the whole time domain in finding Laplace inversion numerically. Laplace transforms is known to be an important tool in solving mathematical equations that arise in engineering problem. Engineers often opt for Laplace transform method to solve initial value problem which involves a step input function which is typical of many control system problems, differential

equations involving impulse and step functions and partial differential equation. For example, through this approach the partial differential equation is transformed into ordinary differential equation and lastly into an algebraic equation which is normally easy to deal with. Since its discovery by a French mathematician, Pierre - Simon Marquis De Laplace (1749-1827) (Kreyszig, 2006), it has been widely applied and continuously researched by scholars from various fields. Those scholars had put through enormous amount of efforts in finding its inverse function numerically and analytically. This is because finding the inverse of Laplace transform is considered to be a difficult task due to its limitation in the inversion table of inverse Laplace transform, in the sense that it could not cater most of the engineering problems which always associated with complexity of mathematical equation.

Before Haar wavelet operational matrix were used to find inversion of Laplace transform numerically, there are other literatures that used other orthogonal functions as well. Cheng and Tsay (1977) have been using Walsh operational matrix for solving various distributed-parameters systems such as heat conduction and percolation problem. Later, a more rigorous approach has been taken by Chi-Hsu (1983) to derive generalized block pulse operational matrices. According to Chi-Hsu (1983), Laplace inversion for rational and irrational transfer function illustrated by using generalized block pulse operational matrices is proven to be more accurate compare to previous work by Cheng and Tsay (1977).

CHAPTER 3

MATHEMATICAL BACKGROUND OF HAAR WAVELET

3.1 Introduction

The history of Haar wavelet dates back to the year of July 1909 which came from the content of inaugural thesis written by Alfréd Haar, a Jewish Hungarian mathematician.   The title of the thesis *'Zur Theorie der orthogonalen Funktionensysteme'* or in English means 'On the Theory of Orthogonal Function Systems' was written for his doctorate study in University of Göttingen under supervision of one of the most influential mathematician in that century, David Hilbert (Haar and Zimmermann, 1911).

(a) Alfréd Haar (1885 -1933)   (b) David Hilbert (1862 -1943)

Figure 3.1: Alfréd Haar and his Ph.D supervisor, David Hilbert (Chang, 2010)

However, the name of Haar wavelet and the study of wavelet was not immediately recognized after he submitting the thesis until around the year 1975. During this time the concept of wavelet was first pioneered and introduced by Jean Morlet, a French geophysicist whom need to analyze the backscattered

seismic signals which carry the information related to the geological layers (Meyer, 2008). Later then, he collaborated with Alexander Grossmann, a Croatian-French physicist to perform wavelet analysis and for the first time the word wavelet emerged in the academic world. The equivalent word for wavelet in French is '*ondellete*' which means small wave.

Haar wavelet is a wavelet family or basis that form from a sequence of rescaled square wave function series. In order to define Haar series, it is crucial to define the fundamental square wave function. Then the subsequent Haar wavelet functions are generated from fundamental square wave function with translation and dilation process. Haar wavelet is the simplest and oldest wavelet. One property of the Haar wavelet is that it has compact support, which means that it vanishes outside of a finite interval. Unfortunately, Haar wavelets are not continuously differentiable which somewhat limits its applications. The other known property is that Haar wavelet is categorized as an orthogonal function.

In this chapter, a brief introduction to Haar wavelet function, its series expansion, matrix form and operational matrix is given. Many literatures have defined Haar wavelet operational matrix on the interval $[0, 1)$. Here we extend the usual defined interval to $[0, X)$ as actual problem does not necessarily hold up to one only.

3.2 Haar Wavelet Function

An analytic function $f(x)$ can be expanded in a series as

$$f(x) = \sum_{n=0}^{\infty} a_n \psi_n(x) \qquad (3.1)$$

where $\psi_n(x)$ is the basis in the Hilbert space $L^2(R)$ and a_n is coefficient of the series. The coefficients can be obtained as follows,

$$a_n = \int_{-\infty}^{\infty} f(x)\psi_n(x)dx \qquad (3.2)$$

For example, if we have a bases function $\psi_n(x) = x^n$, we could expand the function, $f(x)$ using power series expansion such as Taylor series expansion. Same goes to a function with sinusoidal bases, we could use Fourier series expansion for $f(x)$. In this work an orthogonal function namely Haar wavelet function is considered. Haar wavelet functions are not continuous. The set of this function is a group of square waves in interval of $[0, X)$ and defined as below,

$$h_0(x) = \frac{1}{m^{1/2}} \qquad (0 \le x < X) \qquad (3.3)$$

$$h_1(x) = \frac{1}{m^{1/2}} \begin{cases} 1 & 0 \le x < \dfrac{X}{2} \\ -1 & \dfrac{X}{2} \le x < X \\ 0 & \text{elsewhere} \end{cases} \qquad (3.4)$$

$$h_i(x) = \frac{1}{m^{1/2}} \begin{cases} 2^{\frac{j}{2}} & \dfrac{k-1}{2^j}X \le x < \dfrac{k-\frac{1}{2}}{2^j}X \\ -2^{\frac{j}{2}} & \dfrac{k-\frac{1}{2}}{2^j}X \le x < \dfrac{k}{2^j}X \\ 0 & \text{elsewhere} \end{cases} \qquad (3.5)$$

where $i = 1, 2, \cdots, m-1$, $m = 2^J$ and the resolution J is a positive integer. While j and k denote the integer decomposition of the index i, for example $i = 2^j + k - 1$

in which $k = 1, 2, 3, \cdots, 2^j$. $h_0(x)$ is defined as a constant and is called Haar scaling function, while $h_1(x)$ is called Haar mother wavelet function or fundamental square wave function.

All the others subsequent Haar wavelet functions are generated from mother wavelet function, $h_1(x)$ with translation and dilation process.

$$h_i(x) = 2^{\frac{j}{2}} h_1(2^j x - k). \tag{3.6}$$

Haar wavelet functions are also orthogonal functions, so that it holds the property as below

$$(h_p(x), \quad h_q(x)) = \int_0^X h_p(x) h_q(x) dt = \begin{cases} \dfrac{X}{m} & \text{if } p = q \\ 0 & \text{if } p \neq q \end{cases} \tag{3.7}$$

Eqn. (3.7) can be proven as below. If $p = q$, then we have

$$\begin{aligned}
(h_p(x), \quad h_q(x)) &= \int_0^X h_p(x) h_q(x) dt \\
&= \int_0^X h_n^2(x) dx \\
&= \|h_n(x)\|^2 \tag{3.8} \\
&= \int_{\frac{k-1}{2^j} X}^{\frac{k-\frac{1}{2}}{2^j} X} \frac{2^j}{m} dx + \int_{\frac{k-\frac{1}{2}}{2^j} X}^{\frac{k}{2^j} X} \frac{2^j}{m} dx \\
&= \frac{2^j}{m} \left[\frac{k-\frac{1}{2}}{2^j} X - \frac{k-1}{2^j} X \right] + \frac{2^j}{m} \left[\frac{k}{2^j} X - \frac{k-\frac{1}{2}}{2^j} X \right] \\
&= \frac{2^j X}{m} \left[\frac{1}{2^j} \right] \\
&= \frac{X}{m}, \tag{3.9}
\end{aligned}$$

and if $p \neq q$, then we have

$$\int_0^X h_p(x) h_q(x) dt = 0, \tag{3.10}$$

18

as all integrals in Eqn. (3.10) are zero. The orthogonal set of the first four Haar function ($m = 4$) and first eight Haar function ($m = 8$) in the interval of $(0 \leq x < 1)$ can be shown in Figure 3.2 and Figure 3.3, respectively.

(a) Haar function of $h_0(x)$

(b) Haar function of $h_1(x)$

(c) Haar function of $h_2(x)$

(d) Haar function of $h_3(x)$
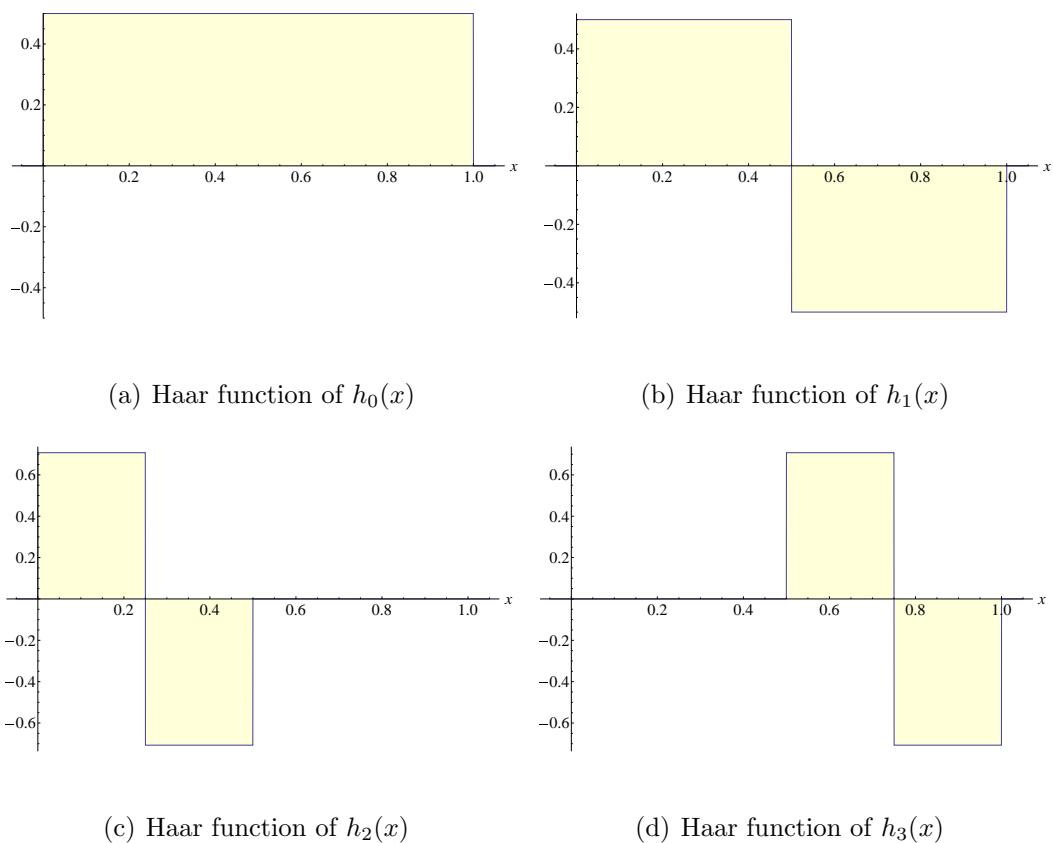
Figure 3.2: First four Haar functions
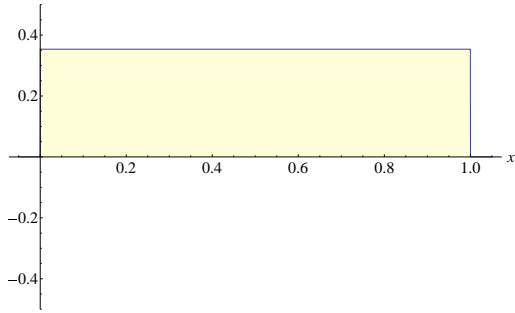
(a) Haar function of $h_0(x)$
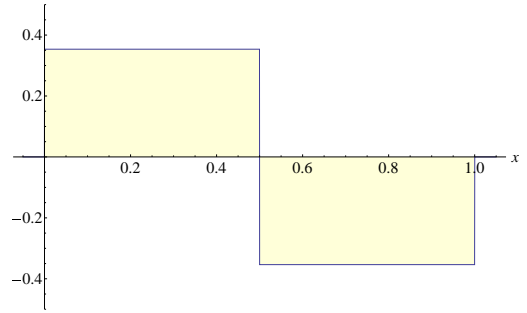
(b) Haar function of $h_1(x)$
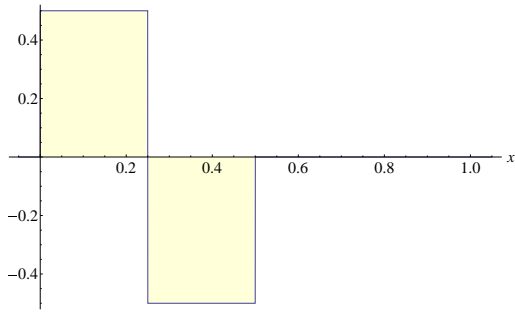
(c) Haar function of $h_2(x)$
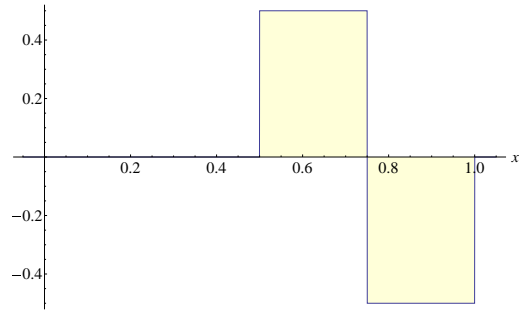
(d) Haar function of $h_3(x)$
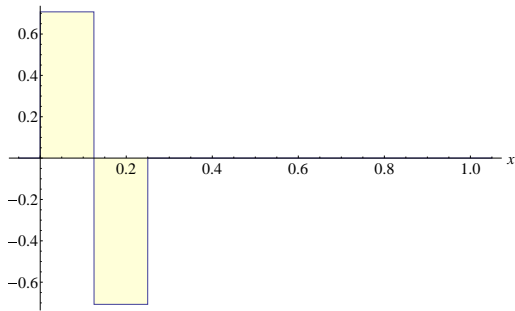
(e) Haar function of $h_4(x)$
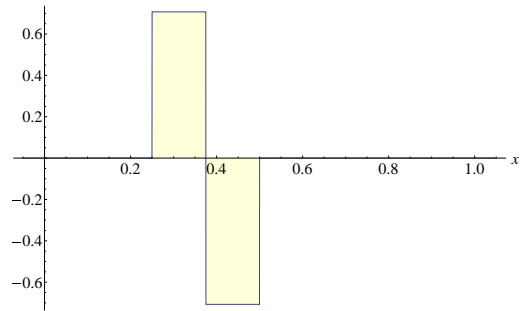
(f) Haar function of $h_5(x)$
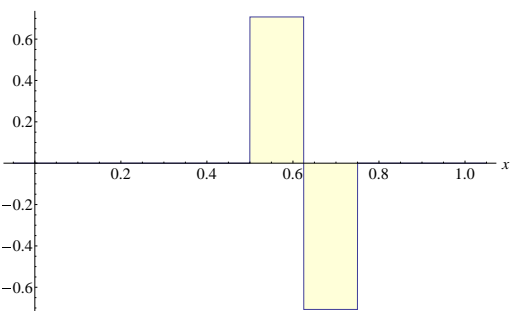
(g) Haar function of $h_6(x)$
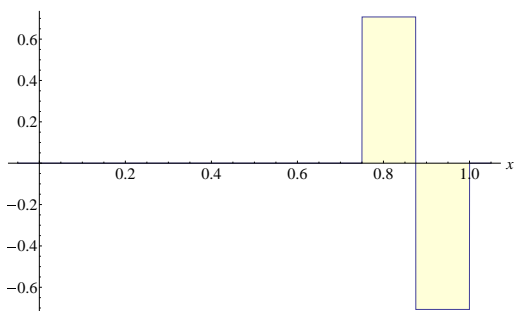
(h) Haar function of $h_7(x)$

Figure 3.3: First eight Haar functions

3.3 Haar Series Expansion

As for Haar series expansion, any function $f(x) \in L^2([0, X))$ can be decomposed into Haar series and can be written as

$$f(x) = \sum_{i=0}^{\infty} c_i h_i(x). \tag{3.11}$$

If the function $f(x)$ may be approximated as a piecewise constant, then the sum in Eqn. (3.11) may be truncated after m terms, then it becomes

$$f_m(x) \approx \sum_{i=0}^{m-1} c_i h_i(x). \tag{3.12}$$

Haar wavelet coefficient, c_i can be easily determined. Suppose $\{h_i(x)\}$ is an orthogonal set of functions on an interval $[0, X)$. It is possible to determine a set of coefficients c_i, where $i = 0, 1, 2, \ldots$, for which

$$f(x) = c_0 h_0(x) + c_1 h_1(x) + \cdots + c_n h_n(x) + \cdots \tag{3.13}$$

the coefficient c_i can be determined by utilizing the inner product in Eqn. (3.7). Multiplying Eqn. (3.13) by $h_p(x)$ and integrating over the interval $[0, X)$ gives

$$\begin{aligned}
\int_0^X f(x) h_p(x) dx &= c_0 \int_0^X h_0(x) h_p(x) dx + c_1 \int_0^X h_1(x) h_p(x) dx + \\
&\quad \cdots + c_n \int_0^X h_n(x) h_p(x) dx + \cdots \\
&= c_0 (h_0, h_p) + c_1 (h_1, h_p) + \cdots + c_n (h_n, h_p) + \cdots
\end{aligned} \tag{3.14}$$

By orthogonality, each term on the right-hand side of the last equation is zero except when $p = n$. In this case we have

$$\int_0^X f(x) h_n(x) dx = c_n \int_0^X h_n^2(x) dx. \tag{3.15}$$

It follows that the required coefficients are

$$c_n = \frac{\int_0^X f(x)h_n(x)dx}{\int_0^X h_n^2(x)dx}, \quad n = 0, 1, 2, \ldots \tag{3.16}$$

in other words, we can rewrite as

$$c_n = \frac{\int_0^X f(x)h_n(x)dx}{\|h_n(x)\|^2}, \quad n = 0, 1, 2, \ldots \tag{3.17}$$

where we know from Eqn. (3.9) that the norm, $\|h_n(x)\|^2 = \dfrac{X}{m}$, therefore the Haar wavelet coefficient become

$$c_n = \frac{m}{X} \int_0^X f(x)h_n(x)dx, \quad n = 0, 1, 2, \ldots \tag{3.18}$$

Thus, any function $f(x)$ which is square integrable within interval $0 \leq x < X$, the Haar wavelet coefficient in Eqn. (3.12) can be determined as

$$c_i = \frac{m}{X} \int_0^X f_m(x)h_i(x)dx. \tag{3.19}$$

If $f(x)$ and $f_m(x)$ in Eqn. (3.12) are the exact and approximate solution, respectively, then the corresponding error is defined as follows

$$e_m(x) = f(x) - f_m(x) \tag{3.20}$$

According to Saeedi et al. (2011), they have shown that the square of the error norm for Haar wavelet approximation has order of accuracy one, or in other words, it is first-order accurate.

$$\|e_m(x)\| = O\left(\frac{1}{m}\right). \tag{3.21}$$

From Eqn. (3.21), it is clear that the error is inversely proportional to the level resolution of Haar wavelet function. This implies that Haar wavelet approximation method will be convergent as m goes to infinity.

3.4 Haar Wavelet Matrix, $\mathbf{H}_m$

As per say Eqn. (3.12) can be expressed in matrix form as

$$f_m(x) = \mathbf{c}_m^t \mathbf{h}_m(x) \tag{3.22}$$

where Haar coefficient vector, $\mathbf{c}_m^t$ and Haar function vector, $\mathbf{h}_m(x)$ are defined as

$$\mathbf{c}_m^t = \begin{bmatrix} c_0 & c_1 & \cdots & c_{m-1} \end{bmatrix} \tag{3.23}$$

and

$$\mathbf{h}_m(x) = \begin{bmatrix} h_0(x) & h_1(x) & \cdots & h_{m-1}(x) \end{bmatrix}^t. \tag{3.24}$$

The superscript t denotes the transpose and the subscript m denotes the dimension of vectors and matrices. Taking the collocation points as following

$$x_j = \frac{2j-1}{2m} X, \quad j = 1, 2, \cdots, m \tag{3.25}$$

and defined m square Haar wavelet matrix, $\mathbf{H}_m$ as

$$\mathbf{H}_m = [H_{ij}] \tag{3.26}$$

where $H_{ij} = h_i(x_j)$.

For instance, the fourth order Haar wavelet matrix, $\mathbf{H}_4$ in the interval of

$0 \leq x < 8$ can be represented in matrix form as below:

$$\mathbf{H}_4 = \begin{bmatrix} h_0(1) & h_0(3) & h_0(5) & h_0(7) \\ h_1(1) & h_1(3) & h_1(5) & h_1(7) \\ h_2(1) & h_3(3) & h_2(5) & h_2(7) \\ h_3(1) & h_3(3) & h_3(5) & h_3(7) \end{bmatrix}$$

(3.27)

$$= \begin{bmatrix} 1/2 & 1/2 & 1/2 & 1/2 \\ 1/2 & 1/2 & -1/2 & -1/2 \\ 1/\sqrt{2} & -1/\sqrt{2} & 0 & 0 \\ 0 & 0 & 1/\sqrt{2} & -1/\sqrt{2} \end{bmatrix}$$

(3.28)

While the eight order of Haar wavelet matrix in the same interval as above can be written as below.

$$\mathbf{H}_8 = \begin{bmatrix} 1/\sqrt{8} & 1/\sqrt{8} & 1/\sqrt{8} & 1/\sqrt{8} & 1/\sqrt{8} & 1/\sqrt{8} & 1/\sqrt{8} & 1/\sqrt{8} \\ 1/\sqrt{8} & 1/\sqrt{8} & 1/\sqrt{8} & 1/\sqrt{8} & -1/\sqrt{8} & -1/\sqrt{8} & -1/\sqrt{8} & -1/\sqrt{8} \\ 1/2 & 1/2 & -1/2 & -1/2 & 0 & 0 & 0 & 0 \\ 0 & 0 & 0 & 0 & 1/2 & 1/2 & -1/2 & -1/2 \\ 1/\sqrt{2} & -1/\sqrt{2} & 0 & 0 & 0 & 0 & 0 & 0 \\ 0 & 0 & 1/\sqrt{2} & -1/\sqrt{2} & 0 & 0 & 0 & 0 \\ 0 & 0 & 0 & 0 & 1/\sqrt{2} & -1/\sqrt{2} & 0 & 0 \\ 0 & 0 & 0 & 0 & 0 & 0 & 1/\sqrt{2} & -1/\sqrt{2} \end{bmatrix}$$

(3.29)

In general, it can be shown that $\mathbf{H}_m$ is an orthogonal matrix (Artisham, 2012). That is the reason why the factor $1/\sqrt{m}$ is inserted in the Haar basis function, Eqns. (3.3), (3.4) and (3.5). This relation implies that the inverse of Haar wavelet matrix is equal to its transpose.

$$\mathbf{H}_m^{-1} = \mathbf{H}_m^t.$$

(3.30)

24

This relationship makes the inverse of Haar wavelet matrix easy to be computed, since computing transpose operation is much simpler than computing an inverse. Particularly, in the hybrid numerical method in Chapter 4, a bigger Haar wavelet matrix is needed. Additionally, $\mathbf{H}_m^{-1}$ and $\mathbf{H}_m^t$ contains many zeros. As m value increases, zeros element in the matrix also increases as can be seen in Eqn. (3.28) and Eqn. (3.29). This factor leads to a faster computation and is one of the reason for rapid convergence of the Haar wavelet series. Hsiao (2004) shows that number of multiplications operation involves in Haar transform is much easier and faster than fast Fourier transform and Walsh transform.

The relative connection between the Haar function vector and block pulse function vector, $\mathbf{b}_m(x)$ is given by Eqn. (3.31).

$$\mathbf{h}_m(x) = \mathbf{H}_m \mathbf{b}_m(x) \tag{3.31}$$

where $\mathbf{b}_m(x) = \begin{bmatrix} b_0(x) & b_1(x) & \cdots & b_{m-1}(x) \end{bmatrix}^t$. Block pulse function is given by

$$b_i(x) = \begin{cases} 1 & \dfrac{(i-1)}{m}X \le x < \dfrac{i}{m}X, \\ 0 & \text{elsewhere,} \end{cases} \tag{3.32}$$

for $i = 0, 1, 2, \ldots, m-1$ and similarly at collocation points as Eqn. (3.25). The m square block pulse matrix, $\mathbf{B}_m$ is an identity matrix since $b_i(x_j) = \delta_{ij}$ where δ_{ij} is a unit step function.

$$\delta_{ij} = \begin{cases} 1 & i = j, \\ 0 & i \ne j. \end{cases} \tag{3.33}$$

For instance, the first four block pulse matrix ($m = 4$) is shown as below.

$$\mathbf{B}_4 = \begin{bmatrix} 1 & 0 & 0 & 0 \\ 0 & 1 & 0 & 0 \\ 0 & 0 & 1 & 0 \\ 0 & 0 & 0 & 1 \end{bmatrix} \tag{3.34}$$

Using the Haar wavelet matrix, the coefficient $\mathbf{c}_m^t$ in Eqn. (3.23) can be easily obtained as

$$\mathbf{c}_m^t = \mathbf{f}_m \cdot \mathbf{H}_m^t \tag{3.35}$$

where

$$\mathbf{f}_m = \begin{bmatrix} f\left(\dfrac{X}{2m}\right) & f\left(\dfrac{3X}{2m}\right) & \cdots & f\left(\dfrac{(2m-1)X}{2m}\right) \end{bmatrix}. \tag{3.36}$$

3.5 Integration of Haar Wavelet Function and Its Operational Matrix

Wu et al. (2001) has proposed a new unified method to derive operational matrix of an orthogonal functions for integration within the interval of $0 \leq x < 1$. They applied the method to find operational matrices of square wave group function and sinusoidal group function. The former group includes block pulse function, Walsh function and Haar wavelet function while the latter includes discrete Fourier transform, discrete cosine transform and discrete Hartley transform (Wu, 2003).

In this work we derive Haar wavelet operational matrix based on Wu et al. (2001) works but using generalized block pulse function operational matrix which is derived by Kilicman and Zhour (2007). By doing this the Haar operational matrix will be in the interval of $0 \leq x < X$ instead of $0 \leq x < 1$. We name this operational matrix as generalized Haar wavelet operational matrix.

Let consider the integration of a Haar wavelet function, $\mathbf{h}_m(x)$ given by

$$\int_0^x \mathbf{h}_m(\tau)d\tau = \mathbf{Q}_m\mathbf{h}_m(x) \tag{3.37}$$

where $\mathbf{Q}_m$ is the Haar operational matrix for integration of Haar wavelet function, $\mathbf{h}_m(x)$. With Eqn. (3.31), integration of Haar wavelet function can also be written as

$$\int_0^x \mathbf{h}_m(\tau)d\tau = \int_0^x \mathbf{H}_m\mathbf{b}_m(\tau)d\tau = \mathbf{H}_m \int_0^x \mathbf{b}_m(\tau)d\tau \tag{3.38}$$

It is known that the integration of block pulse function can be calculated as below

$$\int_0^x \mathbf{b}_m(\tau)d\tau \cong \mathbf{F}_m\mathbf{b}_m(x) \tag{3.39}$$

where $\mathbf{F}_m$ is taken from generalized block pulse operational matrix for integration in the interval of $(0 \le x < X)$ (Kilicman and Zhour, 2007) .

$$\mathbf{F}_m = \frac{X}{2m} \begin{bmatrix} 1 & 2 & \cdots & 2 \\ 0 & 1 & \cdots & \vdots \\ \vdots & 0 & \ddots & 2 \\ 0 & \cdots & 0 & 1 \end{bmatrix}_{m \times m} \tag{3.40}$$

From Eqns. (3.37), (3.38) and (3.39), we obtain

$$\mathbf{Q}_m\mathbf{h}_m(x) = \mathbf{H}_m\mathbf{F}_m\mathbf{b}_m(x) \tag{3.41}$$

Taking the collocation points as Eqn. (3.25) and the fact that $\mathbf{H}_m$ is an orthogonal matrix and $\mathbf{B}_m$ is an identity matrix, we can write Eqn. (3.41) as

$$\mathbf{Q}_m\mathbf{H}_m = \mathbf{H}_m\mathbf{F}_m\mathbf{B}_m \tag{3.42}$$

$$\mathbf{Q}_m = \mathbf{H}_m\mathbf{F}_m\mathbf{H}_m^t \tag{3.43}$$

For example, the generalized Haar operational matrix when $m = 4$ and $X = 8$, from Eqn. (3.43), we will have the matrix as below

$$\mathbf{Q}_4 = \mathbf{H}_4 \mathbf{F}_4 \mathbf{H}_4^t$$

$$= \begin{bmatrix} 4 & -2 & -\dfrac{1}{\sqrt{2}} & -\dfrac{1}{\sqrt{2}} \\[2ex] 2 & 0 & -\dfrac{1}{\sqrt{2}} & \dfrac{1}{\sqrt{2}} \\[2ex] \dfrac{1}{\sqrt{2}} & \dfrac{1}{\sqrt{2}} & 0 & 0 \\[2ex] \dfrac{1}{\sqrt{2}} & -\dfrac{1}{\sqrt{2}} & 0 & 0 \end{bmatrix} \tag{3.44}$$

Besides that the generalized Haar operational matrix for integration, $\mathbf{Q}_m$ also can be obtained from the recursive formula by Chen and Hsiao (1997) after some modifications were made to cover the whole domain $[0, X)$. The generalized Haar operational matrix from recursive formula can be calculated by equation as below,

$$\mathbf{Q}_m = \frac{1}{2m} \begin{bmatrix} 2m\mathbf{Q}_{m/2} & -X\mathbf{H}_{m/2}^t \\[2ex] X\mathbf{H}_{m/2}^t & \mathbf{0}_{m/2} \end{bmatrix}. \tag{3.45}$$

The above recursive formula starts with

$$\mathbf{Q}_1 = \left[\frac{X}{2} \right]. \tag{3.46}$$

For example, in order to find $\mathbf{Q}_2$, the steps are shown as below.

$$\mathbf{Q}_2 = \frac{1}{4} \begin{bmatrix} 4\mathbf{Q}_1 & -X\mathbf{H}_1 \\[2ex] X\mathbf{H}_1^t & \mathbf{0} \end{bmatrix} \tag{3.47}$$

$$= \begin{bmatrix} \mathbf{Q}_1 & -\dfrac{X}{4}\mathbf{H}_1 \\[2ex] \dfrac{X}{4}\mathbf{H}_1^t & \mathbf{0} \end{bmatrix} \tag{3.48}$$

$$= \begin{bmatrix} \dfrac{X}{2} & -\dfrac{X}{4} \\[2ex] \dfrac{X}{4} & \mathbf{0} \end{bmatrix} \tag{3.49}$$

Following the same steps, $\mathbf{Q}_4$ can be determined as shown below.

$$\mathbf{Q}_4 = \frac{1}{8} \begin{bmatrix} 8\mathbf{Q}_2 & -X\mathbf{H}_2 \\[2mm] X\mathbf{H}_2^t & \mathbf{0}_2 \end{bmatrix} \tag{3.50}$$

$$= \begin{bmatrix} \dfrac{X}{2} & -\dfrac{X}{4} & -\dfrac{X}{8\sqrt{2}} & -\dfrac{X}{8\sqrt{2}} \\[3mm] \dfrac{X}{4} & 0 & -\dfrac{X}{8\sqrt{2}} & \dfrac{X}{8\sqrt{2}} \\[3mm] \dfrac{X}{8\sqrt{2}} & \dfrac{X}{8\sqrt{2}} & 0 & 0 \\[3mm] \dfrac{X}{8\sqrt{2}} & -\dfrac{X}{8\sqrt{2}} & 0 & 0 \end{bmatrix} \tag{3.51}$$

The generalized Haar wavelet operational matrix, $\mathbf{Q}_4$ when $X = 8$ yields

$$\mathbf{Q}_4 = \begin{bmatrix} 4 & -2 & -\dfrac{1}{\sqrt{2}} & -\dfrac{1}{\sqrt{2}} \\[3mm] 2 & 0 & -\dfrac{1}{\sqrt{2}} & \dfrac{1}{\sqrt{2}} \\[3mm] \dfrac{1}{\sqrt{2}} & \dfrac{1}{\sqrt{2}} & 0 & 0 \\[3mm] \dfrac{1}{\sqrt{2}} & -\dfrac{1}{\sqrt{2}} & 0 & 0 \end{bmatrix}. \tag{3.52}$$

The generalized Haar wavelet operational matrix, $\mathbf{Q}_4$ obtained by this recursive formula gives the same matrix as calculated using combination work of Wu et al. (2001) and Kilicman and Zhour (2007) as example shown before in Eqn. (3.44).

3.6 Repeated Integration of Haar Wavelet Function

A repeated integral is an integral taken multiple times over a single variable. It is different from a multiple integral as it consists of a number of integrals taken with respect to different variables. If we integrate the Haar wavelet function, $\mathbf{h}_m(\tau)$

twice in the interval $(0, x)$, we have

$$\int \int \mathbf{h}_m(\tau)(d\tau)^2 = \int_0^x \left(\int_0^{\tau_2} \mathbf{h}_m(\tau_1) d\tau_1 \right) d\tau_2 \tag{3.53}$$

$$\simeq \int_0^x \mathbf{Q}_m \mathbf{h}_m(\tau_2) d\tau_2 \tag{3.54}$$

$$\simeq \mathbf{Q}_m^2 \mathbf{h}_m(x). \tag{3.55}$$

Now we can extend Eqn. (3.53) to the case of n times repeated integrations, so then we have

$$\underbrace{\int_0^x \int_0^{\tau_3} \dots \int_0^{\tau_2}}_{n \text{ times}} \mathbf{h}_m(\tau_1) d\tau_1 d\tau_2 \dots d\tau_n \simeq \mathbf{Q}_m^n \mathbf{h}_m(x). \tag{3.56}$$

In Eqn. (3.56), we can see that instead of performing integration on the left side of equation, we could simply have the solution by matrix multiplication. Thus making this method is more computer-friendly as in terms of easy to programme.

CHAPTER 4

NUMERICAL ANALYSIS FOR SOLVING HYPERBOLIC HEAT CONDUCTION EQUATION IN THIN SURFACE LAYERS

4.1 Introduction

In this chapter a new method to solve partial differential equation of hyperbolic heat conduction in thin surface layers is introduced. Figure 4.1 illustrates the flow involved in establishing the new numerical method.
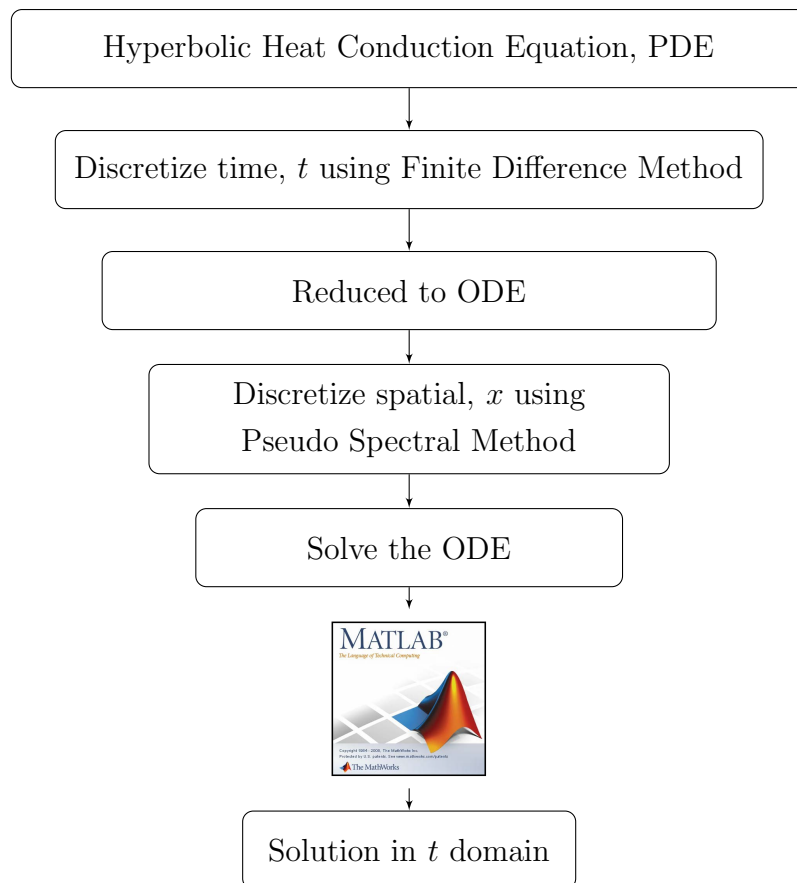
Figure 4.1: Flow of numerical analysis for solving partial differential equation of hyperbolic heat conduction equation.

4.2 Mathematical Formulation in Thin Surface Layers

With recent technology advancement in engineering application, investigating heat transfer under extreme conditions such as in extremely short period of time, in very high flux and in very low temperature is becoming important. It has been shown that under these circumstances, heat propagates with finite speed and non-Fourier effect became significant. Almost in all cases, heat will always initially encounter a thin surface layer near the solid surface when it is conducted. Therefore, for further insight on what is happening at the surface curvature during heat conduction, it is vital to establish the hyperbolic heat conduction equation together with thin surface layer coordinate.

Figure 4.2 shows the coordinate system for this problem (Kao, 1977; Chen, 2007). The $x - y$ plane forms a tangential plane at the surface point of interest. The surface of the body can be described by an equation of the form $z = f(x, y)$.
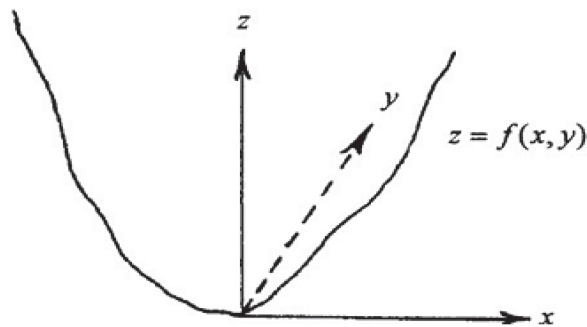
Figure 4.2: Coordinate system

The hyperbolic heat conduction equation is given by

$$\nabla^2 T = \frac{1}{C^2} \frac{\partial^2 T}{\partial t^2} + \frac{1}{\alpha} \frac{\partial T}{\partial t} \qquad (4.1)$$

where C is the propagation speed of the thermal wave and α is the thermal

diffusivity. By introducing a new independent variable $\varsigma = z - f(x,y)$, and neglecting terms of order $\left(\dfrac{\delta}{R}\right)^2$, where δ is the heat penetration length and R is the average radius of curvature at $x = 0$ and $y = 0$, Eqn. (4.1) at $x = 0$, $y = 0$ is given by

$$\frac{\partial^2 T}{\partial \varsigma^2} + \gamma \frac{\partial T}{\varsigma} = \frac{1}{C^2} \frac{\partial^2 T}{\partial t^2} + \frac{1}{\alpha} \frac{\partial T}{\partial t} \tag{4.2}$$

where

$$\gamma = \left(\frac{\partial^2 \varsigma}{\partial x^2} + \frac{\partial^2 \varsigma}{\partial y^2}\right)_{x=0,y=0} = -\left(\frac{1}{R_1} + \frac{1}{R_2}\right) \tag{4.3}$$

For convenience purposes in subsequent numerical analysis, nondimensionalized forms of the hyperbolic heat conduction equation were used, in which the following dimensionless parameters are introduced:

$$\xi = \frac{C^2 t}{2\alpha} \tag{4.4}$$

$$\eta = \frac{C\varsigma}{2\alpha} \tag{4.5}$$

$$\theta(\eta, \xi) = \frac{kC(T - T_0)}{\alpha q_r} \tag{4.6}$$

$$Q(\eta, \xi) = \frac{q}{q_r} \tag{4.7}$$

where ξ is the dimensionless time, η is the dimensionless length, θ is the dimensionless temperature, Q is the dimensionless heat flux and q_r is the reference heat flux. The resulting nondimensionalized hyperbolic heat conduction equation becomes

$$\frac{\partial^2 \theta}{\partial \xi^2} + 2\frac{\partial \theta}{\partial \xi} = \frac{\partial^2 \theta}{\partial \eta^2} + \varepsilon \frac{\partial \theta}{\partial \eta} \tag{4.8}$$

where

$$\varepsilon = \frac{2\gamma\alpha}{C}. \tag{4.9}$$

ε value gives indication whether the surface is convex or concave with value of -1

and 1 respectively. In addition, if the value of ε is 0, it indicates that the surface is being semi-infinite surface.

4.3 Numerical Analysis - Finite Difference and Haar Wavelet Operational Matrix

Consider that we have a dimensionless hyperbolic heat conduction equation as below

$$A\frac{\partial^2 \theta}{\partial \xi^2} + B\frac{\partial \theta}{\partial \xi} = C\frac{\partial^2 \theta}{\partial \eta^2} + D\frac{\partial \theta}{\partial \eta} \tag{4.10}$$

with initial conditions

$$\theta(x,0) = g_1(x) \quad , \quad \theta_\xi(x,0) = g_2(x) \tag{4.11}$$

and boundary conditions

$$\theta(0,t) = f_1(t) \quad , \quad \theta(X,t) = f_2(t). \tag{4.12}$$

Firstly we divide the dimensionless time interval, $[0,\tau)$ into N equal parts of length,

$$\Delta\xi = \frac{\tau}{N} \tag{4.13}$$

and discretize the time as

$$\xi_n = n\Delta\xi, \quad n = 0, 1, 2, \ldots, N. \tag{4.14}$$

For solving the governing Eqn. (4.10), the dimensionless time derivatives are approximated using backward finite differences as it will give stability to the method (Chen and Lin, 1993). Thus we have

$$\theta_\xi^{i+1} \approx \frac{\theta^{i+1} - \theta^i}{\Delta\xi} + O(\Delta\xi), \tag{4.15}$$

$$\theta_{\xi\xi}^{i+1} \approx \frac{\theta^{i+1} - 2\theta^i + \theta^{i-1}}{\Delta\xi^2} + O(\Delta\xi^2). \tag{4.16}$$

Substituting Eqns. (4.15) and (4.16) into Eqn. (4.10), we have

$$C\Delta\xi^2\theta_{\eta\eta}^{i+1} + D\Delta\xi^2\theta_\eta^{i+1} + (-A - B\Delta\xi)\theta^{i+1} = (-2A - B\Delta\xi)\,\theta^i + A\theta^{i-1}. \quad (4.17)$$

The partial differential equation, Eqn. (4.10), now become an ordinary differential equation. Let us consider this notation for the sake of simplicity, $\theta^{i+1}(\eta) = U(\eta, i) \equiv U(\eta)$. Therefore, Eqn. (4.17) can be rewritten as

$$aU''(\eta) + bU'(\eta) + cU(\eta) = k(\eta) \quad (4.18)$$

where $k(\eta) \equiv k(\eta, i) = d\theta^i(\eta) + e\theta^{i-1}(\eta)$ with coefficients, listed as below

$$a = C\Delta\xi^2, \quad (4.19)$$

$$b = D\Delta\xi^2, \quad (4.20)$$

$$c = (-A - B\Delta\xi), \quad (4.21)$$

$$d = (-2A - B\Delta\xi), \quad (4.22)$$

$$e = A. \quad (4.23)$$

Although Eqn. (4.17) is an implicit equation, it can however be solved quite easily using generalized Haar wavelet operational matrix method (Chen and Hsiao, 1997). Additionally, implicit method usually enjoy better stability rather than explicit method. For spatial discretization, the highest order term in Eqn. (4.18) is assumed can be expanded in terms of Haar wavelet series expansion as Eqn. (4.24).

$$U''(\eta) = \mathbf{c}^t\mathbf{h}_m(\eta) \quad (4.24)$$

By integrating Eqn. (4.24) with respect to η, we obtained $U'(\eta)$ and $U(\eta)$ in which are expressed in terms of Haar wavelet functions and the generalized Haar

operational matrix as

$$U'(\eta) = \mathbf{c}^t \mathbf{Q}_m \mathbf{h}_m(\eta) + U'(0)$$

$$= \mathbf{c}^t \mathbf{Q}_m \mathbf{h}_m(\eta) + \sqrt{m}U'(0)\Theta^t \mathbf{h}_m(\eta) \tag{4.25}$$

and

$$U(\eta) = \mathbf{c}^t \mathbf{Q}_m^2 \mathbf{h}_m(\eta) + \sqrt{m}U'(0)\Theta^t \mathbf{Q}_m \mathbf{h}_m(\eta) + U(0)$$

$$U(\eta) = \mathbf{c}^t \mathbf{Q}_m^2 \mathbf{h}_m(\eta) + \sqrt{m}U'(0)\Theta^t \mathbf{Q}_m \mathbf{h}_m(\eta) + \sqrt{m}U(0)\Theta^t \mathbf{h}_m(\eta). \tag{4.26}$$

The following formula which can be derived from Eqns. (3.37) and (3.53) will be helpful for solving this boundary value problem.

$$\mathbf{Q}_m \mathbf{h}_m(X) = \frac{X}{\sqrt{m}}\Theta_m \tag{4.27}$$

and

$$\mathbf{Q}_m^2 \mathbf{h}_m(X) = \frac{X}{\sqrt{m}}\Lambda_m \tag{4.28}$$

where

$$\Theta_m^t = \left[X, 0, 0, \ldots, 0\right], \tag{4.29}$$

$$\Lambda_m^t = \left[\frac{X}{2}, \frac{X}{2^2}, \frac{X}{2^{7/2}}, \ldots, \ldots, \ldots\right]. \tag{4.30}$$

In general Λ_m^t is same as the first column of generalized Haar wavelet operational matrix, $\mathbf{Q}_m$. These terms $\mathbf{Q}_m \mathbf{h}_m(\eta)$ and $\mathbf{Q}_m^2 \mathbf{h}_m(\eta)$ are appeared in Eqns. (4.25) and (4.26).

$U'(0)$ appeared in Eqns. (4.25) and (4.26) can be determined using boundary conditions in Eqns. (4.12). The boundary conditions with the new notation will be as follows:

$$U(0) = f_1(t) \quad , \quad U(X) = f_2(t). \tag{4.31}$$

Substituting Eqn. (4.31) into Eqn. (4.26), yields

$$U(X) = \mathbf{c}^t \mathbf{Q}_m^2 \mathbf{h}_m(X) + \sqrt{m} U'(0) \Theta^t \mathbf{Q}_m \mathbf{h}_m(X) + \sqrt{m} U(0) \Theta^t \mathbf{h}_m(X) \qquad (4.32)$$

$$f_2(t) = \mathbf{c}^t \frac{X}{\sqrt{m}} \Lambda_m + \sqrt{m} U'(0) \Theta^t \frac{X}{\sqrt{m}} \Theta_m + f_1(t). \qquad (4.33)$$

By further simplification, we can determine $U'(0)$ as follows

$$U'(0) = \frac{1}{X} \left(f_2(t) - f_1(t) - \frac{X}{\sqrt{m}} \mathbf{c}^t \Lambda_m \right). \qquad (4.34)$$

We consider the collocation points as mentioned in Eqn. (3.25). Substituting Eqns. (4.24), (4.25) and (4.26) with $U'(0)$ into Eqn. (4.18), we obtain

$$\mathbf{c}^t \left[a \mathbf{I}_m + b \mathbf{Q}_m + c \mathbf{Q}_m^2 \right] = \mathbf{k}^t - \sqrt{m} \left[b U'(0) \Theta^t + c U'(0) \Theta^t \mathbf{Q}_m + \sqrt{m} U(0) \Theta^t \right] \quad (4.35)$$

where $\mathbf{I}_m$ is an identity matrix and $\mathbf{k}^t$ can be obtained using Eqn. (3.35). The calculation is started out by using initial condition information. From Eqn. (4.35), Haar wavelet coefficients, $\mathbf{c}^t$ can be calculated provided that the matrix, on the left side of Eqn. (4.35), $\left[a \mathbf{I}_m + b \mathbf{Q}_m + c \mathbf{Q}_m^2 \right]$ is non-singular. The final solution of Eqn. (4.8) will be solved iteratively using Eqn. (4.17).

This method has been applied to solve general equation of one-dimensional wave equation with initial and boundary conditions. Details can be seen in Appendix D.

4.4 Numerical Results and Discussion

In this section, we applied the proposed method to solve hyperbolic heat conduction equation in thin surface layers problem. Eqn. (4.8) will be solved with given two sets of boundary and initial conditions. All the computations were carried out using MATLAB®.

4.4.1 Example 1 - Prescribed Wall Temperature

For this case, the dimensionless boundary conditions is given by

$$\theta(0, \xi) = 1 \quad \text{and} \quad \theta(\eta \to \infty, \xi) = 0. \tag{4.36}$$

While the initial conditions is given by

$$\theta(\eta, 0) = 0 \quad \text{and} \quad \frac{\partial \theta}{\partial \xi}(\eta, 0) = 0. \tag{4.37}$$

The new notation as Eqn. (4.31) for boundary conditions in this case are

$$U(0) = 1 \quad \text{and} \quad U(\infty) = 0. \tag{4.38}$$

First we solve Eqn. (4.18) with boundary conditions in Eqn. (4.38). $U'(0)$ in Eqn. (4.35) in this case is unknown and can be found by utilizing the given boundary condition in Eqn. (4.38). Let say X is the value in dimensionless length domain that is sufficiently approaching ∞. Using Eqn. (4.26)

$$U(X) = \mathbf{c}^t \mathbf{Q}_m^2 \mathbf{h}_m(X) + \sqrt{m} U'(0) \Theta^t \mathbf{Q}_m \mathbf{h}_m(X) + \sqrt{m} U(0) \Theta^t \mathbf{h}_m(X), \tag{4.39}$$

we have $U'(0)$, as

$$U'(0) = -\frac{1}{X} - \frac{1}{\sqrt{m}} \mathbf{c}^t \Lambda_m. \tag{4.40}$$

Substituting Eqn. (4.40) into Eqns. (4.24), (4.25) and (4.26), and and rearranging Eqn. (4.18), we obtain

$$\mathbf{c}^t \left[a\mathbf{I}_m + b\mathbf{Q}_m - b\Lambda_m \Theta^t - c\mathbf{Q}_m^2 - c\Lambda_m \Theta^t \mathbf{Q}_m \right] =$$
$$\mathbf{k}^t + \left[b\frac{\sqrt{m}}{X}\Theta^t + c\frac{\sqrt{m}}{X}\Theta^t \mathbf{Q}_m - c\sqrt{m}\Theta^t \right]. \tag{4.41}$$

The Haar wavelet coefficients, $\mathbf{c}^t$ are calculated by solving Eqn. (4.41) provided that matrix in the left side of the equation is non-singular. Finally, the solution

for dimensionless temperature is given by

$$U(\eta) = \mathbf{c}^t \left[\mathbf{Q}_m^2 - \Lambda_m \Theta^t \mathbf{Q}_m \right] \mathbf{h}_m(\eta) - \frac{\sqrt{m}}{X} \Theta^t \mathbf{Q}_m \mathbf{h}_m(\eta). \qquad (4.42)$$

Analytic solution for this case is given by Kao (1977),

$$\theta(\eta, \xi) = e^{-\frac{\eta}{2}\varepsilon} \left\{ e^{-\eta} + \left(1 - \frac{\varepsilon^2}{4} \right)^{\frac{1}{2}} \right.$$

$$\left. \eta \int_\eta^\xi e^{-\tau} \frac{I_1 \left\{ \left[\left(1 - \frac{\varepsilon^2}{4} \right) (\tau^2 - \eta^2) \right]^{\frac{1}{2}} \right\}}{(\tau^2 - \eta^2)} d\tau \right\} U(\xi - \eta). \quad (4.43)$$

Figure 4.3 illustrates the dissipation behaviour for present numerical solution with $m = 2^9$ for $\varepsilon = 0$ at various dimensionless time $\xi = 0.5$, 1.0, 1.5 and 2.0, against analytical solution. From the figure we can clearly see that the solution of present numerical results, dissipate before and after the wave front. However there is no numerical oscillations propagate either in front or behind of wave front as the virtue of backward finite difference scheme (Carey and Tsai, 1982).

This dissipative nature is contributed by the first order accuracy in the Eqn. (4.15) which is dominant than the dissipation errors by second order accuracy in Eqn. (4.16). If dissipation errors by second order accuracy become dominant, it will always be associated with the dispersion behaviour and can be observed by numerical oscillations in the resultant solution (Tannehill et al., 1997). Thus we could only see the dissipative behaviour in these solutions.

Noted that $\varepsilon = 0$ will give the solution of the hyperbolic heat conduction equation for a semi-infinite medium. This has been shown by Baumeister and Hamill (1969) and reported by Chen and Lin (1993). Figure 4.3 is almost identical with Figure 1 in (Chen and Lin, 1993) with 11 nodes. They further improve the

accuracy by increasing the nodes up to 101 nodes and had shown that it could produce better results.
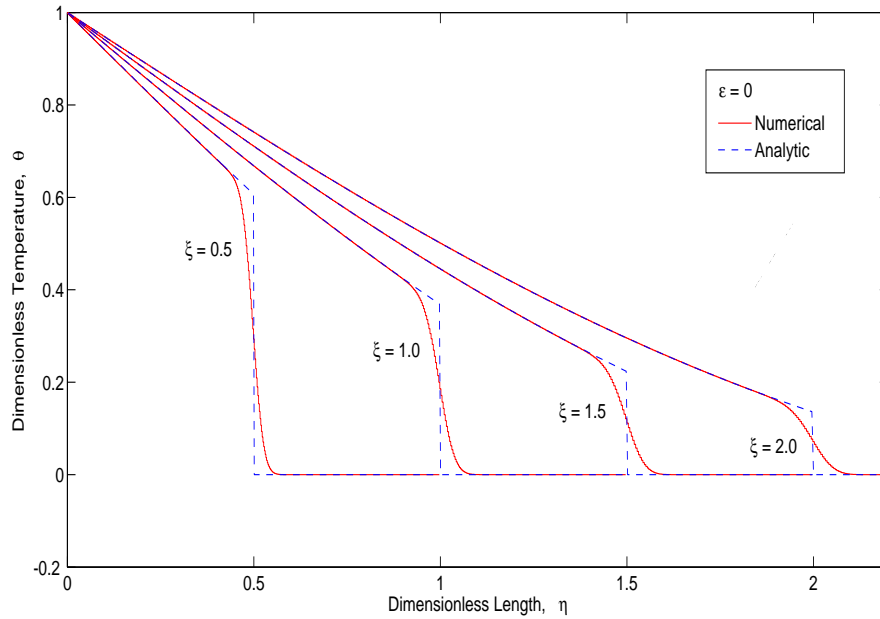
Figure 4.3: Present numerical solutions and analytical solutions when $\varepsilon = 0$ at $\xi = 0.5$, $\xi = 1.0$, $\xi = 1.5$ and $\xi = 2.0$ with $m = 2^9$ and $\Delta\xi = 0.001$

Table 4.1 shows the comparison of dimensionless temperature, θ for prescribed wall temperature with $m = 2^9$ and $\Delta\xi = 0.001$ at different dimensionless time, $\xi = 0.5$ and $\xi = 1.0$ with three ε values, $\varepsilon = -0.1$, $\varepsilon = 0$ and $\varepsilon = 0.1$ between present numerical solution obtained by Eqn. (4.42) and the analytical solution given by Eqn. (4.43). It can be seen from Table 4.1 that absolute error are small for all collocation points between numerical and exact solution except in the vicinity of sharp

continuity, around $\eta = 511/2m$ when $\xi = 0.5$ and $\eta = 717/2m$ when $\xi = 1.0$. Results obtained in the present numerical solution has a good agreement with analytic solution except in the neighbourhood of jump discontinuity.

The results differences in the vicinity of jump continuities can be explained by

dissipative behaviour that is noticeable in Figure 4.3. This dissipative behaviour is associated with the numerical dissipation resulted by truncation errors from backward finite difference discretization for time domain used in the present numerical method which originated from terms in Eqns. (4.15) and (4.16).

Table 4.1: Comparison between the present numerical solution and exact solution for prescribed wall temperature with $m = 2^9$ and $\Delta\xi = 0.001$

$\eta(/2m)$	$\varepsilon = -0.1$			$\varepsilon = 0$			$\varepsilon = 0.1$		
	Haar	Exact	Error*	Haar	Exact	Error*	Haar	Exact	Error*
$\xi = 0.5$									
1	0.9993	0.9993	0.000	0.9992	0.9992	0.000	0.9992	0.9992	0.000
103	0.9240	0.9240	0.000	0.9194	0.9194	0.000	0.9148	0.9148	0.000
205	0.8484	0.8484	0.000	0.8400	0.8400	0.000	0.8316	0.8316	0.000
309	0.7712	0.7713	0.000	0.7597	0.7598	0.000	0.7483	0.7483	0.000
411	0.6959	0.6959	0.000	0.6821	0.6821	0.000	0.6685	0.6685	0.000
511	0.3234	0.6226	0.299	0.3154	0.6073	0.292	0.3076	0.5923	0.285
615	0.0000	0.0000	0.000	0.0000	0.0000	0.000	0.0000	0.0000	0.000
717	0.0000	0.0000	0.000	0.0000	0.0000	0.000	0.0000	0.0000	0.000
821	0.0000	0.0000	0.000	0.0000	0.0000	0.000	0.0000	0.0000	0.000
923	0.0000	0.0000	0.000	0.0000	0.0000	0.000	0.0000	0.0000	0.000
1023	0.0000	0.0000	0.000	0.0000	0.0000	0.000	0.0000	0.0000	0.000
$\xi = 1.0$									
1	0.9991	0.9991	0.000	0.9990	0.9990	0.000	0.9989	0.9989	0.000
103	0.9052	0.9052	0.000	0.8985	0.8985	0.000	0.8916	0.8916	0.000
205	0.8108	0.8108	0.000	0.7988	0.7989	0.000	0.7868	0.7868	0.000
309	0.7148	0.7148	0.000	0.6990	0.6990	0.000	0.6832	0.6832	0.000
411	0.6219	0.6220	0.000	0.6036	0.6037	0.000	0.5856	0.5856	0.000
511	0.5328	0.5329	0.000	0.5134	0.5134	0.000	0.4944	0.4944	0.000
615	0.4426	0.4431	0.001	0.4232	0.4237	0.001	0.4045	0.4050	0.000
717	0.0198	0.0000	0.020	0.0188	0.0000	0.019	0.0178	0.0000	0.018
821	0.0000	0.0000	0.000	0.0000	0.0000	0.000	0.0000	0.0000	0.000
923	0.0000	0.0000	0.000	0.0000	0.0000	0.000	0.0000	0.0000	0.000
1023	0.0000	0.0000	0.000	0.0000	0.0000	0.000	0.0000	0.0000	0.000

*$Absolute\ Error = \mid \theta_{exact} - \theta_{numerical} \mid$
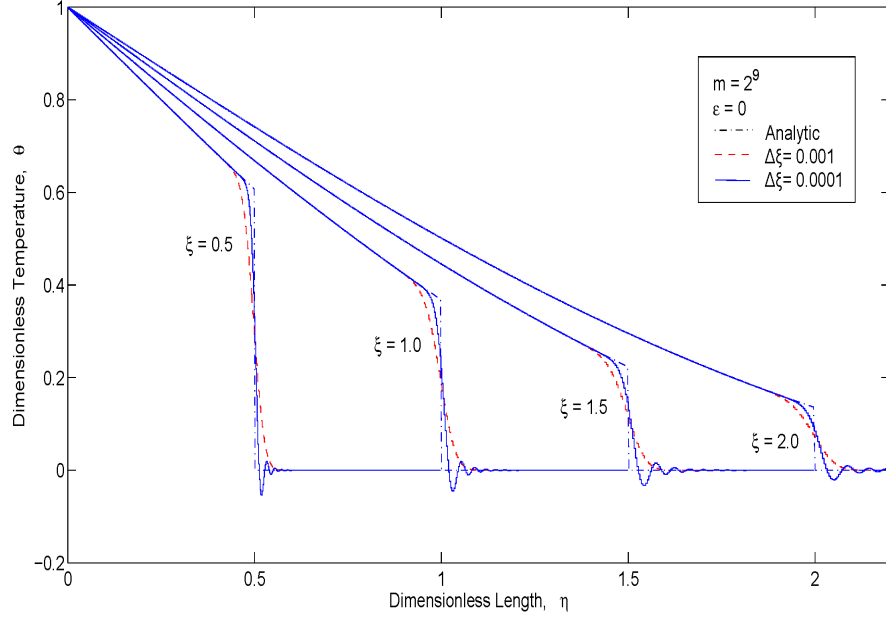
Figure 4.4: The dissipation and dispersion errors in the present numerical solution when $m = 2^9$, $\varepsilon = 0$ with $\Delta\xi = 0.001$ and $\Delta\xi = 0.0001$ at $\xi = 0.5$, $\xi = 1.0$, $\xi = 1.5$ and $\xi = 2.0$

The dissipative and dispersive nature in the present numerical results are shown in Figure 4.4 for prescribed wall temperature for $\Delta\xi = 0.001$ and $\Delta\xi = 0.0001$ when $m = 2^9$ and $\varepsilon = 0$. Numerical results for $\Delta\xi = 0.0001$ has less dissipation than $\Delta\xi = 0.001$, however numerical oscillations started propagating after the wave front, similar to Gibbs-like phenomenon and converge to the analytic solution as η increases. These numerical oscillations are only restricted in the neighborhood after the sharp continuity. Apart from the wave front, the numerical solution is approximately equal to the analytical solution. This ability of wavelet method to keep numerical oscillations only in the vicinity of sharp continuities has been observed by Avudainayagam and Vani (1999).

However, numerical result in Fig. 4.4 has caught our attention in which

numerical oscillations are not supposed to appear when dealing with Haar wavelet analysis. It has been theoretically proven that Haar wavelet basis does not exhibit numerical oscillations near the jump discontinuity at any points (Raeen, 2008; Kelly, 1996). From this knowledge, it affirms us that the numerical oscillations we were experiencing is an outcome from the usage of finite difference method for time discretization. Numerical oscillations occurred in the solution are due to inadequate number of points within the range of sharp discontinuity which is insufficient to precisely compute the large gradient that leads to accumulated errors. This bring to a conclusion that in order to have better numerical solution without numerical oscillation in the vicinity of sharp continuities, we need to add more points in this area. Sufficient number of points to avoid numerical oscillations can be achieved by decreasing $\Delta\xi$ value and increasing Haar wavelet resolution, the m value.
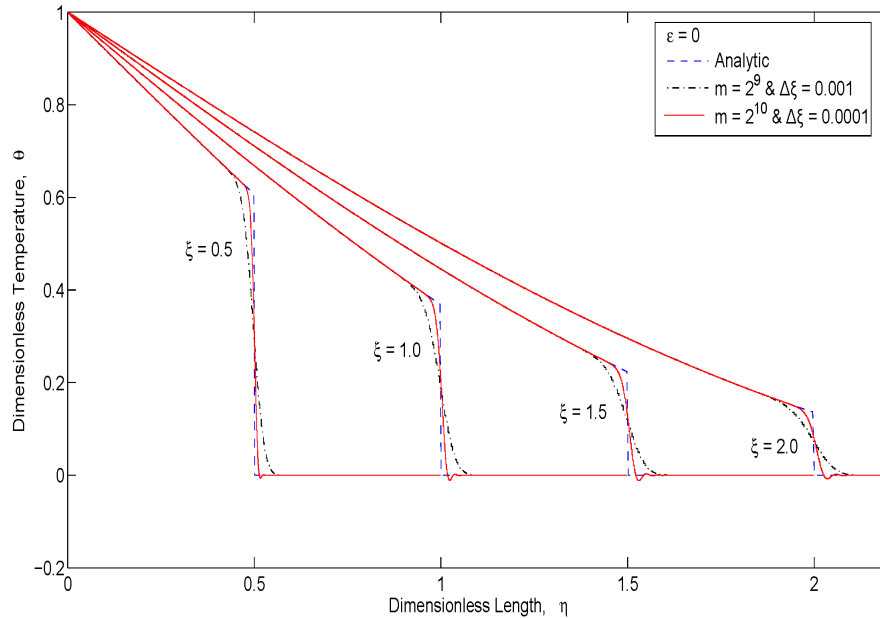
Figure 4.5: Comparison between $m = 2^9$, $\Delta\xi = 0.001$ and $m = 2^{10}$, $\Delta\xi = 0.0001$ for $\varepsilon = 0$ at $\xi = 0.5$, $\xi = 1.0$, $\xi = 1.5$ and $\xi = 2.0$

In Figure 4.5, it can be seen that the numerical oscillations at wave front is suppressed with $m = 2^{10}$ and $\Delta\xi = 0.0001$ as compared to $m = 2^9$ and $\Delta\xi = 0.0001$ in Figure 4.4 . We can see also that by changing $\Delta\xi$ value from 0.001 to 0.0001, the numerical solution is dissipate less and is much closer to analytical solution especially in the vicinity of jump discontinuities. Although numerical results with $m = 2^{10}$ and $\Delta\xi = 0.0001$ are closer to analytical solution around jump discontinuity neighbourhood, relatively small overshoots are still exist at the wave front. We need to have more points here by increasing the amount of Haar wavelet level, thus we proceed with $m = 2^{11}$.
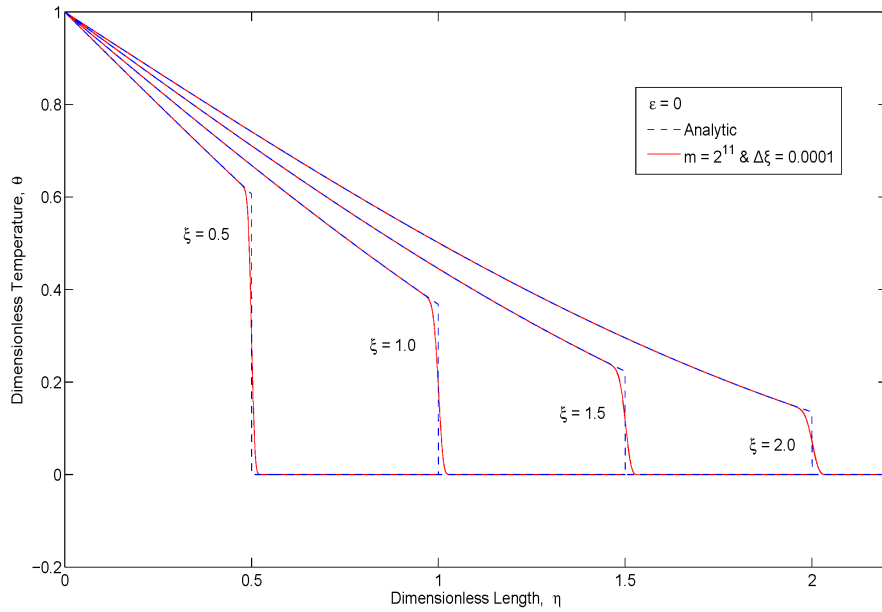
Figure 4.6: Comparison between numerical solution with $m = 2^{11}$, $\Delta\xi = 0.0001$ and analytical solution for $\varepsilon = 0$ at $\xi = 0.5$, $\xi = 1.0$, $\xi = 1.5$ and $\xi = 2.0$

In Figure 4.6 the numerical solutions at the wave front is totally eliminated by increasing Haar wavelet resolution, $m = 2^{11}$ with $\Delta\xi = 0.0001$. In addition, the numerical results is dissipate less compared to numerical results with $m = 2^9$

and $\Delta\xi = 0.001$ (Figure 4.4). This means that numerical results gained by this combination are nearer to the analytical solutions.
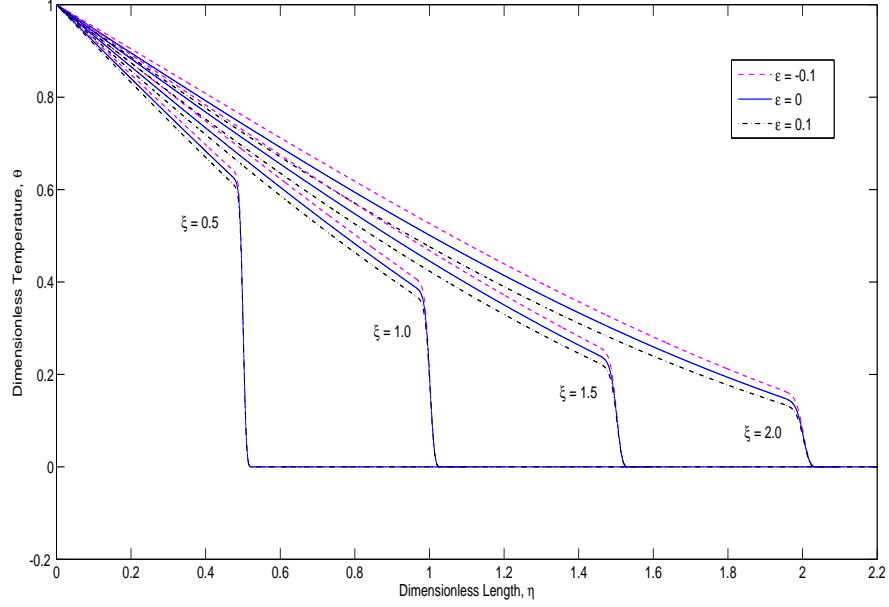
Figure 4.7: The effect on the surface curvature of non-Fourier heat conduction equation with prescribed wall temperature.

Figure 4.7 shows the influence of the surface curvature of a solid body on non-Fourier heat conduction effect with a prescribed wall temperature. The curvature will increase or decrease the dimensionless temperature of the wave front, depending on whether the surface is either concave or convex. The present numerical solution in Figure 4.7 is almost identical with solution obtained by Chen (2007) which is presented in Figure 2 in the paper.

4.4.2 Example 2 - Prescribed in a Finite Slab

With prescribed in a finite slab, the boundary conditions is given by

$$\theta(0, \xi) \;=\; 1 \quad \text{and} \quad \frac{\partial \theta}{\partial \xi}(1, \xi) = 0, \tag{4.44}$$

and initial conditions is given by

$$\theta(\eta, 0) \;=\; 0 \quad \text{and} \quad \frac{\partial \theta}{\partial \xi}(\eta, 0) = 0. \tag{4.45}$$

As in Example 1, $U'(0)$ in Eqn. (4.35) is unknown and can be found by using information from the derivation boundary condition, $U'(1) = 0$ and $U(0) = 1$. Thus we have $U'(0)$ from Eqns. (4.25) and (4.26) as below

$$U'(1) \;=\; \mathbf{c}^t \mathbf{Q}_m \mathbf{h}_m(1) + \sqrt{m} U'(0) \Theta^t \mathbf{h}_m(1),$$

$$U'(0) \;=\; -\mathbf{c}^t \frac{1}{\sqrt{m}} \theta_m. \tag{4.46}$$

Substituting Eqns. (4.25), (4.26) and (4.46) into Eq. (4.18), we obtain

$$\mathbf{c}^t \left[a\mathbf{I}_m + b\mathbf{Q}_m - b\Theta_m\Theta^t + c\mathbf{Q}_m^2 - c\Theta_m\Theta^t\mathbf{Q}_m \right] \;=\; \mathbf{k}^t - c\sqrt{m}\Theta^t. \tag{4.47}$$

From Eqn. (4.47), the Haar wavelet coefficient can be calculated. Then the final answer for this case is given by

$$U(\eta) \;=\; \mathbf{c}^t \left[\mathbf{Q}_m^2 - \Theta_m\Theta^t\mathbf{Q}_m \right] \mathbf{h}_m(\eta) + \sqrt{m}\Theta^t\mathbf{h}_m(\eta). \tag{4.48}$$

Figure 4.8 depicts the dimensionless temperature distribution at various dimensionless time with prescribed in a finite slab for $\varepsilon = 0$ with $m = 2^9$ and $\Delta\xi = 0.001$. It shows that overshoot happened after the wave front, which was predicted from experience solving previous example.
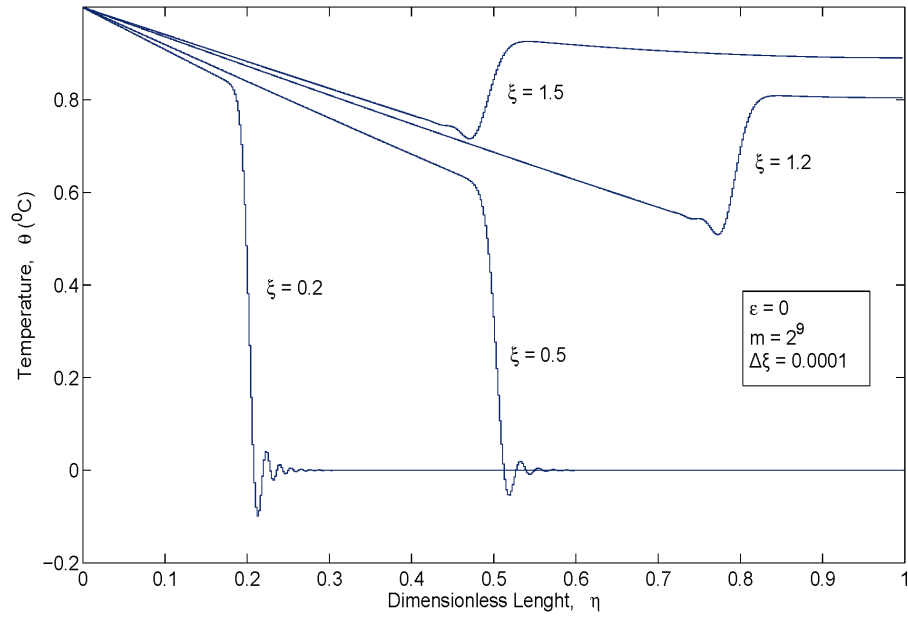
Figure 4.8: Present numerical solution for prescribed finite slab case when $\varepsilon = 0$ with $m = 2^9$ and $\Delta\xi = 0.0001$ at $\xi = 0.2$, $\xi = 0.5$, $\xi = 1.2$ and $\xi = 1.5$

Numerical oscillation could be suppressed by increasing $m = 2^{10}$ with $\Delta\xi = 0.0001$ as illustrates in Figure 4.9. Further increment in Haar wavelet level to $m = 2^{11}$ have shown total elimination of numerical oscillation as can be seen in Figure 4.10.
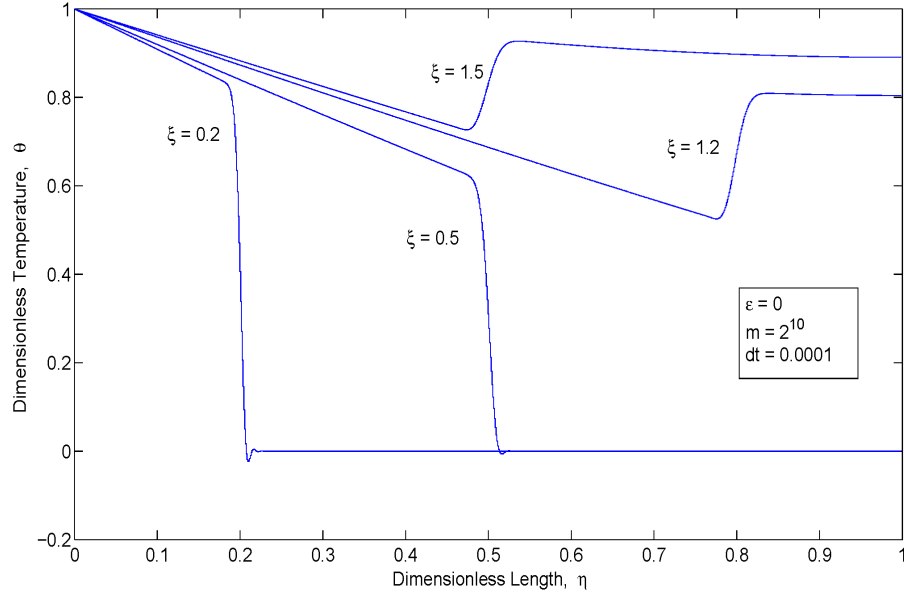
Figure 4.9: Present numerical solution for prescribed finite slab case when $\varepsilon = 0$ with $m = 2^{10}$ and $\Delta\xi = 0.0001$ at $\xi = 0.2$, $\xi = 0.5$, $\xi = 1.2$ and $\xi = 1.5$
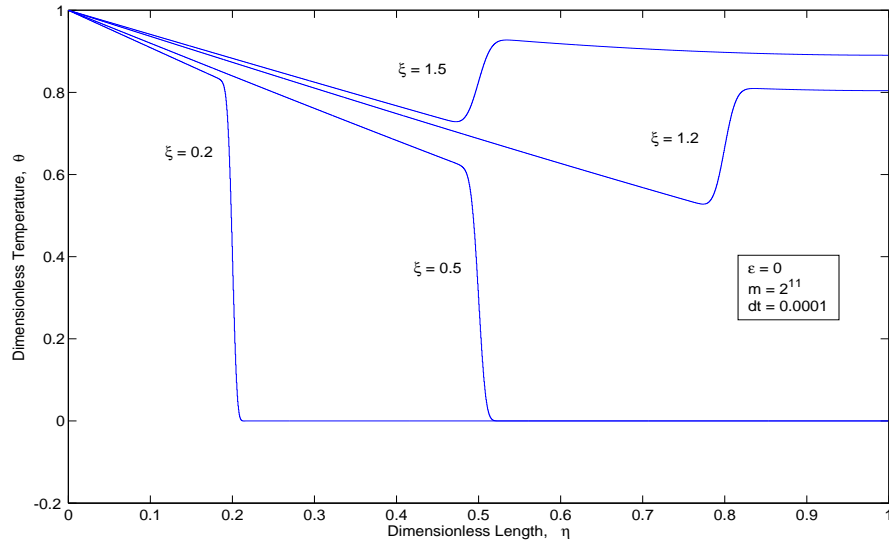
Figure 4.10: Present numerical solution for prescribed finite slab case when $\varepsilon = 0$ with $m = 2^{11}$ and $\Delta\xi = 0.0001$ at $\xi = 0.2$, $\xi = 0.5$, $\xi = 1.2$ and $\xi = 1.5$

Figure 4.11 depicts the effect of the surface curvature of a finite slab body on non-Fourier heat conduction problem with $m = 2^{10}$, $\Delta\xi = 0.0001$ at various dimensionless time. The present numerical solution in Figure 4.11 is almost

identical with solution obtained by Chen (2007) which is presented in Figure 4 in the paper.
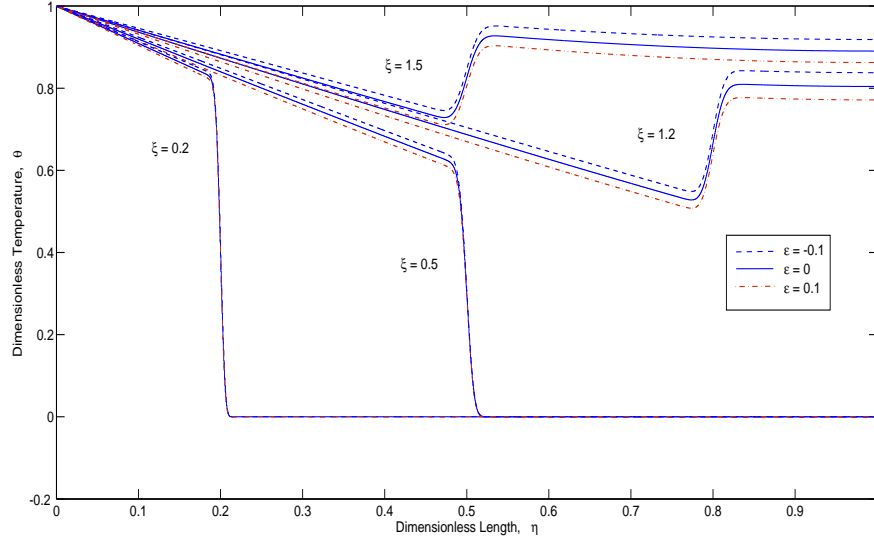
Figure 4.11: The effect of the surface curvature of a finite slab on non Fourier heat conduction problem with $m = 2^{11}$, $\Delta\xi = 0.0001$ at $\xi = 0.2$, $\xi = 0.5$, $\xi = 1.2$ and $\xi = 1.5$

4.5   Conclusion

The present numerical method solves the hyperbolic heat conduction in thin surface layers with two set of initial and boundary conditions, that is for prescribed wall temperature and prescribed in a finite slab. This new method is a combination method of finite difference and pseudo spectral Haar wavelet where the former used time discretization and the latter used spatial discretization. Results have shown that solving the hyperbolic heat conduction equation implicitly using this method could give encouraging results with $m = 2^9$, $\Delta\xi = 0.001$ and $m = 2^{11}$, $\Delta\xi = 0.0001$. Ideally the present numerical method will give more accurate results by increasing Haar wavelet resolution, m. As finite difference is being utilized, the

present numerical result has to be bounded with the effects of the Courant number (Tannehill et al., 1997). However the relationship between m and dimensionless time increment, $\Delta \xi$ is yet to be defined. This method has shown to be stable, convergent and easily coded. The practical implication of this numerical analysis is that when the non-Fourier effect is significant, the surface temperature can be instantaneously modified by the surface curvature (Kao, 1977).

CHAPTER 5

NUMERICAL ANALYSIS OF LAPLACE INVERSION WITH GENERALIZED HAAR WAVELET OPERATIONAL MATRIX

5.1 Introduction

In this chapter, numerical analysis of inverse Laplace transform using generalized Haar operational matrix is introduced. This chapter starts with the overview of Laplace transform and its inversion. Before establishing the numerical analysis of Laplace inversion using generalized Haar wavelet operational matrix, we will explain the underlying concept that leads to operational matrix usage in this work. We proved the method for the case of the transfer function using the extension of Riemann-Liouville fractional integral. Since there is an involvement of Riemann-Liouville fractional integral, we show the Riemann-Liouville fractional integral of Haar wavelet function. From this derivation, it helps us in dealing with expression that appear later in the upcoming section. Subsequently, we will show the derivation of numerical analysis of Laplace inversion base on generalized Haar wavelet operational matrix with transfer function. Numerical results and discussions are shown at the end of this chapter.

5.2 Laplace Transform and Laplace Inversion

The Laplace transform of a function $x(t)$ defined for $t \geq 0$, denoted by $X(s)$ is defined by an integral function equation as below.

$$X(s) = \mathcal{L}\big\{x(t)\big\} = \int_0^\infty e^{-st}x(t)dt \qquad (5.1)$$

In other occasion, we shall use tilde sign to indicate the Laplace transform, for example

$$\tilde{x}(s) = \mathcal{L}\big\{x(t)\big\}. \tag{5.2}$$

$X(s)$ is an integral transform,

$$X(s) = \int_0^\infty k(s,t)x(t)dt \tag{5.3}$$

with $k(s,t) = e^{-st}$ as kernel. Furthermore, the given function $x(t)$ is called the inverse transform of $X(s)$, so that we could write as

$$x(t) = \mathcal{L}^{-1}\big\{X(s)\big\}. \tag{5.4}$$

In other words, we may say $x(t)$ being the inverse transform of $X(s)$.

5.3 Laplace Inversion and Operational Matrix

Let $X(s)$ denotes the transform of a function $x(t)$ which is piecewise continuous for $t \geq 0$, then the Laplace transform of integral can be obtained as below

$$\mathcal{L}\left\{\int_0^t x(\tau)d\tau\right\} = \frac{1}{s} \cdot X(s). \tag{5.5}$$

Sufficient conditions for the validity of Eqn. (5.5) are that $x(\tau)$ be sectionally continuous and of the order $e^{\alpha t}$, that $s > \alpha$ in Eqn. (5.5) and further that the limit of $\dfrac{X(s)}{s}$ exist as $s \to +0$ (Churchill, 1958). We may represent Eqn. (5.5) as

$$\int_0^t x(\tau)d\tau = \mathcal{L}^{-1}\left\{\frac{1}{s} \cdot X(s)\right\}. \tag{5.6}$$

For division by s^n in s domain, with sufficient conditions same as above, we may express Laplace transform of n times repeated integration as

$$\mathcal{L}\left\{\underbrace{\int_0^t \ldots \int_0^{\tau_3} \int_0^2 x(\tau_1)d\tau_1 d\tau_2 \ldots d\tau_n}_{n \text{ times}}\right\} = \frac{1}{s^n} \cdot X(s) \tag{5.7}$$

where n is a whole number. Following Eqn. (5.6), we could rewrite Eqn. (5.7) in other way as below:

$$\underbrace{\int_0^t \ldots \int_0^{\tau_3} \int_0^{\tau_2}}_{n \text{ times}} x(\tau_1)d\tau_1 d\tau_2 \ldots d\tau_n \;=\; \mathcal{L}^{-1}\left\{\frac{1}{s^n}\cdot X(s)\right\} \qquad (5.8)$$

We could summarize the above equation in a table as below:

Table 5.1: Laplace transform of integral

Item	Functions (t domain)	Laplace Transforms (s domain)
1	$\int_0^t x(\tau)d\tau$	$\frac{1}{s}\cdot X(s)$
2	$\underbrace{\int_0^t \ldots \int_0^{t_3} \int_0^{t_2}}_{n \text{ times}} x(\tau_1)\,d\tau_1 d\tau_2 \ldots d\tau_n$	$\frac{1}{s^n}\cdot X(s)$

Table 5.1 shows two functions which are in t domain and its Laplace transform form in s domain. From Item 1 and Item 2, it is obvious that the integration respected to time domain is equivalent to multiplication of $1/s$ and $1/s^n$ in the s domain respectively.

Table 5.2: Integration of Haar wavelet function

Item	Functions	Integration Results
1	$\int_0^t \mathbf{h}_m(\tau)d\tau$	$\mathbf{Q}_m\mathbf{h}_m(t)$
2	$\underbrace{\int_0^t \int_0^t \cdots \int_0^t}_{n \text{ times}} \mathbf{h}_m(\tau)(d\tau)^n$	$\mathbf{Q}_m^n\mathbf{h}_m(t)$

Table 5.2 shows the integration of Haar wavelet function that appeared in Eqn. (3.37) and Eqn. (3.56). Looking at the integration of Haar wavelet function in Table 5.2 and Laplace transform of integral in Table 5.1, it can be seen that

the integration in time domain is comparable with substituting the term $1/s$ or $1/s^n$ in s domain by the generalized Haar wavelet operational matrix, $\mathbf{Q}_m$ or $\mathbf{Q}_m^n$ respectively in the corresponding matrix. In other words, the generalized Haar wavelet operational matrix performs like an integrator in the time domain and $1/s$ in s domain.

The computation of operational matrix, $\mathbf{Q}_m$ and powers of $\mathbf{Q}_m$ are easy comparatively by performing repeated integration. This property is very helpful for problems simplification.

5.4 Riemann-Liouville Fractional Integral and Haar Wavelet Function

Let us consider the below n times repeated integration of function $f(t)$ with integral operator I,

$$(I^n f)(t) = \underbrace{\int \int \ldots \int}_{n \text{ times}} f(\tau_1) d\tau_1 \ldots d\tau_n. \tag{5.9}$$

It is shown in Ross (1975) that the repeated integration with $(n-1)$ fold can be written as a single integral. Below is the generalization form for natural order integrals of function $f(t)$.

$$(I^n f)(t) = \int_0^t \frac{(t - t_n)^{n-1}}{(n-1)!} f(t_n) dt_n \tag{5.10}$$

From the definition of repeated integration of Haar wavelet function, $\mathbf{h}_m$ in Eqn. (3.56) in Chapter 3 and generalization form for natural order integration in Eqn. (5.10), we will have $(n-1)$ fold integral of Haar wavelet function as below.

$$(I^n \mathbf{h}_m)(t) \;=\; \frac{1}{(n-1)!} \int_0^t (t - t_1)^{n-1} \mathbf{h}_m(t_1) dt_1 \approx \mathbf{Q}_m^n \mathbf{h}_m(t). \tag{5.11}$$

Generalization can be made to deal with fractional integral by substituting $(n-1)!$

with Gamma function, $\Gamma(\alpha)$ (Ross, 1975) , thus Eqn. (5.11) become

$$(I^\alpha \mathbf{h}_m)(t) \;=\; \frac{1}{\Gamma(\alpha)} \int_0^t (t - t_1)^{\alpha-1} \mathbf{h}_m(t_1) dt_1 \approx \mathbf{Q}_m^\alpha \mathbf{h}_m(t). \qquad (5.12)$$

This is Riemann-Liouville fractional integral of Haar wavelet function, $\mathbf{h}_m(t)$ with integral order of $\alpha > 0$.

Some modification is necessary to accommodate with expression in finding inversion of Laplace transform later. Firstly we consider the fractional integral of Haar wavelet scaling function, $h_0(x)$ of order $\alpha > 0$ and Eqn. (5.12) is then become

$$
\begin{aligned}
(I^\alpha h_0)(t) &= \frac{1}{\Gamma(\alpha)} \int_0^t (t - t_1)^{\alpha-1} h_0(t_1) dt_1 \\
&= \frac{1}{\Gamma(\alpha)} \frac{1}{\sqrt{m}} \int_0^t (t - t_1)^{\alpha-1} dt_1 \\
&= \frac{1}{\sqrt{m}} \frac{t^\alpha}{\Gamma(\alpha+1)}.
\end{aligned} \qquad (5.13)
$$

By cross multiplying the Eqn. (5.13), it then becomes

$$
\begin{aligned}
\frac{t^\alpha}{\Gamma(\alpha+1)} &= \frac{\sqrt{m}}{\Gamma(\alpha)} \int_0^t (t - t_1)^{\alpha-1} h_0(t_1) dt_1 \\
&= \frac{\sqrt{m}}{\Gamma(\alpha)} \int_0^t (t - t_1)^{\alpha-1} \begin{bmatrix} 1 & 0 & \cdots & 0 \end{bmatrix} \mathbf{h}_m(t_1) dt_1 \\
&= \mathbf{e} \frac{1}{\Gamma(\alpha)} \int_0^t (t - t_1)^{\alpha-1} \mathbf{h}_m(t_1) \, dt_1
\end{aligned} \qquad (5.14)
$$

where $\mathbf{e} = \begin{bmatrix} \sqrt{m} & 0 & \cdots & 0 \end{bmatrix}$. Then, with Eqn. (5.12) and take collocation point as

$$t_i = \frac{2i - 1}{2m} T, \quad i = 1, 2, \cdots, m \qquad (5.15)$$

thus, Eqn. (5.14) is then becomes,

$$\frac{t^\alpha}{\Gamma(\alpha+1)} = \mathbf{e}\mathbf{Q}^\alpha \mathbf{h_m}(t). \qquad (5.16)$$

Expression in Eqn. (5.16) is very helpful during calculation to find inversion of Laplace transform later in the transfer function expression.

5.5 Laplace Inversion of Transfer Function with Generalized Haar Wavelet Operational Matrix

Let $X(s)$ be a transfer function that has a form as below:

$$X(s) = \frac{a_0 s^n + a_1 s^{n-1} + a_2 s^{n-2} + \cdots + a_n}{s^{\alpha+1}(b_0 s^n + b_1 s^{n-1} + b_2 s^{n-2} + \cdots + b_n)} \tag{5.17}$$

where $0 \leq \alpha < 1$, a and b are real numbers and is truncated to n $(n \in \mathbb{Z}^+)$. By dividing each terms in Eqn. (5.17) with s^n, the equation can be expressed in terms of $1/s$. Eqn. (5.17) can be rewritten as

$$X(s) = \frac{a_0 + \dfrac{a_1}{s} + \dfrac{a_2}{s^2} + \cdots + \dfrac{a_n}{s^n}}{s^{\alpha+1}\left(b_0 + \dfrac{b_1}{s} + \dfrac{b_2}{s^2} + \cdots + \dfrac{b_n}{s^n}\right)} \tag{5.18}$$

or

$$\hat{X}\left(\frac{1}{s}\right) = \frac{1}{s^{\alpha+1}} \frac{G_1\left(\dfrac{1}{s}\right)}{G_2\left(\dfrac{1}{s}\right)} \tag{5.19}$$

where

$$G_1\left(\frac{1}{s}\right) = a_0 + \frac{a_1}{s} + \frac{a_2}{s^2} + \cdots + \frac{a_n}{s^n} \tag{5.20}$$

and

$$G_2\left(\frac{1}{s}\right) = b_0 + \frac{b_1}{s} + \frac{b_2}{s^2} + \cdots + \frac{b_n}{s^n}. \tag{5.21}$$

By cross multiplying Eqn. (5.18), we have

$$\left(b_0 + \frac{b_1}{s} + \frac{b_2}{s^2} + \cdots + \frac{b_n}{s^n}\right) X(s) = \frac{1}{s^{\alpha+1}}\left(a_0 + \frac{a_1}{s} + \frac{a_2}{s^2} + \cdots + \frac{a_n}{s^n}\right). \tag{5.22}$$

Taking Laplace inversion of Eqn. (5.22) at both sides yields

$$b_0 x(t) + b_1 \int_0^t x(\tau)d\tau + \ldots + b_n \underbrace{\int_0^t \cdots \int_0^{\tau_3} \int_0^{\tau_2} x(\tau_1)d\tau_1 d\tau_2 \ldots d\tau_n}_{n \text{ times}} =$$

$$\frac{a_0 t^\alpha}{\Gamma(\alpha+1)} + \frac{a_1 t^{\alpha+1}}{\Gamma(\alpha+2)} + \frac{a_2 t^{\alpha+2}}{\Gamma(\alpha+3)} + \cdots + \frac{a_n t^{\alpha+n}}{\Gamma(\alpha+n+1)}. \tag{5.23}$$

Using Eqn. (5.16) and taking the collocation points as Eqn. (5.15) and factorize $\mathbf{c}_m^t$, $\mathbf{e}$ and $\mathbf{H}_m$, Eqn. (5.23) becomes

$$\mathbf{c}_m^t(b_0\mathbf{I}_m + b_1\mathbf{Q}_m + b_2\mathbf{Q}_m^2 + \cdots + b_n\mathbf{Q}_m^n)\mathbf{H}_m$$

$$= \mathbf{e}\mathbf{Q}_m^\alpha(a_0\mathbf{I}_m + a_1\mathbf{Q}_m + a_2\mathbf{Q}_m^2 + \cdots + a_n\mathbf{Q}_m^n)\mathbf{H}_m \quad (5.24)$$

where $\mathbf{e} = \begin{bmatrix} \sqrt{m} & 0 & \cdots & 0 \end{bmatrix}$. Rewrite Eqn. (5.24) with

$$g_1(\mathbf{Q}_m) = a_0\mathbf{I}_m + a_1\mathbf{Q}_m + a_2\mathbf{Q}_m^2 + \cdots + a_n\mathbf{Q}_m^n \quad (5.25)$$

and

$$g_2(\mathbf{Q}_m) = b_0\mathbf{I}_m + b_1\mathbf{Q}_m + b_2\mathbf{Q}_m^2 + \cdots + b_n\mathbf{Q}_m^n, \quad (5.26)$$

Eqn. (5.24) becomes

$$\mathbf{c}_m^t g_2(\mathbf{Q}_m) = \mathbf{e}\mathbf{Q}_m^\alpha g_1(\mathbf{Q}_m). \quad (5.27)$$

$g_1(\mathbf{Q}_m)$ and $g_2(\mathbf{Q}_m)$ are matrix functions yield by substituting $1/s$ terms with the generalized Haar wavelet operational matrix in $G_1(1/s)$ and $G_2(1/s)$ defined in Eqn. (5.20) and (5.21) respectively. Multiplying both sides with $g_2^{-1}(\mathbf{Q}_m)$, the vector coefficient, $\mathbf{c}_m^t$ can be easily calculated by multiplication of matrices as below.

$$\mathbf{c}_m^t = \mathbf{e}\mathbf{Q}_m^\alpha g_1(\mathbf{Q}_m)g_2^{-1}(\mathbf{Q}_m) \quad (5.28)$$

Once the Haar wavelet coefficient, $\mathbf{c}_m^t$ is known, the Laplace inversion of the transfer function $X(s)$ is given by

$$\mathbf{x}(t) = \mathbf{c}_m^t\mathbf{H}_m(t). \quad (5.29)$$

Substituting, the Haar coefficient, $\mathbf{c}_m^t$ calculated in Eqn. (5.28) into Eqn. (5.29), we have

$$\mathbf{x}(t) = \mathbf{e}\mathbf{Q}_m^\alpha g_1(\mathbf{Q}_m)g_2(\mathbf{Q}_m)^{-1}\mathbf{H}_m(t). \quad (5.30)$$

By introducing an identity matrix,

$$\mathbf{E} = \mathbf{Q}_m^{-1}\mathbf{H}_m(t)\mathbf{H}_m^t(t)\mathbf{Q}_m \qquad (5.31)$$

and

$$\hat{\mathbf{X}}(\mathbf{Q}_m) = \mathbf{Q}^{\alpha+1}g_1(\mathbf{Q}_m)g_2(\mathbf{Q}_m)^{-1} \qquad (5.32)$$

into Eqn. (5.30), we can rewrite as

$$\mathbf{x}(t) = \mathbf{e}\mathbf{Q}_m^{-1}\mathbf{H}_m(t)\mathbf{H}_m^t(t)\hat{\mathbf{X}}(\mathbf{Q}_m)\mathbf{H}_m(t). \qquad (5.33)$$

Taking the collocation points as Eqn. (5.15) and use Eqn. (3.43), yields

$$\mathbf{x} = \mathbf{e}\mathbf{H}_m\mathbf{F}_m^{-1}\mathbf{H}_m^t\hat{\mathbf{X}}(\mathbf{Q}_m)\mathbf{H}_m \qquad (5.34)$$

where

$$\mathbf{F}_m^{-1} = \frac{2m}{\tau}\begin{bmatrix} 1 & -2 & \cdots & -2 \\ 0 & 1 & \cdots & 2 \\ \vdots & 0 & \ddots & -2 \\ 0 & \cdots & 0 & 1 \end{bmatrix}_{m \times m} \qquad (5.35)$$

Multiplying $\mathbf{e}\mathbf{H}_m\mathbf{F}_m^{-1}$ in Eqn. (5.34), thus we have Laplace inversion as

$$\mathbf{x} = \begin{bmatrix} \dfrac{2m}{\tau} & -\dfrac{2m}{\tau} & \cdots & -\dfrac{2m}{\tau} \end{bmatrix}\mathbf{H}_m^t\hat{\mathbf{X}}(\mathbf{Q}_m)\mathbf{H}_m \qquad (5.36)$$

where $\hat{\mathbf{X}}(\mathbf{Q}_m) = \mathbf{Q}^{\alpha+1}g_1(\mathbf{Q}_m)g_2(\mathbf{Q}_m)^{-1}$ is from Eqn. (5.19) by replacing $1/s$ with

the generalized Haar operational matrix, $\mathbf{Q}_m$.

From the derivation above, finding Laplace inversion for a transfer function, it

can be concluded that numerical Laplace inversion can be easily computed by the

following steps as figure below.

```
┌─────────────────────────────────────────────────┐
│         Transfer function, X(s)                 │
└─────────────────────────────────────────────────┘
                        │
                        ▼
┌─────────────────────────────────────────────────┐
│    Express the transfer function X(s) in        │
│    terms of 1/s and denotes as X̂(1/s)           │
└─────────────────────────────────────────────────┘
                        │
                        ▼
┌─────────────────────────────────────────────────┐
│    Substitute 1/s with the generalized          │
│    Haar wavelet operational matrix, Q_m.        │
└─────────────────────────────────────────────────┘
                        │
                        ▼
┌─────────────────────────────────────────────────┐
│       Calculate the Laplace inversion by        │
│                                                 │
│  x = [2m/τ  −2m/τ  ···  −2m/τ] H^t_m X̂(Q_m)H_m │
└─────────────────────────────────────────────────┘
```
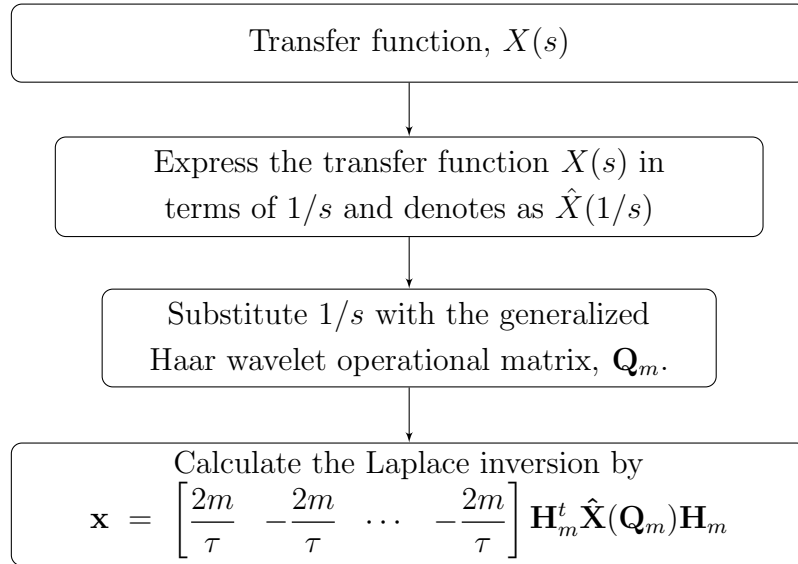
Figure 5.1: Steps of finding Laplace inversion from irrational transfer function using generalized Haar wavelet operational matrix method.

Through this method, there is no need to do integration operations. Laplace inversion can be calculated by multiplication of matrices.

5.6 Numerical Results

In this section a few examples of transfer function is solved using this method. Examples in the next section includes rational and irrational transfer function. Examples start with rational transfer function followed by irrational transfer function and exponential transfer function. Examples of initial value problem and partial differential equation of heat equation are also illustrated to demonstrate the simplicity and effectiveness of this method.

5.6.1 Rational Transfer Function

5.6.1.1 Example 1

Find the Laplace inversion for rational transfer function

$$X(s) = \frac{1}{s^2 + 1}. \qquad (5.37)$$

Expressing Eqn. (5.37) in terms of $1/s$, we have

$$\hat{X}\left(\frac{1}{s}\right) = \frac{1}{s^2} \frac{1}{1 + \left(\dfrac{1}{s}\right)^2}. \qquad (5.38)$$

Substituting $1/s$ terms with generalized Haar operational matrix, $\mathbf{Q}_m$, it becomes

$$\hat{\mathbf{X}}(\mathbf{Q}_m) = \mathbf{Q}_m^2 (\mathbf{I}_m + \mathbf{Q}_m^2)^{-1}. \qquad (5.39)$$

The inversion of Laplace transform with $\tau = 10$ and $m = 64$ is given by

$$\mathbf{x} = \begin{bmatrix} \dfrac{128}{10} & -\dfrac{128}{10} & \cdots & -\dfrac{128}{10} \end{bmatrix}_{1 \times 64} \cdot \mathbf{H}_{64}^t \cdot \mathbf{Q}_{64}^2 (\mathbf{I}_{64} + \mathbf{Q}_{64}^2)^{-1} \cdot \mathbf{H}_{64}. \qquad (5.40)$$

Analytical solution for Eqn. (5.37) is

$$\mathcal{L}^{-1}\left(\frac{1}{s^2 + 1}\right) = \sin t. \qquad (5.41)$$

The results is shown in Figure 5.3 for $m = 2^5$ and Figure 5.4 for $m = 2^6$. Table 5.3 presents the data for Figure 5.4.

Figure 5.2: Comparison between numerical solution and analytical solution of inverse Laplace transform for rational transfer function $X(s) = \dfrac{1}{s^2 + 1}$ with $\tau = 1$ and $m = 2^5$.

Figure 5.3: Comparison between numerical solution and analytical solution of inverse Laplace transform for rational transfer function $X(s) = \dfrac{1}{s^2 + 1}$ with $\tau = 10$ and $m = 2^5$.

Figure 5.4: Comparison between numerical solution and analytical solution of inverse Laplace transform for rational transfer function $X(s) = \dfrac{1}{s^2 + 1}$ with $\tau = 10$ and $m = 2^6$.

Table 5.3: Data of Figure 5.4

x ($\times 10/128$)	Numerical Solution	Analytic Solution	Absolute Error	Relative Error
1	0.077651	0.078046	0.000394	0.005048
9	0.643556	0.646605	0.003049	0.004715
17	0.967102	0.9707	0.003597	0.003706
25	0.926445	0.927798	0.001353	0.001458
33	0.536896	0.534121	0.002775	0.005195
41	-0.054844	-0.061494	0.006649	0.108124
49	-0.625931	-0.633859	0.007928	0.012508
65	-0.934645	-0.933861	0.000784	0.000840
73	-0.556013	-0.548074	0.007939	0.014485
81	0.032009	0.044925	0.012916	0.287501
89	0.607977	0.620939	0.012962	0.020875
97	0.954985	0.962192	0.007207	0.007490
113	0.574838	0.561877	0.012961	0.023067
121	-0.009157	-0.028343	0.019187	0.676957
127	-0.457708	-0.476876	0.019168	0.040195

5.6.1.2 Example 2

Find the Laplace inversion for rational transfer function

$$X(s) = \frac{10}{s+3}. \tag{5.42}$$

Express in terms of $1/s$, yields

$$\hat{X}\left(\frac{1}{s}\right) = \frac{10/s}{1+3/s}. \tag{5.43}$$

Substitute the terms $1/s$ with generalized Haar wavelet operational matrix, $\mathbf{Q}_m$, we have,

$$\hat{\mathbf{X}}\left(\mathbf{Q}_m\right) = 10\mathbf{Q}_m(\mathbf{I}_m + 3\mathbf{Q}_m)^{-1}. \tag{5.44}$$

The inversion of Laplace transform with $\tau = 2$ and $m = 2^5$ is given by

$$\mathbf{x} = 10 \cdot \left[\frac{32}{2} \quad -\frac{32}{2} \quad \cdots \quad -\frac{32}{2}\right]_{1\times32} \cdot \mathbf{H}_{32}^t \cdot \mathbf{Q}_{32} \cdot (\mathbf{I}_{32} + 3\mathbf{Q}_{32}) \cdot \mathbf{H}_{32}. \tag{5.45}$$

Analytical solution for Laplace inversion of Eqn. (5.42) is

$$\mathcal{L}^{-1}\left(\frac{10}{s+3}\right) = 10e^{-3t}. \tag{5.46}$$

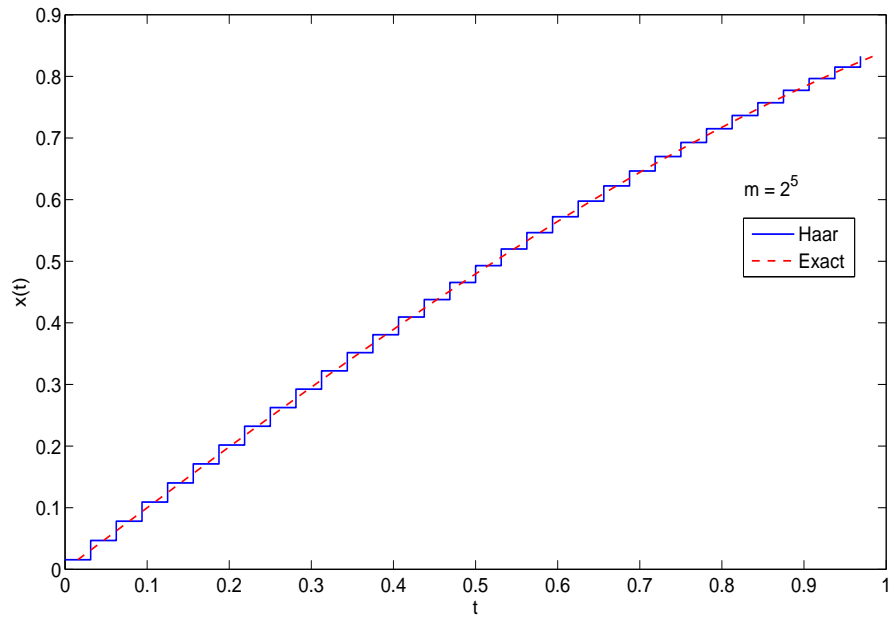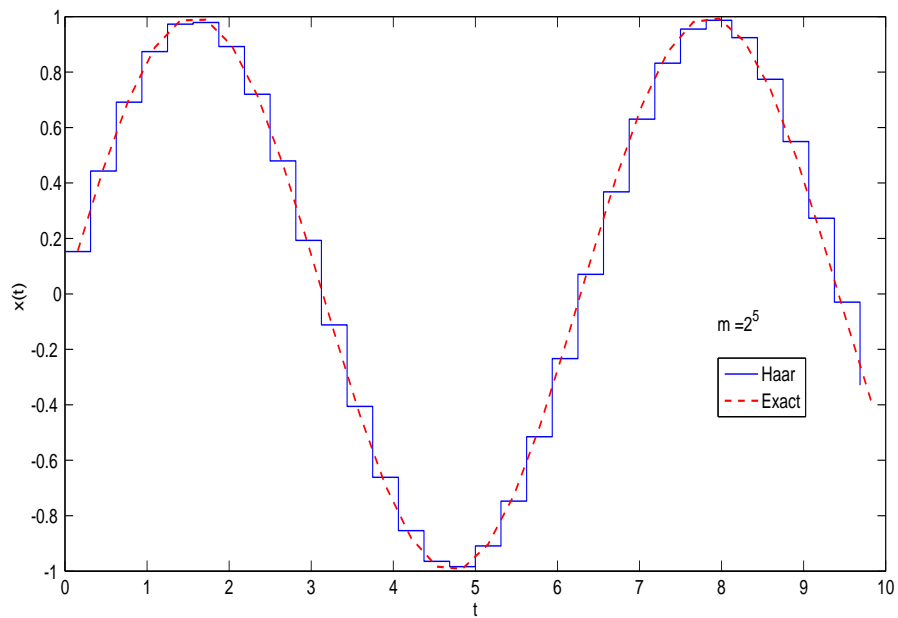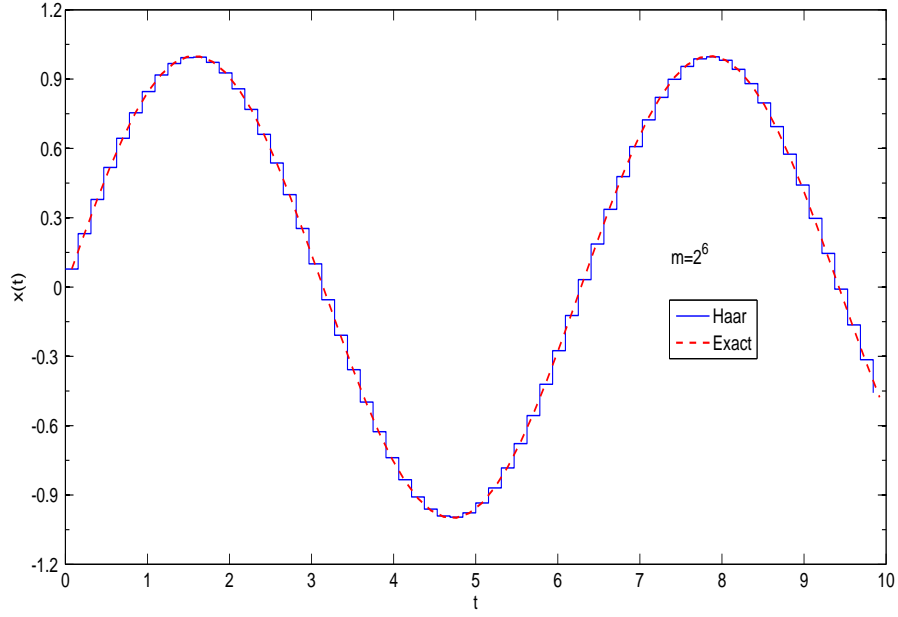The result is shown in Figure 5.6 and its data in Table 5.4.

Figure 5.5: Comparison between numerical solution and analytical solution of inverse Laplace transform for rational transfer function $X(s) = \dfrac{10}{s+3}$ with $m = 2^5$ and $\tau = 2$.

Figure 5.6: Comparison between numerical solution and analytical solution of inverse Laplace transform for rational transfer function $X(s) = \dfrac{10}{s+3}$ with $m = 2^6$ and $\tau = 2$.

Table 5.4: Data of Figure 5.6

x (×2/64)	Numerical Solution	Analytic Solution	Absolute Error	Relative Error
1	9.142857	9.105104	0.037754	0.004146
5	6.276851	6.257840	0.019011	0.003038
9	4.309251	4.300946	0.008304	0.001931
13	2.958432	2.955994	0.002438	0.000825
17	2.031054	2.031623	0.000569	0.000280
21	1.394381	1.396313	0.001932	0.001384
25	0.957285	0.959671	0.002386	0.002486
29	0.657206	0.659571	0.002366	0.003587
33	0.451192	0.453316	0.002125	0.004688
37	0.309757	0.311560	0.001803	0.005787
41	0.212658	0.214132	0.001474	0.006884
45	0.145996	0.147170	0.001174	0.007977
49	0.100231	0.101149	0.000918	0.009076
53	0.068811	0.069518	0.000707	0.010170
57	0.047241	0.047779	0.000538	0.011260
61	0.032433	0.032838	0.000406	0.012364
63	0.026873	0.027224	0.000351	0.012893

5.6.2 Irrational Transfer Function

5.6.2.1 Example 1

Find the inversion of Laplace transform for irrational transfer function below

$$X(s) = \frac{1}{s^n \sqrt{s}}. \tag{5.47}$$

Express above equation in terms of $1/s$, we have,

$$\hat{X}\left(\frac{1}{s}\right) = \left(\frac{1}{s}\right)^n \left(\frac{1}{s}\right)^{\frac{1}{2}}. \tag{5.48}$$

Substitute $1/s$ terms with generalized Haar operational matrix, $\mathbf{Q}_m$, it becomes

$$\hat{\mathbf{X}}\left(\mathbf{Q}_m\right) = \mathbf{Q}_m^n \mathbf{Q}_m^{1/2}. \tag{5.49}$$

Notice that square root of generalized Haar wavelet operational matrix, $\mathbf{Q}_m^{1/2}$ term in Eqn. (5.49) is calculated using MATLAB® built-in command, `sqrtm(Q)`. Haar wavelet operational matrix is always positive definite, hence the existence of Haar wavelet operational matrix inverses and its square root are never unavailable (Chen and Hsiao, 1997). The numerical Laplace inversion is given by

$$\mathbf{x} = \begin{bmatrix} \dfrac{2m}{\tau} & -\dfrac{2m}{\tau} & \cdots & -\dfrac{2m}{\tau} \end{bmatrix}_{1 \times m} \cdot \mathbf{H}_m^t \cdot \mathbf{Q}_m^n \cdot \mathbf{Q}_m^{1/2} \cdot \mathbf{H}_m. \tag{5.50}$$

Analytical solution of Laplace inversion for Eqn. (5.47) is

$$\mathcal{L}^{-1}\left(\frac{1}{s^n \sqrt{s}}\right) = \frac{4^n n!}{(2n)! \sqrt{\pi}} t^{n-1/2}. \tag{5.51}$$

The results is shown in Figure 5.7 and its data in Table 5.5 with $n = 3$, $\tau = 30$ and $m = 32$.
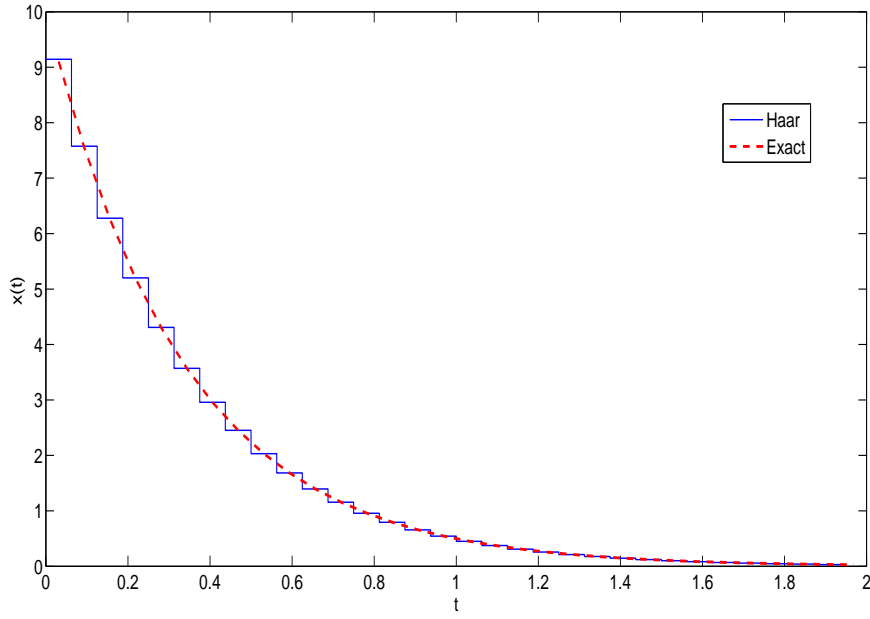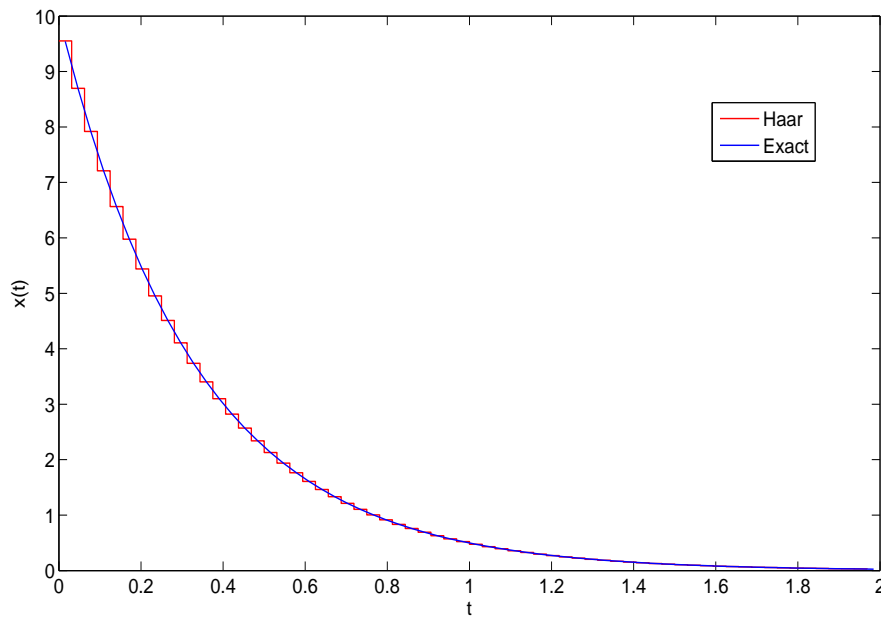

Figure 5.7: Comparison between numerical solution and analytical solution of inverse Laplace transform for rational transfer function $X(s) = \dfrac{1}{s^n \sqrt{s}}$ with $m = 2^5$ and $\tau = 30$.

Table 5.5: Data of Figure 5.7

x ($\times 30/64$)	Numerical Solution	Analytic Solution	Absolute Error	Relative Error
1	0.150436	0.045267	0.105170	2.323326
7	6.167896	5.868432	0.299464	0.051030
13	27.990590	27.582611	0.407979	0.014791
19	71.722949	71.229680	0.493268	0.006925
25	142.023656	141.457838	0.565818	0.004000
31	242.834029	242.203954	0.630076	0.002601
37	377.636235	376.947879	0.688357	0.001826
43	549.585080	548.843004	0.742076	0.001352
49	761.586360	760.794201	0.792160	0.001041
55	1016.348121	1015.508861	0.839260	0.000826
61	1316.416351	1315.532498	0.883854	0.000672
63	1426.927258	1426.029031	0.898227	0.000630

5.6.2.2 Example 2

Find the Laplace inversion for exponential transfer function

$$X(s) = \frac{e^{-a\sqrt{s}}}{\sqrt{s}}. \tag{5.52}$$

Express above equation in terms of $1/s$, we have,

$$\hat{X}\left(\frac{1}{s}\right) = \left(\frac{1}{s}\right)^{\frac{1}{2}} e^{-a\left(\frac{1}{s}\right)^{-\frac{1}{2}}}. \tag{5.53}$$

Substitute $1/s$ terms with generalized Haar operational matrix, $\mathbf{Q}_m$, it becomes

$$\hat{\mathbf{X}}\left(\mathbf{Q}_m\right) = \left(\mathbf{Q}_m\right)^{\frac{1}{2}} \exp(-a\left(\mathbf{Q}_m\right)^{-\frac{1}{2}}). \tag{5.54}$$

The Laplace inversion with $a = 1$, $\tau = 1$ and $m = 16$ is given by

$$\mathbf{x} = \begin{bmatrix} \dfrac{32}{1} & -\dfrac{32}{1} & \cdots & -\dfrac{32}{1} \end{bmatrix} \mathbf{H}_m^t \left(\mathbf{Q}_m\right)^{\frac{1}{2}} e^{-\left(\mathbf{Q}_m\right)^{-\frac{1}{2}}} \mathbf{H}_m. \tag{5.55}$$

Notice that exponential matrix for generalized Haar wavelet operational matrix term, $e^{-\left(\mathbf{Q}_m\right)^{-\frac{1}{2}}}$ in Eqn. (5.55) can be calculated using MATLAB® built-in

command `expm(Q)`. While, the analytical solution for Laplace inversion of Eqn. (5.52) is given by

$$\mathcal{L}^{-1}\left(\frac{e^{-a\sqrt{s}}}{\sqrt{s}}\right) = \frac{e^{-a^2/4t}}{\sqrt{\pi t}}. \tag{5.56}$$

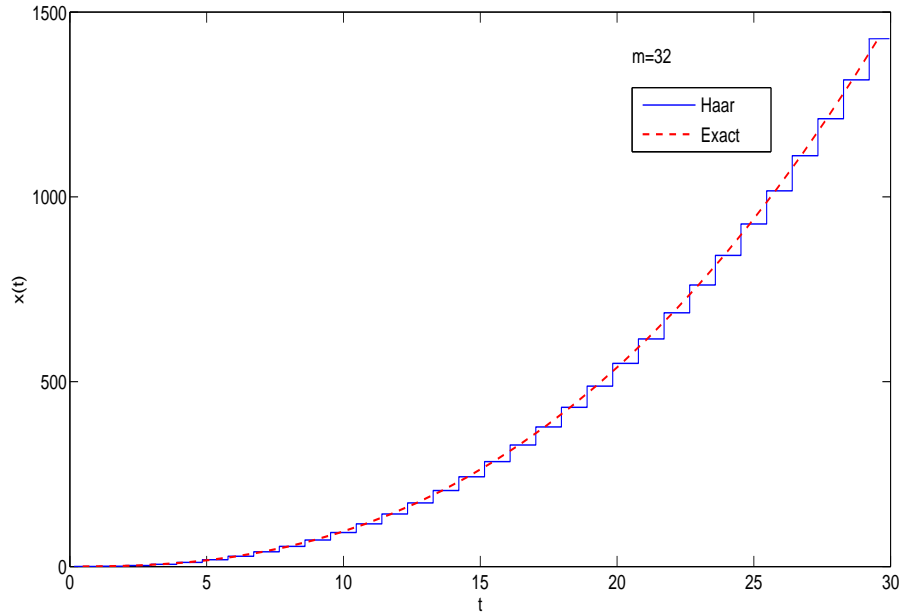The results is shown in Figure 5.8 and its data in Table 5.6.

Figure 5.8: Comparison between numerical solution and analytical solution of inverse Laplace transform for irrational transfer function $X(s) = \dfrac{e^{-a\sqrt{s}}}{\sqrt{s}}$ with $a = 1$, $m = 2^4$ and $\tau = 1$.

x (×1/32)	Numerical Solution	Analytic Solution	Absolute Error	Relative Error
3	0.111791	0.128033	0.016241	0.126850
5	0.270179	0.288167	0.017986	0.062415
7	0.391819	0.384693	0.007126	0.018524
9	0.439733	0.437360	0.002373	0.005426
11	0.465646	0.465000	0.000646	0.001389
13	0.480754	0.478377	0.002377	0.004969
15	0.483684	0.483427	0.000257	0.000532
17	0.484484	0.483506	0.000978	0.002023
19	0.480992	0.480576	0.000416	0.000866
21	0.476124	0.475822	0.000302	0.000635
23	0.470355	0.469978	0.000377	0.000802
25	0.463596	0.463506	0.000089	0.000192
27	0.456960	0.456707	0.000252	0.000552
29	0.449823	0.449775	0.000047	0.000104
31	0.442976	0.442836	0.000140	0.000316

5.6.2.3 Example 3

Find the Laplace inversion for transfer function

$$X(s) = \frac{a}{2\sqrt{\pi}s^{3/2}}e^{-a^2/4s}. \tag{5.57}$$

Express above equation in terms of $1/s$, we have,

$$X\left(\frac{1}{s}\right) = \frac{a}{2\sqrt{\pi}}\left(\frac{1}{s}\right)^{\frac{3}{2}}e^{\frac{-a^2}{4s}}. \tag{5.58}$$

Substitute $1/s$ terms with generalized Haar operational matrix, $\mathbf{Q}_m$, it becomes

$$\hat{\mathbf{X}}(\mathbf{Q}_m) = \frac{a}{2\sqrt{\pi}}(\mathbf{Q}_m)^{\frac{3}{2}}e^{\frac{-a^2}{4}\mathbf{Q}_m} \tag{5.59}$$

The inversion of Laplace transform with $a = 1$, $\tau = 5$ and $m = 32$ is given by

$$\mathbf{x} = \frac{1}{2\sqrt{\pi}} \cdot \begin{bmatrix} \frac{64}{5} & -\frac{64}{5} & \cdots & -\frac{64}{5} \end{bmatrix} \cdot \mathbf{H}_{32}^t \cdot (\mathbf{Q}_{32})^{\frac{3}{2}} \cdot e^{\frac{-\mathbf{Q}_{32}}{4}} \cdot \mathbf{H}_{32} \tag{5.60}$$

69

Analytical solution for Eqn. (5.57) is given by

$$\mathcal{L}^{-1}\left(\frac{a}{2\sqrt{\pi}s^{3/2}}e^{-a^2/4s}\right) = \frac{\sin a\sqrt{t}}{\pi}. \tag{5.61}$$

The results is shown in Figure (5.9) and its data in Table (5.7).
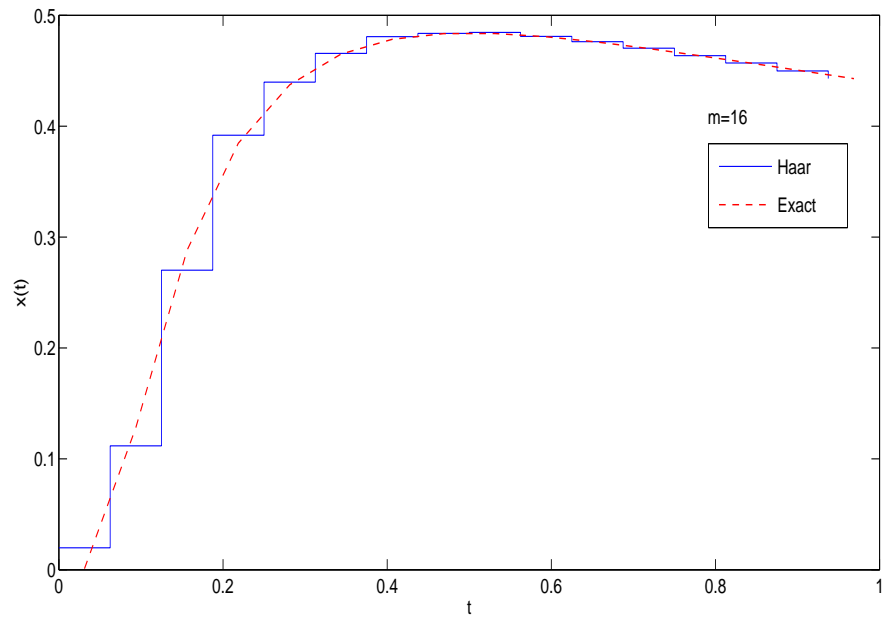

Figure 5.9: Comparison between numerical solution and analytical solution of inverse Laplace transform for irrational transfer function $X(s) = \dfrac{a}{2\sqrt{\pi}s^{3/2}}e^{-a^2/4s}$ with $a = 1$, $m = 2^5$ and $\tau = 5$.

Table 5.7: Data of Figure 5.9

x ($\times 5/64$)	Numerical Solution	Analytic Solution	Absolute Error	Relative Error
1	0.077323	0.087816	0.010494	0.119500
5	0.184305	0.186242	0.001937	0.010400
9	0.235848	0.236714	0.000866	0.003658
13	0.268667	0.269179	0.000511	0.001898
17	0.290515	0.290859	0.000344	0.001183
21	0.304777	0.305025	0.000248	0.000813
25	0.313357	0.313544	0.000187	0.000596
29	0.317480	0.317625	0.000146	0.000460
33	0.318001	0.318117	0.000115	0.000362
37	0.315557	0.315649	0.000093	0.000295
41	0.310637	0.310712	0.000075	0.000241
45	0.303634	0.303695	0.000061	0.000201
49	0.294869	0.294918	0.000049	0.000166
53	0.284607	0.284647	0.000040	0.000141
57	0.273076	0.273108	0.000032	0.000117
61	0.260469	0.260494	0.000025	0.000096

5.6.2.4 Example 4

Find the inversion of Laplace transform for below rational transfer

$$X(s) = \frac{e^{\frac{1}{s}}}{s\sqrt{s}}. \tag{5.62}$$

Express Eqn. (5.62) above equation in terms of $1/s$, we have,

$$X\left(\frac{1}{s}\right) = \frac{1}{s}\left(\frac{1}{s}\right)^{\frac{1}{2}} e^{\frac{1}{s}}. \tag{5.63}$$

Substitute $1/s$ terms with generalized Haar operational matrix, $\mathbf{Q}_m$, it becomes

$$\hat{\mathbf{X}}(\mathbf{Q}_m) = \mathbf{Q}_m(\mathbf{Q}_m)^{\frac{1}{2}} e^{\mathbf{Q}_m}. \tag{5.64}$$

The inversion of Laplace transform with $\tau = 10$ and $m = 16$ is given by

$$\mathbf{x} = \begin{bmatrix} \frac{32}{10} & -\frac{32}{10} & \cdots & -\frac{32}{10} \end{bmatrix} \mathbf{H}_{16}^t \cdot \mathbf{Q}_{16} \cdot (\mathbf{Q}_{16})^{\frac{1}{2}} \cdot e^{\mathbf{Q}_{16}} \cdot \mathbf{H}_{16}. \tag{5.65}$$

Analytical solution for Eqn. (5.62) is given by.

$$\mathcal{L}^{-1}\left(\frac{e^{\frac{1}{s}}}{s\sqrt{s}}\right) = \frac{\sinh 2\sqrt{t}}{\sqrt{\pi}}. \tag{5.66}$$

The results is shown in Figure 5.10 and its data in Table 5.8.
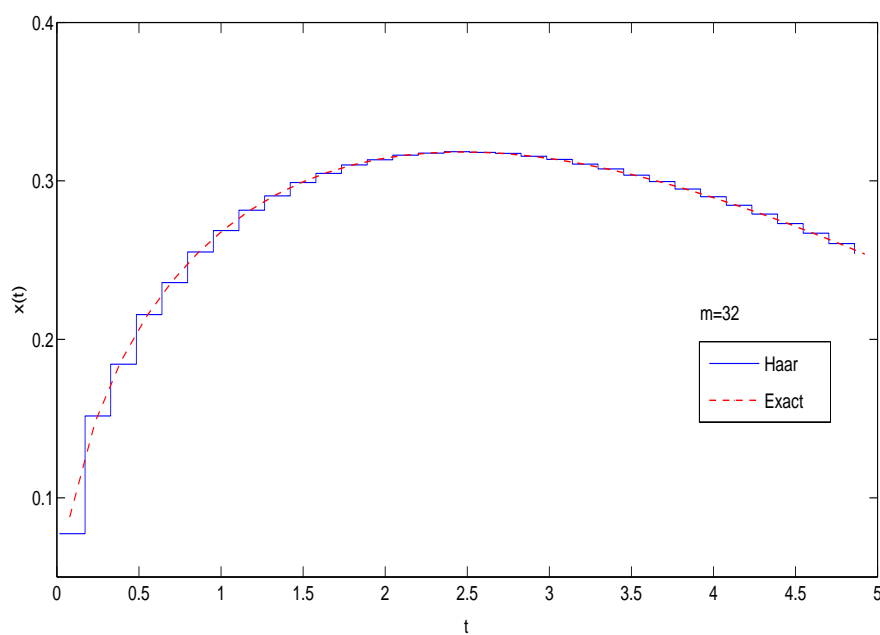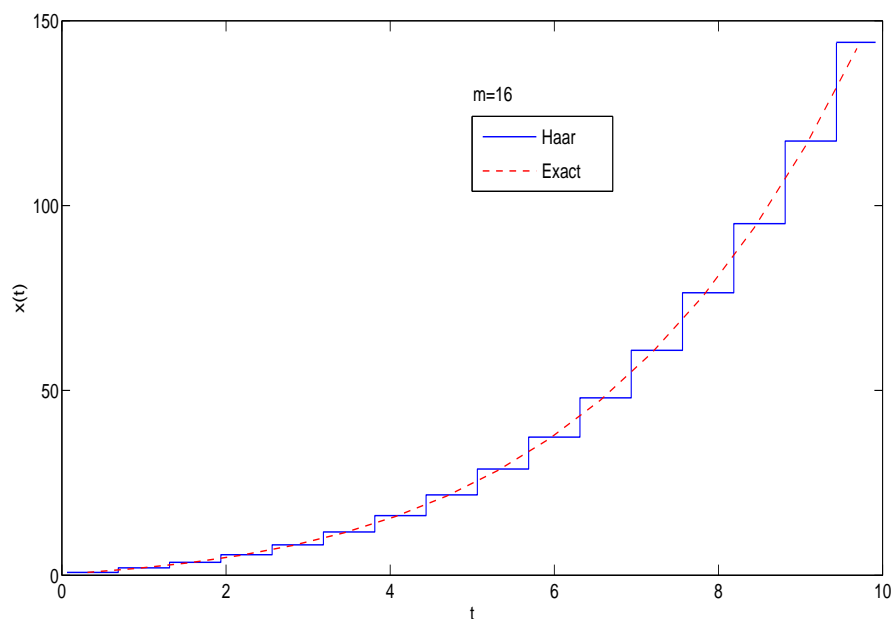

Figure 5.10: Comparison between numerical solution and analytical solution of inverse Laplace transform for irrational transfer function $X(s) = \dfrac{e^{\frac{1}{s}}}{s\sqrt{s}}$ with $m = 2^4$ and $\tau = 10$.

Table 5.8: Data of Figure 5.10

x (10/128)	Numerical Solution	Analytic Solution	Absolute Error	Relative Error
1	0.302221	0.332077	0.029856	0.089907
7	1.181332	1.173735	0.007597	0.006473
13	2.082231	2.079523	0.002708	0.001302
19	3.207519	3.201149	0.006370	0.001990
25	4.605088	4.598966	0.006122	0.001331
31	6.336745	6.327982	0.008762	0.001385
37	8.456198	8.446414	0.009785	0.001158
43	11.030775	11.018246	0.012529	0.001137
49	14.129035	14.114571	0.014464	0.001025
55	17.832289	17.814598	0.017692	0.000993
61	22.227128	22.206584	0.020544	0.000925
67	27.413283	27.388771	0.024511	0.000895
73	33.498756	33.470356	0.028400	0.000849
79	40.605882	40.572531	0.033351	0.000822
85	48.868057	48.829593	0.038464	0.000788
91	58.434784	58.390125	0.044658	0.000765
97	69.469518	69.418281	0.051237	0.000738
103	82.154120	82.095149	0.058971	0.000718
109	96.687539	96.620228	0.067312	0.000697
115	113.289936	113.213008	0.076928	0.000679
121	132.202055	132.114670	0.087385	0.000661
127	153.689186	153.589904	0.099282	0.000646

5.6.3 Initial Value Problem

Consider the initial value problem

$$t\frac{d^2x}{dt^2} + \frac{dx}{dt} + tx = 0. \tag{5.67}$$

Initial conditions for this case are given by

$$x(0) = 1 \quad \text{and} \quad x'(0) = 0 \tag{5.68}$$

We are going to solve this problem with Laplace transform method. Firstly we have to take Laplace transform of Eqn. (5.67) with respect to t, so that the expression becomes

$$\frac{d}{ds}\left\{ s^2 X - sx(0) - x'(0) \right\} + sX - x(0) - \frac{dX}{ds} = 0. \tag{5.69}$$

Substituting above equation with given initial condition in Eqn. (5.68) gives

$$(s^2 + 1)\frac{dX}{ds} + sX = 0 \tag{5.70}$$

By integrating the above equation gives solution in s domain as below

$$X(s) = \frac{1}{\sqrt{s^2 + 1}}. \tag{5.71}$$

To find the final answer in t domain, we have to find Laplace inversion of Eqn. (5.71). Finding the inversion of Laplace transform with this numerical method will start with expressing Eqn. (5.71) in terms of $1/s$. Thus, the equation becomes

$$\hat{X}\left(\frac{1}{s}\right) = \frac{1/s}{\sqrt{1 + (1/s)^2}}. \tag{5.72}$$

Then, all terms with $1/s$ is substituted with generalized Haar wavelet operational matrix,

$$\hat{\mathbf{X}}\left(\mathbf{Q}_m\right) = \mathbf{Q}_m(\mathbf{I}_m + \mathbf{Q}_m^2)^{\frac{1}{2}}. \tag{5.73}$$

Therefore, the Laplace inversion for this problem with $m = 2^8$ and $\tau = 30$ is given by

$$\mathbf{x} = \begin{bmatrix} \dfrac{512}{30} & -\dfrac{512}{30} & \cdots & -\dfrac{512}{30} \end{bmatrix} \mathbf{H}_m^t \mathbf{Q}_m(\mathbf{I}_m + \mathbf{Q}_m^2)^{\frac{1}{2}}(\mathbf{Q}_m)\mathbf{H}_m. \tag{5.74}$$

The solution is shown in Figure 5.11 and its data in Table 5.9. The analytical solution for Eqn. (5.67) is the first kind Bessel function of zeroth order, $J_0(t)$.

74
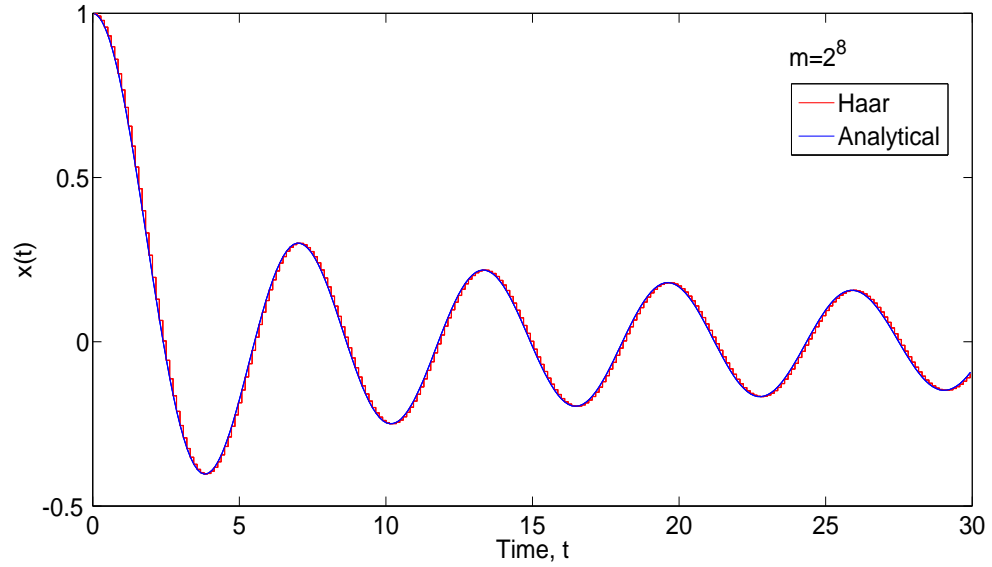
Figure 5.11: Comparison between numerical solution and analytical solution for initial value problem, $t\dfrac{d^2x}{dt^2} + \dfrac{dx}{dt} + tx = 0$ with $m = 2^8$ and $\tau = 30$.

Table 5.9: Data of Figure 5.11

x ($\times 30/512$)	Numerical solution	Analytic solution	Absolute Error	Relative Error
1	0.998288	0.999142	0.000854	0.000855
31	0.331278	0.330444	0.000834	0.002524
61	-0.388527	-0.389169	0.000642	0.001650
91	-0.066750	-0.064718	0.002032	0.031398
151	-0.049088	-0.051735	0.002647	0.051165
211	0.120132	0.122830	0.002698	0.021965
271	-0.160514	-0.162654	0.002140	0.013157
301	-0.083414	-0.079964	0.003450	0.043144
337	0.178919	0.178542	0.000378	0.002117
355	0.073666	0.069880	0.003786	0.054179
367	-0.045525	-0.049582	0.004057	0.081824
373	-0.099023	-0.102458	0.003435	0.033526
385	-0.162780	-0.163792	0.001013	0.006185
397	-0.148710	-0.146735	0.001975	0.013460
403	-0.113853	-0.110624	0.003229	0.029189
415	-0.010319	-0.005835	0.004484	0.768466
451	0.138176	0.135982	0.002194	0.016134
511	-0.096959	-0.093181	0.003778	0.040545

5.6.4　Heat Equation

Heat equation is one of the prominent example of partial differential equation and it is a parabolic equation. This problem is taken from Carrier and Pearson (1976). Despite the simplicity of this example, it will show that our method is usable in solving heat equation.

Consider one-dimensional heat equation problem which is given by below equation.

$$\frac{\partial U}{\partial t} = a^2 \frac{\partial U}{\partial x^2} \tag{5.75}$$

We have to determine the $U(x,t)$ in the region of $0 < x < \infty$ and $0 < t < \infty$. The initial condition is given by

$$U(x,0) = 0, \quad x > 0 \tag{5.76}$$

and boundary condition by

$$U(0,t) = 1, \quad t > 0. \tag{5.77}$$

Taking Laplace transform at both side of Eqn. (5.75) with respect to time, t we obtain,

$$-U(x,0) + s\tilde{U}(x,s) = s^2 \tilde{U}_{xx} \tag{5.78}$$

where

$$\tilde{U}(x,s) = \int_0^\infty e^{-st} U(x,t) dt \tag{5.79}$$

and we assume that $U(x,t)$ to be sufficiently well behaved that the processes of integration with respect to time, t and differentiation with respect to spatial, x are

interchangeable, so that

$$\int_0^\infty e^{-st} U_{xx}(x,t)dt = \left(\int_0^\infty e^{-st} U(x,t)dt\right)_{xx}. \tag{5.80}$$

Substitute the initial condition then the solution of Eqn. (5.78) is

$$\tilde{U}(x,s) = A\exp\left(\sqrt{s}x/a\right) + B\exp\left(\sqrt{s}x/a\right), \tag{5.81}$$

where A and B is yet to be determined unknown constant. For large x, it is anticipated that the function $U(x,t)$ will be bounded function of t, so that its Laplace transform must approach to zero as s approach to ∞. Therefore, the coefficient B must be set equal to zero. To determine A, we know that from initial condition based on given Eqn. (5.76), we have

$$\tilde{U}(x,s) = \frac{1}{s}\exp\left(\frac{-\sqrt{s}x}{a}\right). \tag{5.82}$$

To find the solution numerically using this method, we need to express Eqn. (5.82) in terms of $1/s$, then we have

$$\tilde{U}\left(\frac{1}{s}\right) = \frac{1}{s}\exp\left(\frac{-\left(\frac{1}{s}\right)^{-1/2}x}{a}\right). \tag{5.83}$$

Next, we have to substitute $1/s$ terms with the generalized Haar wavelet operational matrix, $\mathbf{Q}_m$. Thus Eqn. (5.83) become

$$\tilde{\mathbf{u}}\left(\mathbf{Q}_m\right) = \mathbf{Q}_m\exp\left(\frac{-\left(\mathbf{Q}_m\right)^{-1/2}x}{a}\right). \tag{5.84}$$

If $x = 100$ and $a = 10$, we have

$$\tilde{\mathbf{u}}\left(\mathbf{Q}_m\right) = \mathbf{Q}_m\exp\left(\frac{-100\cdot\mathbf{Q}_m}{10}\right)^{-1/2}. \tag{5.85}$$

Finally, the numerical solution for Laplace inversion of Eqn. (5.82) with $m = 2^5$ and $\tau = 50$ can be calculated by

$$\mathbf{x} = \begin{bmatrix} \dfrac{64}{50} & -\dfrac{64}{50} & \cdots & -\dfrac{64}{50} \end{bmatrix} \mathbf{H}_{32}^t \cdot \mathbf{Q}_{32} \cdot \exp\left(-\mathbf{Q}_{32}\right)^{-1/2} \cdot \mathbf{H}_{32}. \tag{5.86}$$

We could invert directly Eqn. (5.82) using table of Laplace transform to find the solution analytically. By inverting both sides we have analytical solution for Eqn. (5.75) as

$$u(x,t) = \mathrm{erfc}\ \left(\frac{x}{2a\sqrt{t}}\right). \tag{5.87}$$

Figure 5.12 and Figure 5.13 illustrate result obtained by numerical and analytical solution for heat equation with $m = 2^5$ and $m = 2^7$ respectively. Table 5.10 shows data for Figure 5.12 .
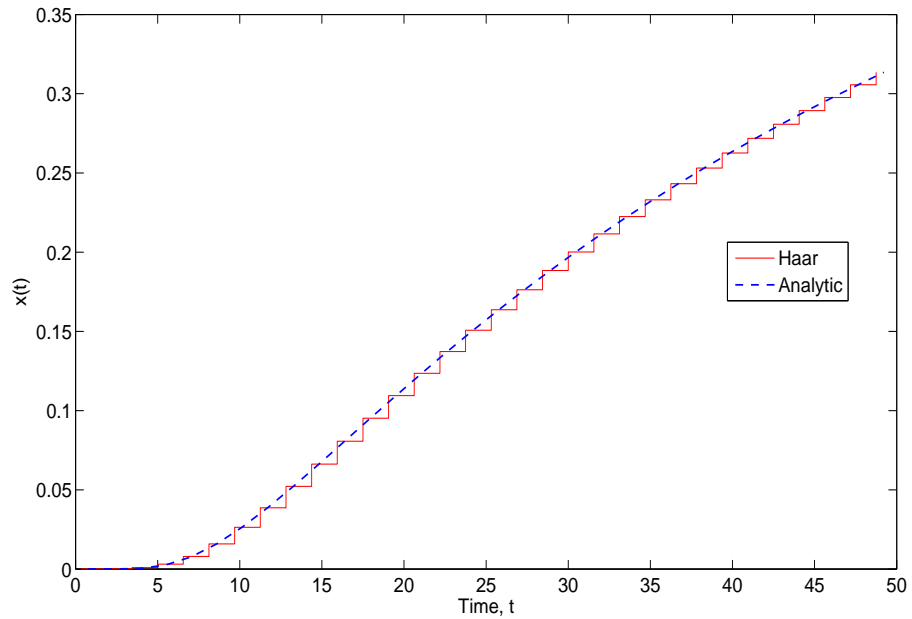
Figure 5.12: Comparison between numerical solution and analytical solution of inverse Laplace transform for heat equation, $U_t = a^2 U_{xx}$ with $a = 10$, $m = 2^5$ and $\tau = 50$.
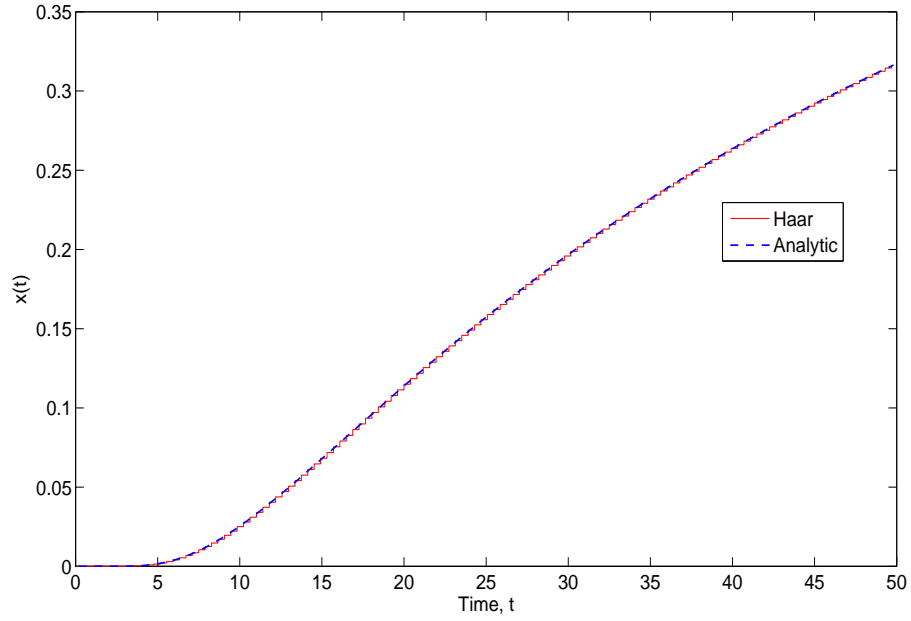
Figure 5.13: Comparison between numerical solution and analytical solution of inverse Laplace transform for heat equation, $U_t = a^2 U_{xx}$ with $a = 10$, $m = 2^7$ and $\tau = 50$.

Table 5.10: Data of Figure 5.12

x ($\times 50/64$)	Numerical solution	Analytic Solution	Absolute Error	Relative Error
7	0.003096	0.002497	0.000599	0.239910
9	0.007934	0.007661	0.000273	0.035617
13	0.026334	0.026500	0.000166	0.006268
19	0.066259	0.066457	0.000198	0.002983
23	0.095142	0.095293	0.000151	0.001582
27	0.123551	0.123658	0.000107	0.000866
29	0.137306	0.137395	0.000089	0.000650
33	0.163673	0.163734	0.000061	0.000376
37	0.188404	0.188445	0.000042	0.000222
41	0.211494	0.211522	0.000028	0.000133
47	0.243228	0.243243	0.000015	0.000061
51	0.262609	0.262618	0.000009	0.000035
55	0.280707	0.280713	0.000005	0.000019
59	0.297636	0.297638	0.000002	0.000008
63	0.313500	0.313500	0.000000	0.000001

5.7   Numerical Discussions

The results of all examples are shown in figures and tables. Each figure is plotted with solution obtained from present numerical analysis and exact solution. Results from the figures provide a better visualization regarding the agreement between numerical and exact solution. On the other hand, results in table format display digits obtained from numerical and exact solution which will give insights in terms of solutions' accuracy of our method. Furthermore, from this digits we calculate absolute error and relative error which illustrate the difference between approximated valued from the present numerical analysis and the true value from the exact solution.

Even though the exact solution is available in all examples, the use of numerical Haar wavelet operational matrix method is much simpler than the conventional contour integration method and it can be easily coded. This factor gives Haar wavelet a reason to be ventured further as numerical tools. Additionally, few benefits come from its great features such as faster computation and attractiveness. This work is going to be a stepping stone in finding Laplace inversion for transfer function which is not available in the inversion table of Laplace transform.

It can be observed from the figures that the present numerical method shows good agreement with the exact solution. As shown in all figures, the time domain for numerical results obtained are not restricted to one. This is resulted by the extension work we have done to generalize the Haar wavelet operational matrix. By generalizing the Haar operational matrix enabling us finding the solution in all time domain. Without generalization of Haar wavelet operational matrix, we can

only obtain numerical result within the interval $0 \leq t < 1$, for instance in Figure 5.2.

The present numerical method provides encouraging results even for small values of Haar wavelet resolution, $m = 2^4$. The accuracy of solution in present numerical results increase as bigger value of m is used as showed in Example 1 of rational transfer function, Figure 5.3 and Figure 5.4 from $m = 2^5$ and $m = 2^6$ respectively.

5.8   Conclusion

In this chapter, a numerical method of finding Laplace inversion is derived from transfer function using generalized Haar wavelet operational matrix. Laplace inversion of exponential transfer function also can be calculated by this method as exponential function is expandable using Maclaurin series in which the expansion expression will have $1/s$ terms. Generalized Haar wavelet operational matrix is constructed based on combination work of obtaining the corresponding integral operational matrix of Haar basis (Wu et al., 2001) and generalized block pulse function (Kilicman and Zhour, 2007). This method enable finding the Laplace inversion numerically without limiting its time domain within the interval $0 \leq t < 1$ only.

Some of the most effective methods for the numerical inversion of the Laplace transform are based on the approximation of the Bromwich contour integral. Instead of performing the conventional contour integration, Laplace inversion can be achieved by a series of matrix multiplication via numerical generalized Haar operational matrix method. As a result, this method gives an alternative way to

find the solution for inversion of Laplace transform in a much quicker time. Furthermore, due to sparse matrices which appeared during the calculation, it contributes to a faster computational analysis. Numerical results demonstrate good performance of the method used in term of accuracy and competitiveness compared to analytical solution. Examples on solving differential equation, initial value problem and heat equation by Laplace transform method are also shown and the numerical solution obtained shows good agreement with analytical solution. The present method is very convenient as it requires only simple computing systems, less computing time and less computer memory.

CHAPTER 6

CONCLUSION AND FUTURE WORK

The study of this thesis was started with understanding the mathematical background of Haar wavelet. Many scholars whom proposed numerical method using Haar wavelet basis usually define Haar wavelet operational matrix within the interval of zero to one. This gives limitations to our ultimate goal as the integration involved in partial differential equation does not necessarily cover only in the interval between zero and one. Therefore, it is convenient to derive the Haar wavelet operational matrix that can cover the whole domain of Haar series expansion.

In this thesis, we derived the operational matrix using combination work of new unified method to derive operational matrices of any orthogonal function proposed by Wu et al. (2001) and generalized block pulse operational matrix for integration proposed by Kilicman and Zhour (2007). We named the operational matrix derived from this combination work as generalized Haar wavelet operational matrix.

The first numerical analysis using generalized Haar wavelet operational matrix is an attempt to solve partial differential equation of hyperbolic heat conduction in thin surface layers. We established the numerical method with hybrid concept of time and spatial discretization by finite difference method and pseudo spectral method respectively. As for pseudo spectral method the highest order of differential equation is assumed to be equal to Haar series expansion. The generalized Haar wavelet operational matrix appear in the equation after integrating the highest order term in ordinary differential equation which has

been expanded in Haar series. Before we applied this method to solve our hyperbolic heat conduction equation in thin surface layer, we tried to solve simpler type of partial differential equation. We employed the proposed method to solve wave equation which is one of the example of hyperbolic type partial differential equation. The numerical analysis is shown in Appendix (D) and we obtained a promising result. After the applicability of the proposed method is confirmed, then we employed the numerical method to solve the actual problem, which is the hyperbolic heat conduction problem in thin surface layers.

As mentioned in Chapter 3, the paramount challenge of solving partial differential equation of hyperbolic heat conduction equation is the exhibits of numerical oscillation in the vicinity of sharp discontinuities. Through this method we found that with a certain discretization, the numerical oscillation is totally eliminated, thus making this numerical method competitive with others. Two sets of initial and boundary conditions were investigated as evidence to the accuracy and efficiency of the proposed numerical method for the hyperbolic heat conduction problem in thin surface layers. Further investigation of the present methods' accuracy and efficiency can be examined by solving the equation with other sets of initial and boundary conditions. For instance, conditions in a pulsed energy source, surface radiation and in a composite region. To the best of our knowledge, this is the first effort to solve hyperbolic type partial differential equation through this method.

In this thesis, we did not go in depth into mathematically proving the numerical stability of the method. We also do not measure the magnitude of dissipation and dispersion appeared in the numerical method. It is often to state

the Courant-Friedrichs-Lewy condition, or CFL condition in establishing numerical solution method for hyperbolic partial differential equations if finite difference method is being used. As finite difference method were used for time discretization, somehow the present numerical method has to be bounded with CFL condition. This is going to be our next goal in future work in which we want to establish the numerical stability analysis.

The second numerical analysis is finding Laplace inversion via generalized Haar wavelet operational matrix. This is an extension work of Wu et al. (2001) that covers the whole time domain for Laplace inversion in its solution. We have derived the proposed method for the case of the transfer function using the extension of Riemann-Liouville fractional integral. Examples of finding Laplace inversion is illustrated from rational, irrational and exponential transfer function. Solution of initial value problem and heat equation via Laplace transform are also given. The resulting approximation in the present numerical method are in a good agreement with exact solution even for small m. This method does not involve conventional and complex integration but only a few of matrices multiplication. The present method is considered to be simple compared to conventional method and can be easily be coded. It is our hope to extend the numerical method to find Laplace inversion for multidimensional Laplace transform. This problem is useable in analysing continuous nonlinear and time-varying which always expressed by Volterra functional series and distributed systems expressed by partial differential equation.

APPENDIX A

MATLAB CODE FOR GENERALIZED HAAR WAVELET

OPERATIONAL MATRIX

```
m=2^5; % Haar wavelet level with J=5

S=10;  % Haar series expansion domain


t=0.5/m:1/m:(m-0.5)/m; % generate collocation points

M=2*m*ones(1,m);

for i=2:2:m

    M(i)=-M(i);

end

zeta1=@(j,k) (k-1)/2^j;

zeta2=@(j,k) (k-0.5)/2^j;

zeta3=@(j,k) k/2^j;


% generating Haar wavelet matrix size of (m x m)

H(1,1:m)=1;

for i=1:(m-1)

    j=floor(log(i)/log(2));

    k=i-2^j+1;

   % fprintf(' i= %d  , aa= %d  and  k = %d  \n', i, aa, k)

    for s=1:m

        if ( t(s) >= zeta1(j,k)) && ( t(s) < zeta2(j,k))
```

```
                H(i+1,s)= 2^(j/2);

            elseif (t(s) >= zeta2(j,k)) && (t(s) < zeta3(j,k))

                H(i+1,s)= -2^(j/2);

            else

                H(i+1,s)= 0;

            end

        end

end

H=H/sqrt(m); % Haar wavelet matrix


% generating generalized block pulse operational matrix

QB=triu(ones(m));

for i=1:m

    QB(i,i)=0.5;

end

QB=QB/m; % generalized block pulse operational matrix


% generating generalized Haar wavelet operational matrix

% with Wu et. al method.

QH=H*QB*H';

QH=S*QH; generalized Haar wavelet operational matrix
```

APPENDIX B

MATLAB CODE FOR HYBRID METHOD OF SOLVING

HYPERBOLIC HEAT CONDUCTION IN THIN SURFACE LAYERS

B.1 The MATLAB code for Prescribed Wall Temperature (Example 1)

```
% Haar wavelet resolution

m=2^3; L=1;

% Parameters that change

epsilon=0; %concave or convex

T=0.5; %dimensionless time has 4 values

dt=0.001; %time increment

% Generate block pulse matrix

Q=2*triu(ones(m,m));

for i=1:m

    Q(i,i)=Q(i,i)-1;

end

QB=Q/(2*m);

% Generate Haar matrix

H=ones(m);

J=log2(m);

x=1:2:(2*m-1); x=x/(2*m);

for alpha=0:(J-1)
```

```matlab
    for k=1:pow2(alpha)

        fun=@(x) (( x >= (k-1)/pow2(alpha)) &&...

         ( x < (k-0.5)/pow2(alpha)))...

            - (( x < k/pow2(alpha)) && ( x >= (k-0.5)/pow2(alpha)));

        i=pow2(alpha)+k;

        for j=1:m

            H(i,j)=pow2(alpha/2)*fun(x(j));

        end

    end

end

H=H/sqrt(m);

% Haar operational matrix via Wu formula

Q=H*QB*H';

% For boundary value problem matrix

lambda=Q(:,1); theta=zeros(m,1); theta(1,1)=1;

x=L*x; Q=L*Q;

% Coefficients for ODE

A=(dt)^2;

B=epsilon*(dt)^2;

C=(-1-2*dt);

% Time increment

N=T/dt;

% Initial condition

uim1=zeros(1,m);
```

```matlab
ui=uim1;

for s=1:N

    u=-2*(1+dt)*ui+uim1;

    k=u*H'+sqrt(m)*(B*theta'/L+C*theta'*Q/L-C*theta');

    left=A*eye(m) +B*Q -B*L*lambda*theta'+C*Q^2-C*L*lambda*theta'*Q;

    c=k/left;

    uip1=(c*(Q-L*lambda*theta')*Q*H + sqrt(m)*(theta'-theta'*Q/L)*H);

    uim1=ui;

    ui=uip1;

end
% MATLAB code for Analytical Solution Example 1

ep=epsilon;   %epsilon has 3 values -0.1,0,0.1

zeta=T; % fix and has 4 values, dimensionless time

area=zeros(1,m);

% integration value of Bessel function in analytical solution

for i=1:m

    if x(i)<=zeta

    tau=linspace(x(i)+0.0001,zeta,100000);

    %argument for bessel function

    a=(1-(ep^2)/4);b=(tau.^2-x(i)^2);

    Z=(a*b).^(1/2);

    %Modified bessel function

    func=@(tau) (exp(-tau).*besseli(1,Z))./sqrt(b);

    area(i)=trapz(tau,func(tau));
```

```matlab
        else

            area(i)=0;

        end

end

Theta=zeros(1,m);

for i=1:m

    if x(i)<=zeta

    Theta(i)=exp((-x(i)./2)*ep)*(exp(-x(i))+sqrt(a)*x(i).*area(i));

        else

        Theta(i)=0;

        end

end


% Graph command

stairs(x-(1/m),ui,'r'); % numerical solution

hold on

plot(x,Theta,'--'); % analytical solution

axis([0 2.2 -0.2 1]);

xlabel('Dimensionless Length,  \eta');

ylabel('Dimensionless Temperature,  \theta');

hleg3 = legend('Numerical','Analytic');

str1(1) = {'\epsilon=0'};

str1(2) = {'m=2^9'};

str1(3) = {'dt=0.001'};
```

```
text(1.5,0.8,str1,'FontSize',14)
```

B.2 The MATLAB code for Prescribed in a Finite Slab (Example 2)

```
% Haar wavelet resolution

m=2^10;

% Boundary condition interval (0,1)

L=1;

% Parameters that change

epsilon=0; %concave or convex

T=1.5; dt=0.0001;

% Generate block pulse matrix

Q=2*triu(ones(m,m));

for i=1:m

    Q(i,i)=Q(i,i)-1;

end

QB=Q/(2*m);

% Generate Haar wavelet matrix

H=ones(m);

J=log2(m);

x=1:2:(2*m-1); x=x/(2*m);

for alpha=0:(J-1)

    for k=1:pow2(alpha)

        fun=@(x) (( x >= (k-1)/pow2(alpha)) &&...
```

```matlab
                ( x < (k-0.5)/pow2(alpha)))...

                - (( x < k/pow2(alpha)) && ( x >= (k-0.5)/pow2(alpha)));

            i=pow2(alpha)+k;

            for j=1:m

                H(i,j)=pow2(alpha/2)*fun(x(j));

            end

        end

end

H=H/sqrt(m);

% Generate Haar operational matrix via Wu formula

Q=H*QB*H';

lambda=Q(:,1);

theta=zeros(m,1); theta(1,1)=1; beta=theta'*H(:,m);

x=L*x; Q=L*Q;

% Coefficient of ODE

A=(dt)^2./(dt)^2;

B=(epsilon*(dt)^2)./dt^2;

C=(1+2*dt)./dt^2;

% time increment

N=T/dt;

% Iteration

uim1=zeros(1,m);  % initial

ui=uim1;

for s=1:N
```

```
        u=((-2*(1+dt))./dt^2)*ui+uim1/dt^2;

        k=u*H'+C*(sqrt(m)*theta');

        left=A*eye(m)+B*Q-B*theta*theta'-C*Q^2+C*theta*theta'*Q;

        c=k/left;

        uip1=(c*Q^2-c*theta*theta'*Q+sqrt(m)*theta')*H;

        uim1=ui;

        ui=uip1;

end

hold on

stairs(x-(1/m),ui,'b');

axis([0 1 -0.2 1]);

xlabel('Dimensionless Length \eta');

ylabel('Dimensionless Temperature,\theta (^0C)');
```

MATLAB PROGRAMMING FOR NUMERICAL LAPLACE

INVERSION

```matlab
% Haar wavelet resolution, m

m=2^5;

% Generate block pulse operational matrix

Q=2*triu(ones(m,m));

for i=1:m

    Q(i,i)=Q(i,i)-1;

end

QB=Q/(2*m);

% Generate Haar wavelet matrix

H=ones(m);

J=log2(m);

x=1:2:(2*m-1); x=x/(2*m);

for alpha=0:(J-1)

    for k=1:pow2(alpha)

        fun=@(x) (( x >= (k-1)/pow2(alpha)) &&...

            ( x < (k-0.5)/pow2(alpha)))...

            - (( x < k/pow2(alpha)) && ( x >= (k-0.5)/pow2(alpha)));

        i=pow2(alpha)+k;

        for j=1:m

            H(i,j)=pow2(alpha/2)*fun(x(j));
```

```
        end

    end

end

H=H/sqrt(m);

% Generate generalized Haar wavelet operational matrix via...

% Wu et. al formula

Q=H*QB*H'; Q=L*Q;
```

APPENDIX D

NUMERICAL ANALYSIS OF WAVE EQUATION WITH GENERALIZED HAAR WAVELET OPERATIONAL MATRIX METHOD

D.1 Numerical Analysis

Wave equation is a prominent hyperbolic type partial differential equation. The equation is derived from the model of the vibrating string. One-dimensional wave equation is given as below,

$$\frac{\partial^2 u}{\partial x^2} = \frac{1}{a^2}\frac{\partial^2 u}{\partial t^2} \tag{D.1}$$

where $a^2 = 1$ is considered here. Boundary conditions are given as

$$u(0,t) = u(L,t) = 0, \quad t \geq 0, \tag{D.2}$$

and initial conditions are given as

$$u(x,0) = \begin{cases} \dfrac{2x}{L} & 0 \leq x \leq \dfrac{L}{2} \\[2ex] \dfrac{2(1-x)}{L} & \dfrac{L}{2} \leq x < L, \end{cases} \tag{D.3}$$

$$\frac{\partial u}{\partial t}(x,0) = 0. \tag{D.4}$$

From Eqn. (D.1) , using a backward finite difference in t, we have

$$\frac{\partial u}{\partial t} = u_t^{(i+1)} \approx \frac{u^{(i+1)} - u^i}{\Delta t} + O(\Delta t) \tag{D.5}$$

$$\frac{\partial^2 u}{\partial t^2} = u_{tt}^{(i+1)} \approx \frac{u^{(i+1)} - 2u^i + u^{(i-1)}}{\Delta t^2} + O(\Delta t^2) \tag{D.6}$$

Substitute Eqns. (D.5) and (D.6) into Eqn. (D.1), we have

$$\frac{u^{(i+1)} - 2u^i + u^{(i-1)}}{\Delta t^2} = u_{xx}^{(i+1)} \tag{D.7}$$

$$\Delta t^2 u_{xx}^{(i+1)} - u^{(i+1)} = -2u^i + u^{(i-1)} \tag{D.8}$$

Let us consider this notation $U(x) = u^{(i+1)}(x)$. Therefore we can rewrite Eqn. (D.8) as in the form as below

$$\Delta t^2 U''(x) - U(x) = k(x) \tag{D.9}$$

where $k(x) = -2u^i + u^{(i-1)} = \mathbf{k}^t \mathbf{h}_m(x)$. For spatial discretization, the highest order term in Eqn. (D.9) is assumed can be expanded in terms of Haar wavelet series expansion as below

$$U''(x) = \mathbf{c}_m^t \mathbf{h}_m(x). \tag{D.10}$$

Subsequently, $U'(x)$ and $U(x)$ are obtained by integrating Eqn. (D.10). Thus we have

$$U'(x) = \mathbf{c}_m^t \mathbf{Q}_m \mathbf{h}_m(x) + \sqrt{m} U'(0) \theta^t \mathbf{h}_m(x), \tag{D.11}$$

and

$$U(x) = \mathbf{c}_m^t \mathbf{Q}_m^2 \mathbf{h}_m(x) + \sqrt{m} U'(0) \theta^t \mathbf{Q}_m \mathbf{h}_m(x) + \sqrt{m} U(0) \theta^t \mathbf{h}_m(x). \tag{D.12}$$

The following formula will be helpful for solving boundary value problem (BVP).

$$\mathbf{Q}_m \mathbf{h}_m(L) = \frac{L}{\sqrt{m}} \theta_m \tag{D.13}$$

and

$$\mathbf{Q}_m^2 \mathbf{h}_m(L) = \frac{L}{\sqrt{m}} \Lambda_m \tag{D.14}$$

where

$$\Theta_m^t = \begin{bmatrix} 1, 0, 0, \ldots, 0 \end{bmatrix}, \tag{D.15}$$

$$\Lambda_m^t = \begin{bmatrix} \dfrac{L}{2}, \dfrac{L}{2^2}, \dfrac{L}{2^{7/2}}, \ldots, \ldots, \ldots \end{bmatrix}. \tag{D.16}$$

Λ_m^t is taken from the first column of generalized Haar wavelet operational matrix, $\mathbf{Q}_m$. Substituting $U(L) = 0$ into Eqn. (D.12), $U'(0)$ can be determined.

$$U(L) = \mathbf{c}_m^t \mathbf{Q}_m^2 \mathbf{h}_m(L) + \sqrt{m} U'(0) \theta^t \mathbf{Q}_m \mathbf{h}_m(L)$$

$$U'(0) = -\mathbf{c}_m^t \frac{1}{\sqrt{m}} \Lambda_m. \tag{D.17}$$

Substituting Eqn. (D.17) into Eqns. (D.10), (D.11) and (D.12) and rearranging Eqn. (D.9), so we have

$$\mathbf{c}^t \begin{bmatrix} \mathbf{I}_m \Delta t^2 - \mathbf{Q}_m^2 + \Lambda_m \theta^t \mathbf{Q}_m \end{bmatrix} \mathbf{h}_m(x) = \mathbf{k}^t \mathbf{h}_m(x). \tag{D.18}$$
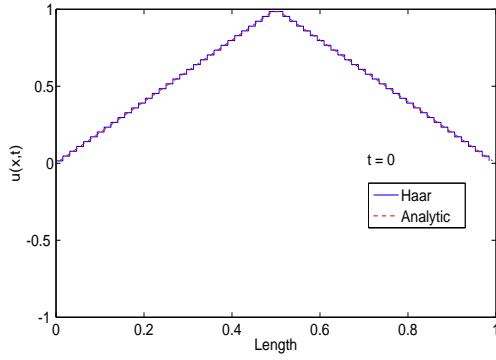
From Eqn. (D.18), Haar coefficient, $\mathbf{c}^t$ can be calculated and finally, the solution for wave equation is given by

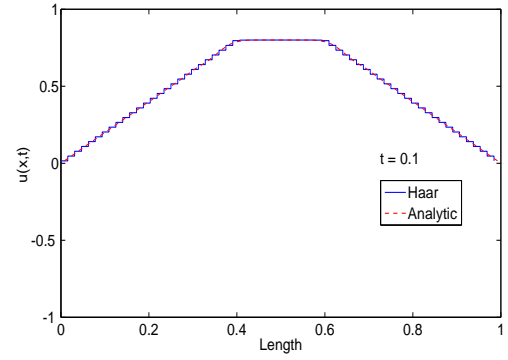$$U(x) = \mathbf{c}^t (\mathbf{Q}_m - \Lambda_m \theta^t) \mathbf{Q}_m \mathbf{h}_m(x). \tag{D.19}$$

Analytical solution using separation of variables for this problem is given by

$$U(x,t) = \frac{8}{\pi^2} \sum_{n=0}^{\infty} \frac{\sin\left(\dfrac{n\pi x}{L}\right) \sin\left(\dfrac{n\pi}{2}\right) \cos\left(\dfrac{n\pi a t}{L}\right)}{n^2}. \tag{D.20}$$

Results of the present numerical and analytical method are shown in Figure D.1 below.
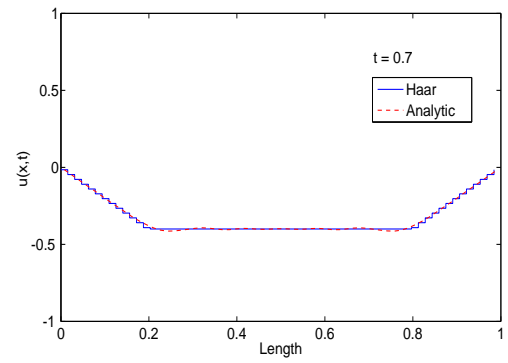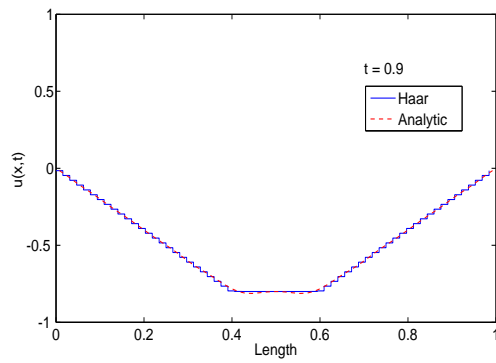
(a) Solutions when $t = 0$

(b) Solutions when $t = 0.1$
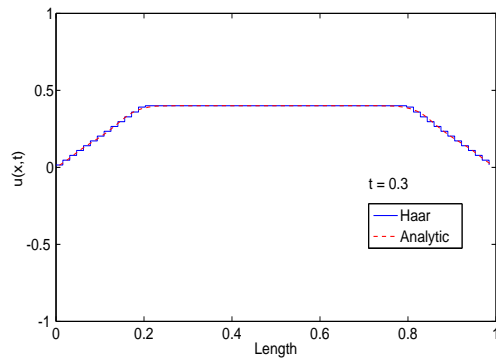
(c) Solutions when $t = 0.3$

(d) Solutions when $t = 0.7$

(e) Solutions when $t = 0.9$
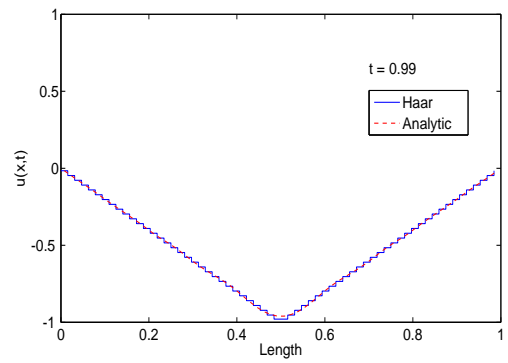
(f) Solutions when $t = 0.99$

Figure D.1: Comparison between numerical and analytical solution for wave equation, $u_{tt} = a^2 u_{xx}$ when $a^2 = 1$, $L = 1$ and $\Delta t = 0.0001$ at various values of time, t.

D.2 MATLAB code for numerical analysis of wave equation

```
% Solving wave equation

% U_tt = c^2*U_xx

% ODE aU" - U'=k

m=2^4;L=3;

% Generate block pulse operational matrix

Q=2*triu(ones(m,m));

for i=1:m

    Q(i,i)=Q(i,i)-1;

end

QB=Q/(2*m);

% Generate Haar matrix

H=ones(m);

J=log2(m);

x=1:2:(2*m-1); x=x/(2*m);

for alpha=0:(J-1)

    for k=1:pow2(alpha)

        fun=@(x) (( x >= (k-1)/pow2(alpha)) &&...

        ( x < (k-0.5)/pow2(alpha)))- (( x < k/pow2(alpha))...

        && ( x >= (k-0.5)/pow2(alpha)));

        i=pow2(alpha)+k;

        for j=1:m

            H(i,j)=pow2(alpha/2)*fun(x(j));
```

```matlab
        end

    end

end

H=H/sqrt(m);

% Haar operational matrix via Wu formula

Q=H*QB*H';

Q=L*Q;

theta=zeros(m,1); theta(1,1)=1;

theta=L*theta;

lambda=Q(:,1);

% initial input

dt=0.001;

v=1;a=(v*dt)^2;T=0.001; N=T/dt;

left=a*eye(m)-Q^2 + lambda*theta'*Q;

x=L*x;

fun = @(x) (2*x)/L.*(0<=x & x< L/2) + 2*(1-x/L).*(L/2 <=x & x< L);


uim1=fun(x);  % initial condition

ui=uim1;


for s=1:N

    u=uim1-2*ui;

    k=u*H'; %right hand side

    c=k/left; %coefficient
```

```
        uip1=c*(Q-lambda*theta')*Q*H;

        uim1=ui;

        ui=uip1;

end



%analytical solution

for s=0; t=0.001;  c=1;

for n=1:20

        s=s+sin(n*pi*x/L)*sin(n*pi/2)*cos(n*pi*c*t/L)/(n*n);

end

f=8*s/(pi^2);

end



stairs(x-3/(2*m),f)

hold on

plot(x,ui,'r')
```

APPENDIX E

TABLE OF LAPLACE TRANSFORMS

Table E.1: Laplace transforms $X(s) = \mathcal{L}\{x(t)\} = \int_0^\infty e^{-st} f(t) dt$

No	Transfer Function, $X(s)$	Laplace Inversion, $x(t)$
1	1	$\delta(t)$
2	$\dfrac{1}{s}$	$1, u(t)$
3	$\dfrac{1}{s^2}$	t
4	$\dfrac{1}{s^{p+1}}$	$\dfrac{t^p}{\Gamma(p+1)}, \quad (p > -1)$
5	$\dfrac{X(s)}{s}$	$\displaystyle\int_0^t x(\tau)d\tau$
6	$\dfrac{X(s)}{s^n}$	$\displaystyle\int_0^t \cdots \int_0^t f(\tau)d\tau^n = \int_0^t \dfrac{(t-\tau)^{n-1}}{(n-1)!}f(\tau)d\tau$
7	$\dfrac{1}{s^2+1}$	$\sin t$
8	$\dfrac{1}{s-a}$	e^{-at}
9	$\dfrac{1}{s^n\sqrt{s}}$	$\dfrac{4^n n!}{(2n)!\sqrt{\pi}}t^{n-1/2}$
10	$\dfrac{e^{-a\sqrt{s}}}{\sqrt{s}}$	$\dfrac{e^{-a^2/4t}}{\sqrt{\pi t}}$
11	$\dfrac{a}{2\sqrt{\pi}s^{3/2}}e^{-a^2/4s}$	$\dfrac{\sin a\sqrt{t}}{\pi}$
12	$\dfrac{e^{\frac{1}{s}}}{s\sqrt{s}}$	$\dfrac{\sinh 2\sqrt{t}}{\sqrt{\pi}}$
13	$s^2 X(s) - sx(0) - x'(0)$	$x''(t)$
14	$s^n x(s) - s^{n-1}x(0) \cdots x^{(n-1)}(0)$	$x^{(n)}(t)$
15	$\dfrac{1}{s}\exp\left(\dfrac{-\sqrt{s}x}{a}\right)$	$\operatorname{erfc}\left(\dfrac{x}{2a\sqrt{t}}\right)$

REFERENCES

Artisham, C. G. N. (2012). Numerical solution of elliptic partial differential equations by Haar wavelet operational matrix method. Master's thesis, University of Malaya.

Avudainayagam, A. and Vani, C. (1999). Wavelet-Galerkin solutions of quasilinear hyperbolic conservation equations. *Commun. Numer. Methods Eng.*, 15:589–601.

Babolian, E. and Fattahzadeh, F. (2007). Numerical computation method in solving integral equations. *Applied Mathematics and Computation*, 188:10161022.

Baumeister, K. J. and Hamill, T. D. (1969). Hyperbolic heat conduction equation a solution for the semi-infinite body problem. *ASME J. Heat Transfer*, 91:543–548.

Beylkin, G. (1993). Wavelets and fast numerical algorithms. *Proceedings of Symposia in Applied Mathematics*, 47.

Bindal, A., Khinast, J. G., and Ierapetritou, M. G. (2003). Adaptive multiscale solution of dynamical systems in chemical processes using wavelets. *Computers and Chemical Engineering*, 27:131–142.

Bokanowski, O. and Zidani, H. (2007). Anti-dissipative schemes for advection and application to Hamilton-Jacobi-Bellman equations. *Journal of Science Computation*, 30:1–33.

Carey, G. F. and Tsai, M. (1982). Hyperbolic heat transfer with reflection. *Numer. Heat Transfer*, pages 309–327.

Carrier, G. F. and Pearson, C. E. (1976). *Partial Differential Equations Theory and Technique.* Academic Press, Inc. (London) Ltd.

Catteneo, C. (1958). A form of heat conduction which eliminates the paradox of instantaneous propagation. *Comp. Rend. Acad. Sci.*, 4:431–433.

Chan, S. H. J., Low, D., and Mueller, W. K. (1971). Hyperbolic heat conduction in catalytic supported crystallites. *AIChE Journal*, 17(6):1499–1501.

Chang, S. (2010). *Academic Genealogy of Mathematicians.* World Scientific Publishing Company, 1 edition.

Chen, C. F. and Hsiao, C. (1997). Haar wavelet method for solving lumped and distributed-parameter systems. *Control Theory and Applications, IEE Proceedings*, 144(1):87–94.

Chen, C. F. and Hsiao, C. H. (1975). A Walsh series direct method for solving variational problems. *J. Franklin Inst*, 300:265–280.

Chen, H.-T. and Lin, J.-Y. (1993). Numerical analysis for hyperbolic heat conduction. *International Journal Heat and Mass Transfer*, 36(11):2891–2898.

Chen, T.-M. (2007). Numerical solution of hyperbolic heat conduction in thin surface layers. *International Journal of Heat and Mass Transfer*, 50:4424–4429.

Cheng, C. F. and Tsay, Y. T. (1977). Walsh operational matrices for fractional calculus and their application to distributed systems. *Journal of the Franklin Institute*, 303(3):267–284.

Chi-Hsu, W. (1983). On the generalization of block pulse operational matrices for fractional and operational calculus. *J. Franklin Inst.*, 315:91–102.

Churchill, R. V. (1958). *Operational Mathematics.* McGraw-Hill Inc., second edition.

Endow, Y. (1989). Optimal control via Fourier series of operational matrix of integration. *IEEE Trans. Autom. Control*, 34:770–773.

Gu, J. and Jiang, W. (1996). The Haar wavelets operational matrix of integration. *Int. J. Syst. Sci.*, 27:623–628.

Guo, Z.-Y. and Xu, Y.-S. (1992). Non-Fourier heat conduction in IC chip. *InterSociety Conference on Thermal Phenomena in Electronic Systems*, pages 271–275.

Haar, A. and Zimmermann, T. G. (1911). Zur theorie der orthogonalen funktionensysteme. *Mathematicsche Annalen*, 71(1):38–53.

Hariharan, G. and Kannan, K. (2011). A comparative study of Haar wavelet method and homotopy pertubation method for solving one-dimensional reaction-diffusion equations. *International Journal of Applied Mathematics and Computation*, 3(1):21–34.

Hess, L. D., Kokorowski, S. A., Olson, G. L., and Yaron, G. (1981). Laser processing of silicon for advanced microelectronic devices and circuits. *Laser and electronic beam solid interaction and material processing*, pages 307–319.

Holmström, M. and Waldén, J. (1998). Adaptive wavelet methods for hyperbolic PDEs. *Journal of Scientific Computing*, 13(1):19–49.

Hsiao, C. (2004). Solution of variational problems via Haar orthonormal wavelet direct method. *International Journal of Computer Mathematics*, 7:871–887.

Jerri, A. J. (1998). *The Gibbs Phenomenon in Fourier Analysis, Splines and Wavelet.* Springer, first edition.

Kao, T. T. (1977). Non Fourier heat conduction in thin surface layers. *Journal Heat Transfer*, 99:343–345.

Karimi, H. (2006). Optimal vibration control of vehicle engine-body system using Haar functions. *Int. J. Control Autom. Syst.*, 4:714–724.

Kelly, S. E. (1996). Gibbs phenomenon for wavelets. *Appl. Comput. Harmonic Analysis 3*, 3:72–81.

Khellat, F. and Yousefi, S. A. (2006). The linear Legendre mother wavelets operational matrix of integration and its application. *Journal of the Franklin Institute*, 343:181–190.

Khuri, S. (1993). Walsh and Haar functions in genetic algorithms. In *Proceedings of the 1994 ACM Symposium on Applied Computing*, pages 201–205. ACM Press.

Kilicman, A. and Zhour, Z. A. A. A. (2007). Kronecker operational matrices for fractional calculus and some applications. *Applied Mathematics and Computation*, 187(1):250–265.

Kreyszig, E. (2006). *Advanced engineering mathematics*. John Wiley Sons, Inc, 9 edition.

Lepik, Ü. (2005). Numerical solution of differential equations using Haar wavelets. *Mathematics and Computers in Simulation*, 68(2):127–143.

Lepik, Ü. (2007a). Application of the Haar wavelet transform to solving integral and differential equations. *Proceeding Estonian Academy Science Physics and Mathematics*, 56:28–46.

Lepik, Ü. (2007b). Numerical solution of evolution equations by the Haar wavelet method. *Applied Mathematics and Computation*, 185:695–704.

Lepik, Ü. (2011). Solving PDEs with the aid of two-dimensional Haar wavelets. *Computers Mathematics with Applications*, 61(7):1873–1879.

Lepik, Ü. and Tamme, E. (2004). Application of the Haar wavelets for solution of linear integral equations. In *Dynamical Systems and Applications Proceeding*, pages 494–507.

Liu, K.-C. and Chen, H.-T. (2004). Numerical analysis for the hyperbolic heat conduction problem under a pulsed surface disturbance. *Applied Mathematics and Computation*, 159(3):887–901.

Mallat, S. (2009). *A Wavelet Tour of Signal Processing, The Sparse Way*. Academic Press, London, 3rd edition.

Meyer, Y. (2008). Tribute to Jean Morlet. In *Continuous Wavelet Transform and Morlet's wavelet: International conference in honor of Jean Morlet*. Centre International de Rencontres Mathmatiques (CIRM), Marseille, France.

Mohan, B. and Kar, S. (2005). Comments on optimal control via Fourier series

of operational matrix of integration. *IEEE Trans. Autom. Control 50 (2005)*, 50:1466–1467.

Ozisik, M. N. and Vick, B. (1984). Propagation and reflection of thermal waves in a finite medium. *International Journal Heat Mass Transfer*, 27:1845–1854.

Paraskevopoulos, P. N. (1987). The operational matrices of integration and differentiation for the Fourier sine-cosine and exponential series. *IEEE Transactions on Automatic Control,*, 32(7):648–651.

Raeen, K. (2008). A study of the Gibbs phenomenon in Fourier series and wavelets. Master's thesis, The University of New Mexico, Albuquerque, New Mexico.

Ross, B. (1975). *Fractional Calculus and its Applications.* Springer-Verlag, Berlin.

Saeedi, H., Mollahasani, N., Moghadam, M. M., and Chuev, G. N. (2011). An operational Haar matrix method for solving fractional Volterra integral equations. *Int. J. Appl. Math. Comput. Sci.*, 21(3):535–547.

Shahsavaran, A. (2011). Haar wavelet method to solve Volterra integral equations with weakly singular kernel by collocation method. *Applied Mathematical Sciences*, 5(65):3201–3210.

Shen, W., Little, L., and Hu, L. (2010.). Anti-diffusive methods for hyperbolic heat transfer. *Computer Methods in Applied Mechanics and Engineering*, 199:1231–1239.

Shong-Leih, L. (1989). Weighting function scheme and its application on multidimensional conservation equations. *International Journal of Heat and Mass Transfer*, 32(11):2065–2073.

Singh, O. P., Singh, V. K., and Pandey, R. K. (2009). New stable numerical solutions of singular integral equations of Abel type by using normalized Bernstein polynomials. *Applied Mathematical Sciences*, 3(5):241–255.

Sinha, S. and Butcher, E. (1997). Symbolic computation of fundamental solution matrices for linear time-periodic dynamical systems. *J. Sound Vib.*, 206.

Taitel, Y. (1984). On the parabolic hyperbolic and discrete formulation of the heat conduction equation. *International Journal Heat Mass Transfer*, 15:369–371.

Tamma, K. and Railkar, S. (1989). Specially tailored transfinite-element formulations for hyperbolic heat conduction involving non-Fourier effects. *Numer. Heat Transfer*, 15 (Part B):211–226.

Tannehill, J. C., Anderson, D. A., and Pletcher, R. H. (1997). *Computational Fluid Mechanics and Heat Transfer*. Taylor and Francis, second edition.

Vernotte, P. (1958). Les paradoxes de la theorie continue de l'equation de la chaleur. *Competes Rendus Hebd. Seances Academy Science*, 246(22):3154–3155.

Wu, J.-L. (2003). *The Operational Matrix of Orthogonal Functions for Differential Equations*. PhD thesis, National Cheng Kung University, Tainan, Taiwan, Republic of China.

Wu, J.-L., Chen, C.-H., and Chen, C.-F. (2001). Numerical inversion of Laplace transform using Haar wavelet operational matrices. *IEEE Transactions on Circuits and Systems - 1: Fundamental Theory and Applications*, 48(1):120–123.

Zhengfu, X. and Chi-Wang, S. (2005). Anti-diffusive flux corrections for high

order finite difference WENO schemes. *Journal of Computational Physics*, 205(2):458–485.